MEASUREMENT NOTES

Note 14

COAXIAL DIELECTRIC WAVEGUIDES

June 1972

J.F. Toth and R. DeVore
The Ohio State University ElectroScience Laboratory
Department of Electrical Engineering
Columbus, Ohio 43212

Abstract

Cutoff frequencies were found for three configurations of cylindrical dielectric waveguides of circular cross-section for the lower order hybrid, E and H modes. The permittivities of the various coaxial layers were varied over a relatively wide range as were the ratios of the radii of the individual layers. Dispersion and attenuation characteristics were determined for the same range of geometrical and physical properties, primarily for the lower order HE_{11}, E_{01}, and H_{01} modes. A prescription for the determination of the cutoff frequencies of any coaxial-type (ℓ-layer) dielectric guide is presented.

Utilizing the information acquired, criteria are set for the design of a coaxial dielectric (ℓ=3) waveguide. An example of this configuration, designed for the X-band region, is given and its performance is compared with that of a dielectric rod (ℓ=1) waveguide.

TABLE OF CONTENTS

P. 9 P. 50
P. 33 P. 66
P. 36 P. 137
P. 37 P. 145
P. 43

CHAPTER I
DESIGN OF A COAXIAL DIELECTRIC WAVEGUIDE

A. Introduction

The dielectric waveguide configurations that have been considered in this report are shown in Fig. 1. The modes of the dielectric guide are the hybrid HE_{nm} (also EH_{nm} for n>1), transverse electric H_{om} (TE_{om}) and transverse magnetic E_{om} (TM_{om}). The first index denotes the number of azimuthal or ϕ-variations while the second index represents the greatest integer number of standing half-waves between the axis and the external boundary interface. Although the only configuration considered in the design is the three coaxial layer, hereinafter called the coaxial dielectric waveguide, representative phase and attenuation properties are shown for the one and two layer (rod and tube) configurations. In addition field amplitude and phase plots are given. The purpose of Figs 2 through 9 is to illustrate the similarities and contrasts between the one, two and three layer coaxial configurations. The dielectrics ($\varepsilon_{diel.}$=2.55; ε_{foam}=1.03; ε_{air}=1.00) used in each construction are the same but, of course, the possible permutations thereof, as well as relative layer thicknesses, increase with the number of interfaces. These parametric characteristics together with the modal cut-off frequencies are certainly necessary conditions and provide the basis for the design of any coaxial dielectric waveguide.

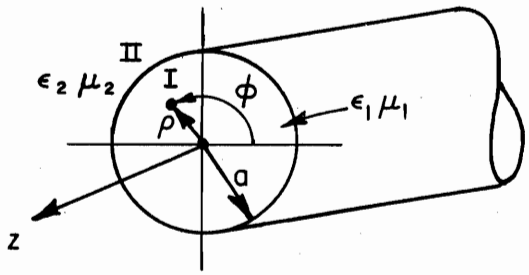

(a) DIELECTRIC ROD GUIDE

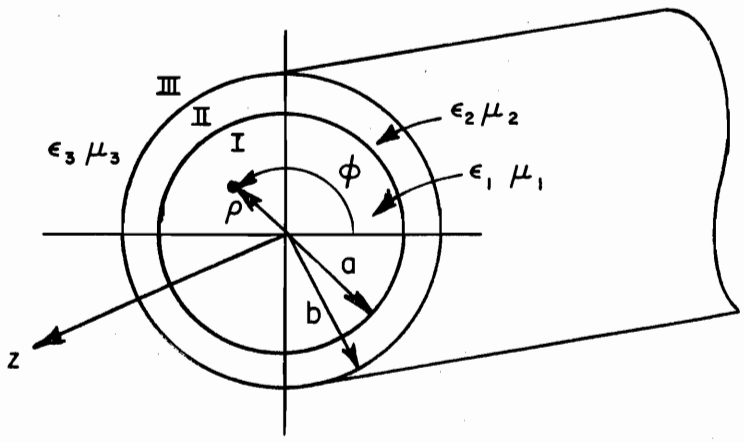

(b) DIELECTRIC TUBE GUIDE

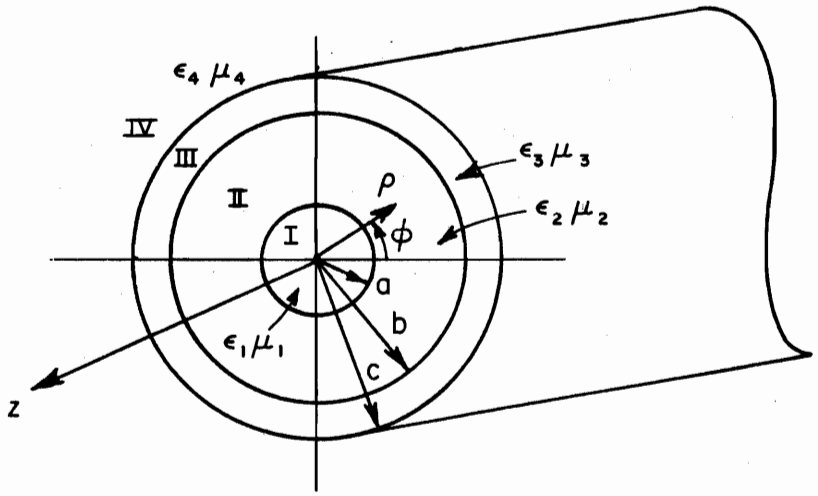

(c) DIELECTRIC COAXIAL GUIDE

Fig. 1.--Dielectric waveguide configurations.

In Figs. 2-9, all geometric parameters (radii a, b, c) and dielectric regions, are defined in Fig. 1. The vacuum wave number is defined by

$$(1) \qquad k_o = \frac{2\pi}{\lambda_o} = \frac{\omega}{c}$$

where λ_o is the vacuum wavelength, ω the angular frequency and c the vacuum speed of light. The axial propagation factor is

$$(2) \qquad \gamma = \text{Re } \gamma + j \text{ Im } \gamma$$

with spatial and temporal dependence $\epsilon^{j(\omega t - \gamma z)}$. The relative complex dielectric constant of medium m is

$$(3) \qquad \varepsilon_m = \frac{\epsilon_m}{\epsilon_o} (1 - j \tan \delta_m) = \text{Re } \varepsilon_m + j \text{ Im } \varepsilon_m$$

where the symbols have their usual meanings. Explicitly, the propagation factor γ as defined herein lies in the fourth quadrant, so $\text{Im } \gamma \leq 0$. The quantity $\text{Im } \varepsilon_m$ is clearly less than or equal to zero. Their ratio, the normalized attenuation factor $\text{Im}(\frac{\gamma}{k_o})/\text{Im } \varepsilon_m$, is shown in the figures as a positive quantity. This scaling or attenuation factor normalization was found to be valid over the range

$$(4) \qquad 0 < |\text{Im} \varepsilon_m| < 0.1.$$

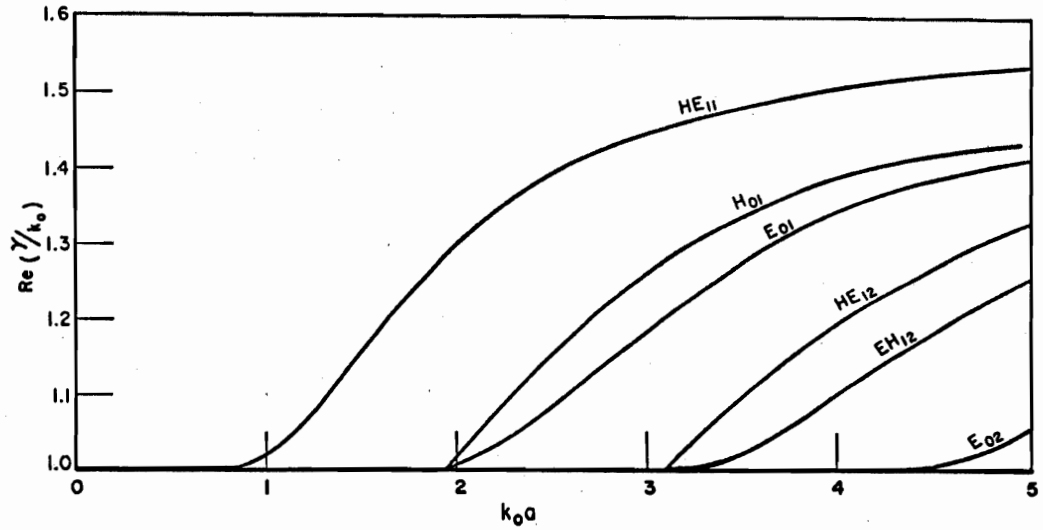

(a)

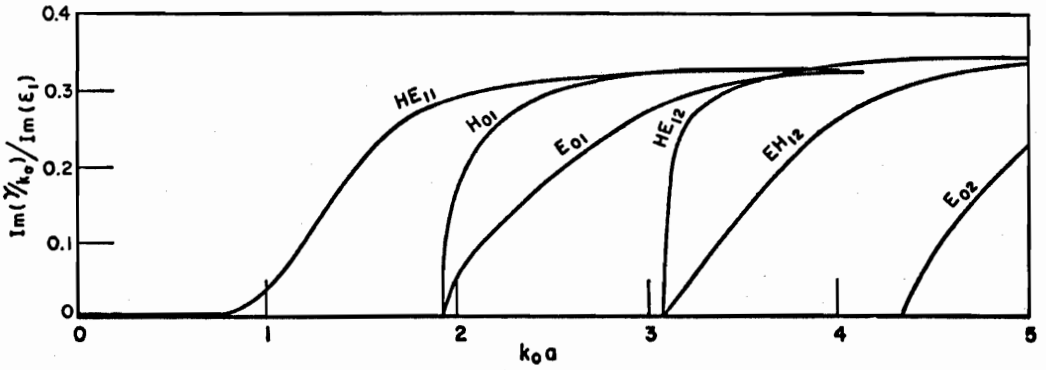

(b)

Fig. 2.--Modal (a) dispersion and (b) attenuation characteristics dielectric rod waveguide: ϵ_1=2.55 (Eqs. (II-8), (II-12) and (II-19)).

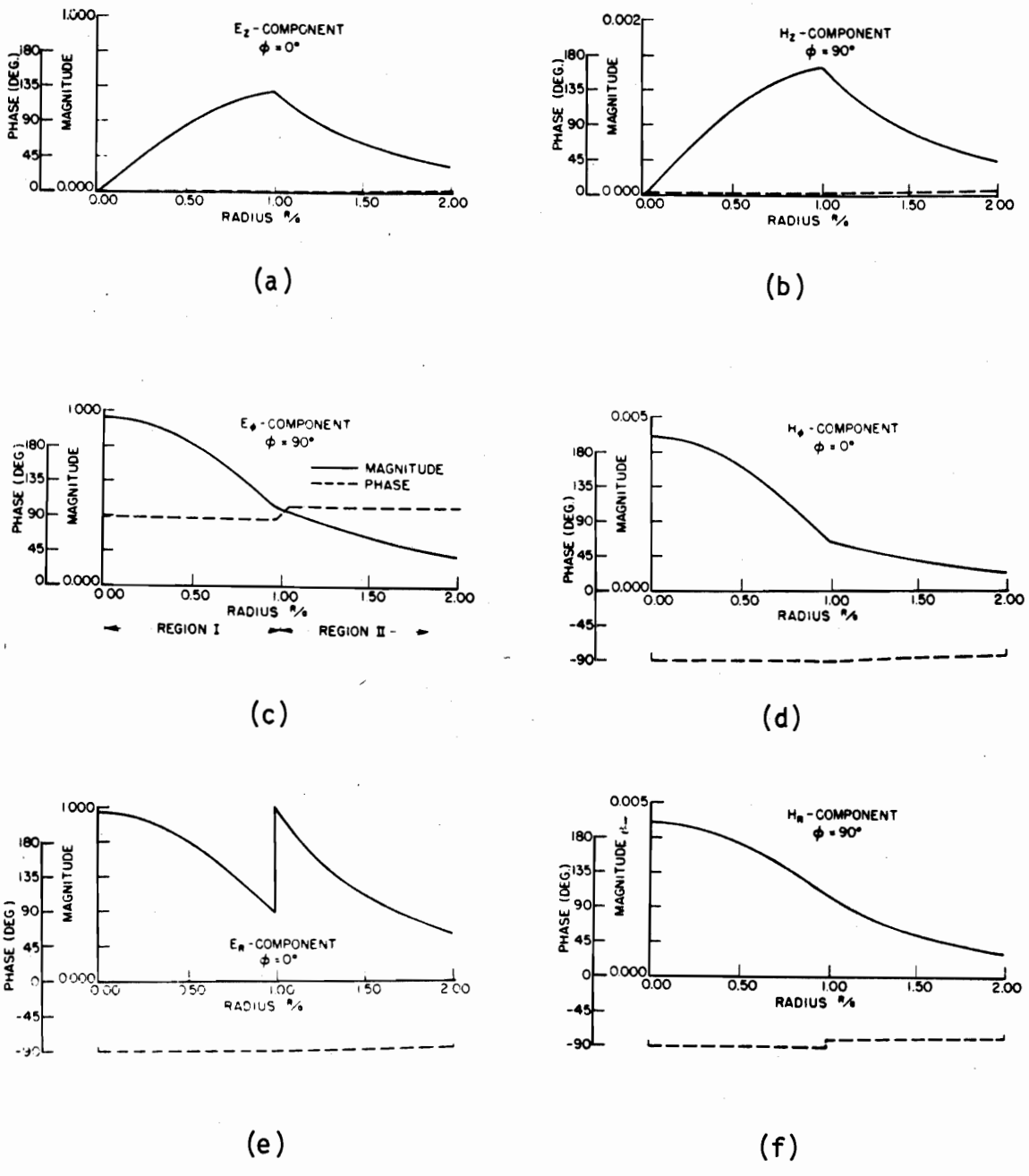

Fig. 3.--Field components for dielectric rod waveguide for the HE_{11} mode with $\epsilon_1=2.55$ and $Re(\gamma/k_0)=1.155$ (transverse plane).

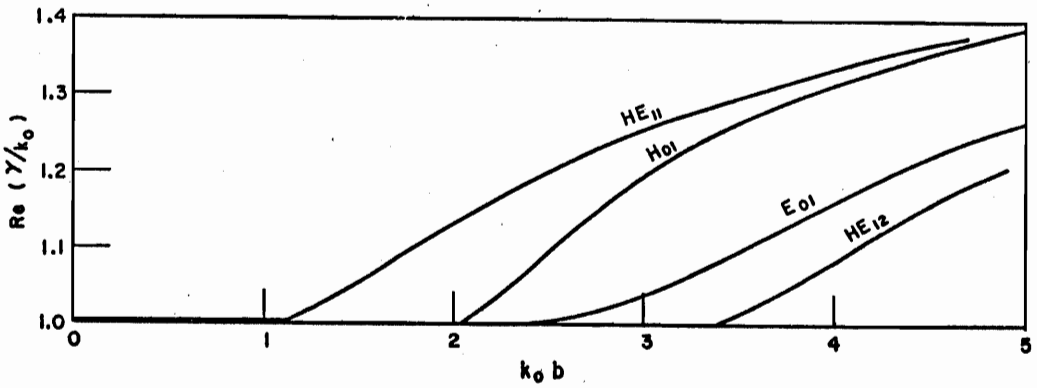

(a)

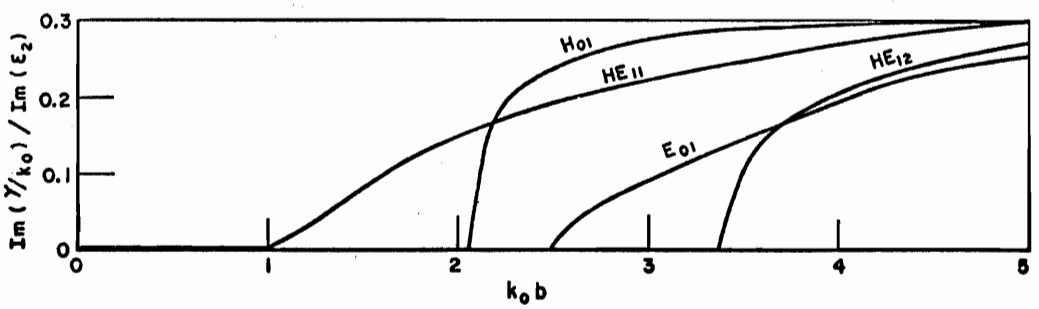

(b)

Fig. 4.--Modal (a) dispersion and (b) attenuation characteristics for airfilled dielectric tube waveguide: ϵ_2=2.55, a/b=.5 (Eqs. (II-23), (II-27) and (II-34)).

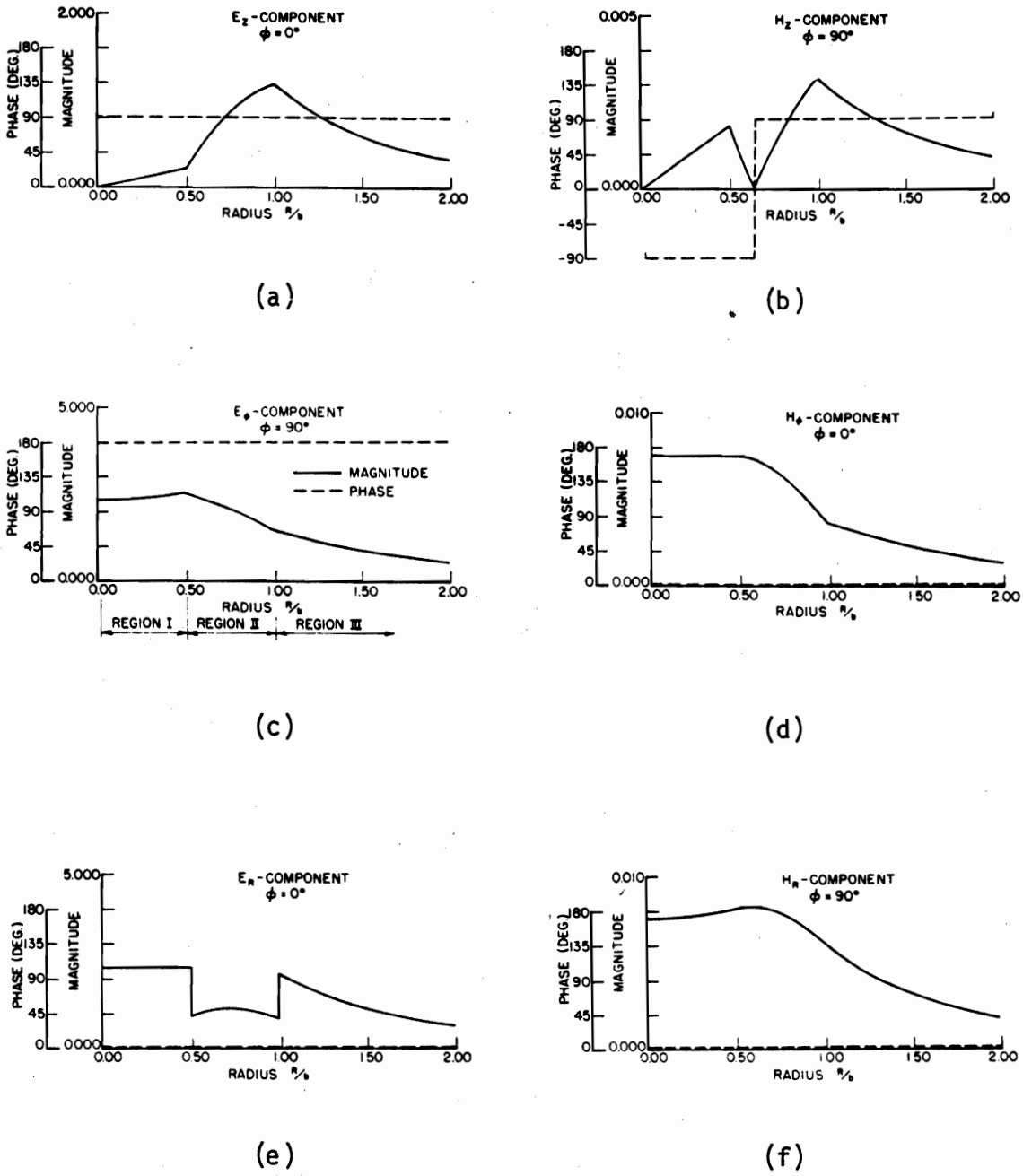

Fig. 5.--Field components for an airfilled dielectric tube waveguide for the HE_{11} mode with ϵ_2=2.55, a/b=.5 and $Re(\gamma/k_0)$=1.101 (transverse plane).

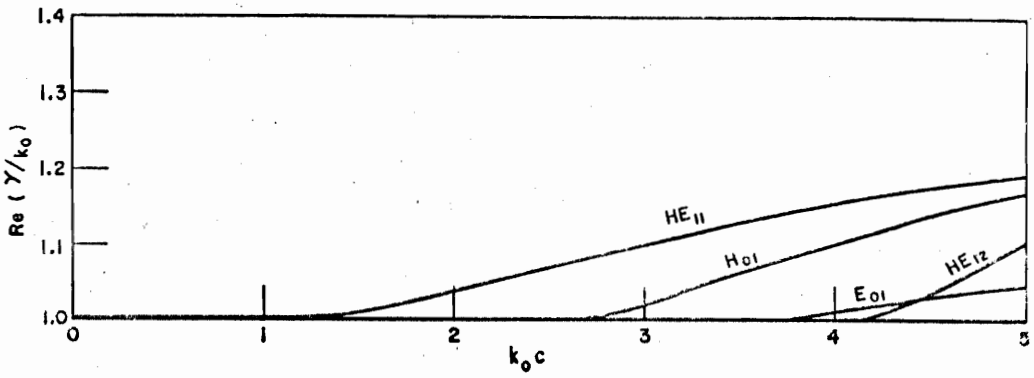

(a)

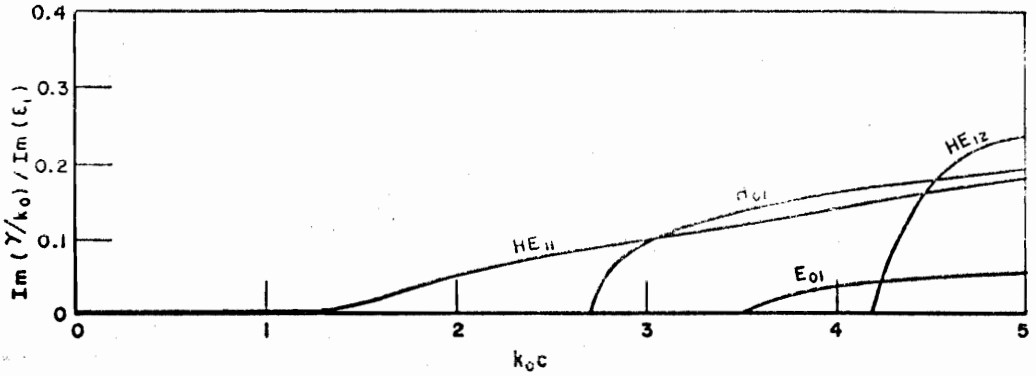

(b)

Fig. 6.--Modal (a) dispersion and (b) attenuation characteristics for dielectric coaxial waveguide: $\epsilon_1=\epsilon_3=2.55$, $\epsilon_2=1.03$, a/c=.3, b/c=.8 (Eqs. (II-38), (II-42) and (II-49)).

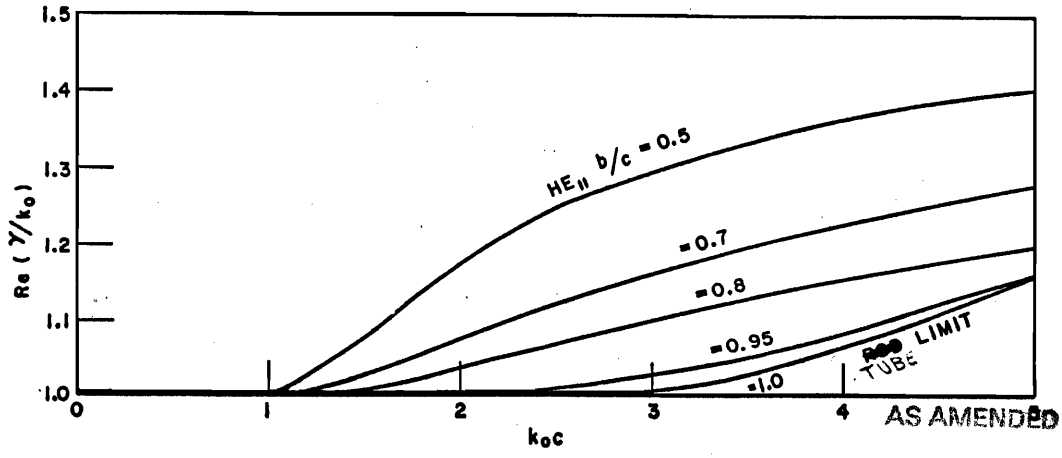

(a)

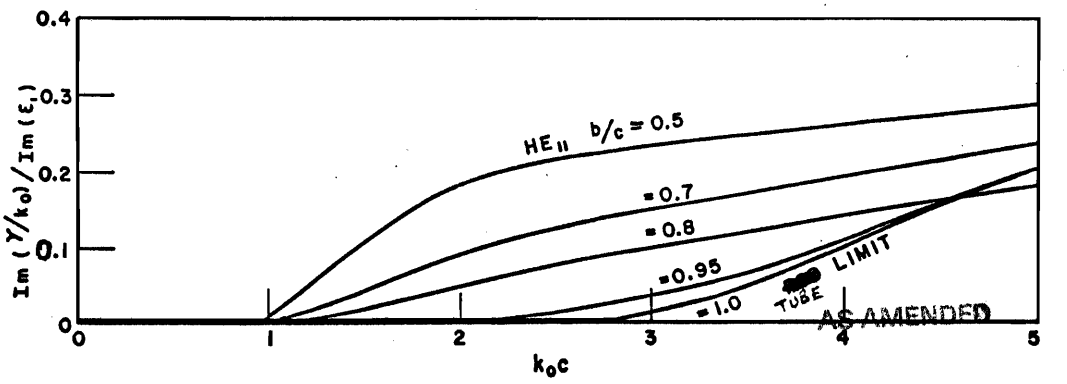

(b)

Fig. 7.--HE_{11} mode (a) dispersion and (b) attenuation characteristics for dielectric coaxial waveguide: $\epsilon_1=\epsilon_3=2.55$, $\epsilon_2=1.03$, a/c=.3 (Eq. (II-49)).

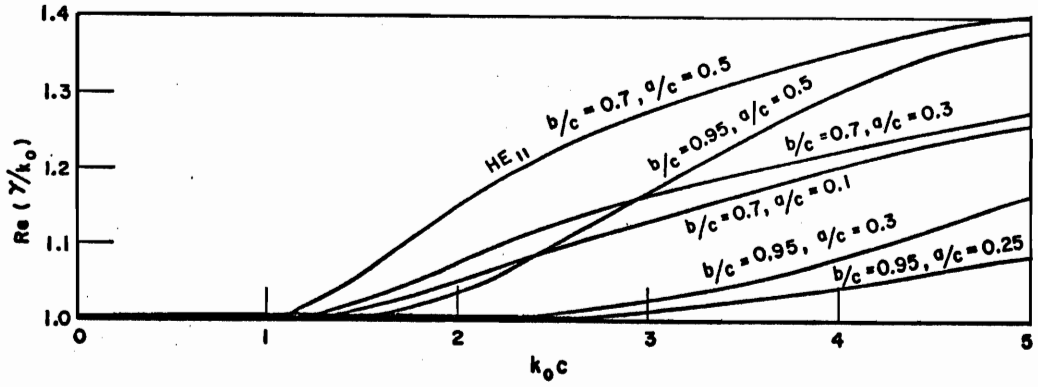

(a)

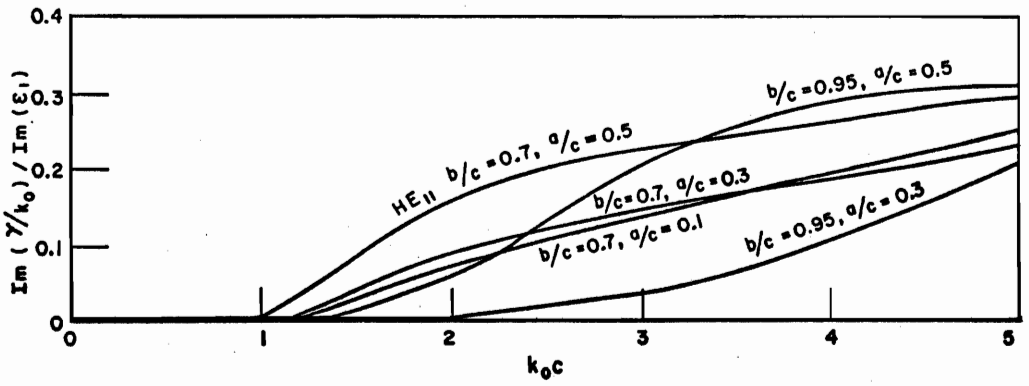

(b)

Fig. 8.--HE_{11} mode (a) dispersion and (b) attenuation characteristics for dielectric coaxial waveguide: $\epsilon_1=\epsilon_3=2.55$, $\epsilon_2=1.03$ (Eq. (II-49)).

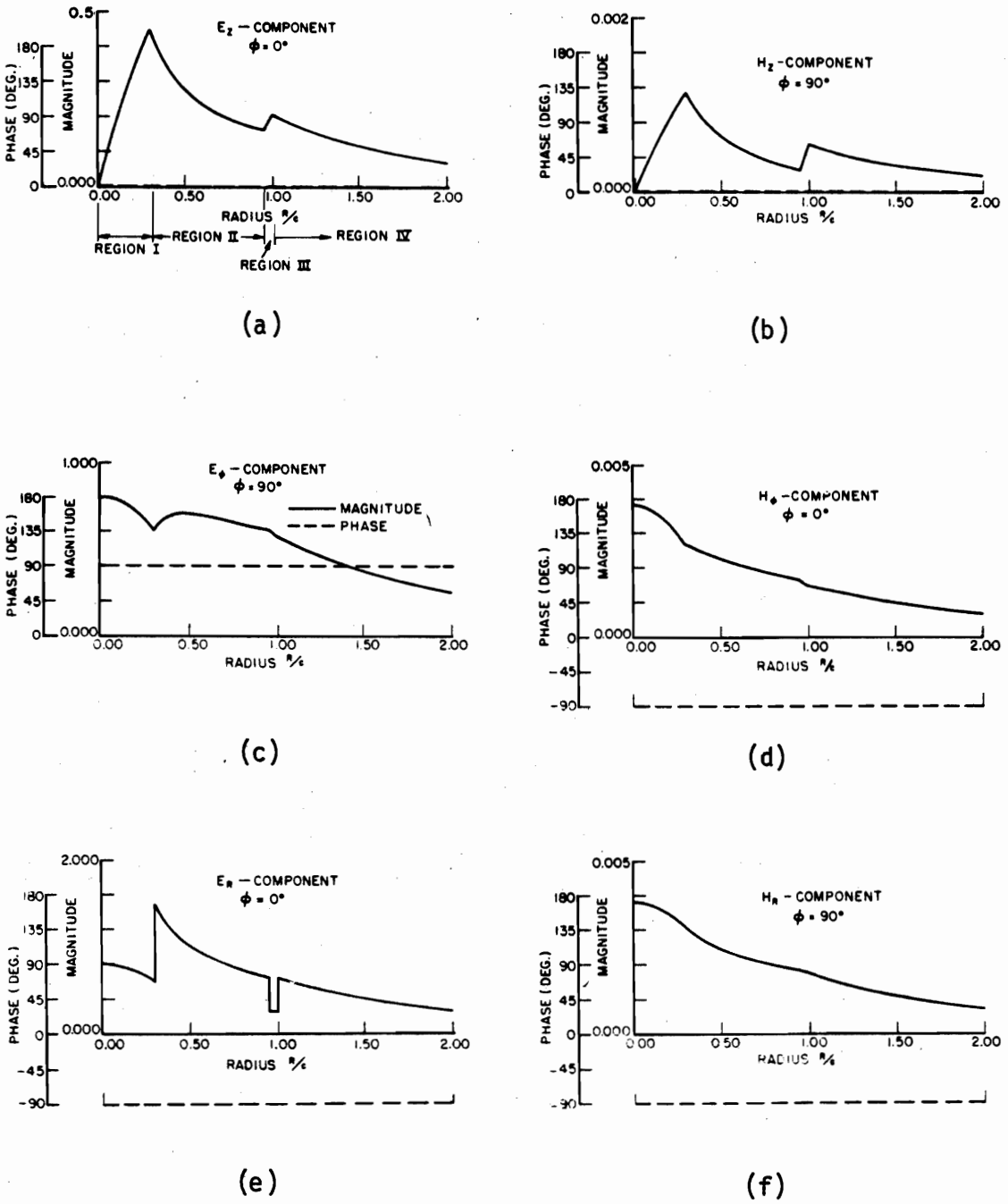

Fig. 9.--Field components for a dielectric coaxial waveguide HE_{11} mode with $\epsilon_1=\epsilon_3=2.55$, $\epsilon_2=1.03$, a/c=.3, b/c=.95 and $Re(\gamma/k_0)=1.021$ (transverse plane).

B. Waveguide Design Considerations

As in metal waveguides, one of the design considerations is the necessity that only one mode be excited in the waveguide so that the complications of multimode operation are avoided. To be sure that the waveguide is operating in this condition, an operating frequency range should be chosen in which only one mode can be excited. The only mode satisfying this requirement is the HE_{11} mode which is never cutoff. All the higher modes in each configuration have distinct cutoff values and can never be excited without the possibility of exciting the HE_{11} mode. Therefore, the operating frequency range is limited on the high end by the cutoff frequency of the next lowest mode. In all the computations that were performed for any of the configurations, this was the H_{01} mode.

Any of the configurations of Fig. 1 could be used as a waveguide, but some practical limitations make the coaxial guide more suitable to transmission over large distances. It is not feasible to remove all objects from the vicinity of the waveguide as guide supports are necessary to support lengths of more than a few meters. Thus there will be interaction between the external fields and the supports for most practical situations. This requires that most of the transmitted signal be transported within the dielectric guide for good transmission properties. This is indeed a problem for the dielectric rod and tube configurations. The dielectric rod cross-section must be increased in size to the point that other modes are excited and the attenuation is greatly increased if most of the energy is to be transported inside

the dielectric. The phase velocity is also greatly reduced in this region. The dielectric tube has the inherent problem that the fields are large in the vicinity of the external dielectric-air interface. This means there is always a relatively large portion of the energy transported in the external region.

The construction of long lengths of waveguide would present problems for the dielectric rod and tube cases which can be overcome in the construction of a long coaxial guide. Shorter lengths of coaxial guide can be made such that the inner dielectric rod would extend slightly from one end of the section and be indented the same amount at the other end. These shorter lengths may be fitted together either by threading the inner rod or force fitting the sections together to obtain the required lengths. No such simple method of construction is apparent for the other configurations without the introduction of some discontinuities and many more supports. From the standpoint of energy considerations and ease of construction, the most suitable configuration is the coaxial waveguide.

In designing a coaxial waveguide there are a number of variables to consider. Attenuation must be kept small if transmission over large distances is to be feasible. This can be accomplished by the use of a dielectric material with low loss tangent and, if feasible, by operating in the frequency range where the attenuation factor is small. Unfortunately, in this frequency range, most of the energy is propagating in the external region. Therefore the operating frequency range must include the region in which the loss becomes significant. The attenuation is also a function of the

relative dielectric constant of the interior rod region ($r<a$). Therefore, the use of material with high dielectric constant in this region should be avoided. The phase velocity, which is a function of the real part of the normalized propagation constant, is also a design consideration although it is not independent of the attenuation. The linearity of the phase characteristic over the bandwidth of the transmitted signal determines the amount of video pulse detail loss.

Probably the most important consideration is that the amount of energy transported outside the guide must be kept reasonably small. Although the HE_{11} mode has no cutoff value, at very low wavenumbers the propagation constant is essentially equal to the free space propagation constant k_o. Over that wavenumber range, a surface wave is only slightly bound to the guide. Therefore, most of the energy is transported external to the waveguide. For this reason, the allowable operating range should be restricted to that range of wavenumbers limited on the high end by the H_{01} mode cutoff wavenumber and on the low end by the wavenumber at which the normalized propagation constant becomes essentially unity. In this operating range, the amount of energy transported internally increases sharply as the wavenumber increases. A drawback is the attenuation also increases over this range.

As power is energy per unit time, one finds, from Poynting's theorem, the time average power density in the axial direction;

$$(5) \qquad P_z(r,\phi) = \frac{1}{2}\,\mathrm{Re}(E \times H^*)_z = \frac{1}{2}\,\mathrm{Re}[E_r H_\phi^* - E_\phi H_r^*],$$

which can be evaluated within the guide and in the exterior region. The fields inside and outside the guide are defined by the expressions given in Appendix II. Substituting the appropriate expressions in Eq. (5), Poynting's relation takes on the following form;

$$P_z(r,\phi) = F(r)\cos^2\phi + G(r)\sin^2\phi, \tag{6}$$

where $F(r)$ and $G(r)$ are functions of only the radial coordinate r. By substituting $-\phi$ for ϕ in Eq. (6), symmetry about $\phi = 0$ axis can be seen. Likewise, substituting $\pi - \phi$ for ϕ in Eq. (6), establishes the symmetry about the $\phi = 90°$ axis. This double symmetry condition allows one to obtain the level lines of $P_z(r,\phi)$ internal and external to the guide as a function of r and ϕ by evaluating over only a quarter of the area ($0° \leq \phi \leq 90°$). The shape of the level contours are somewhat elliptical with interchange of major and minor diameters occurring as the parameters are varied. The eccentricity of these elliptical level lines is very close to zero over the operating range. Therefore, for brevity, a good approximation to the power density percentage in each region can be found by integrating Eq. (5) at $\phi = 45°$. By numerically integrating radially Eq. (5) sufficiently far to include all but a negligible amount of power, the percentage of power transported in each region can be determined. Of special interest is the percentage of power outside the waveguide. Graphs of the percentage of power outside the coaxial guide over the operating frequency range defined previously are plotted in Figs. 10 to 12.

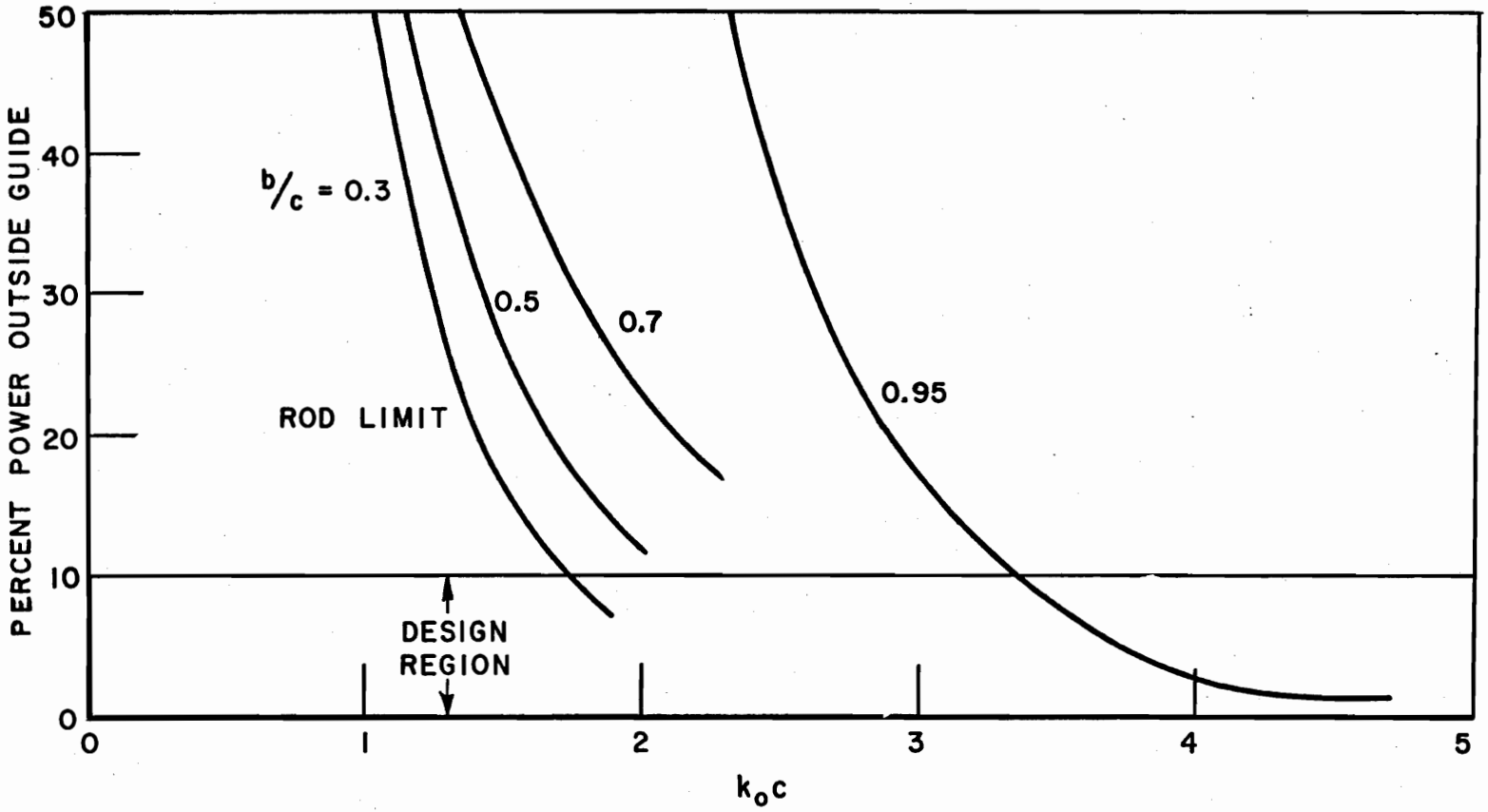

Fig. 10.--Percentage of power outside the guide over the appropriate wavenumber operating range for the dielectric coaxial waveguide with $\epsilon_1 = \epsilon_3 = 2.55$, $\epsilon_2 = 1.03$ and radii ratio a/c=.3.

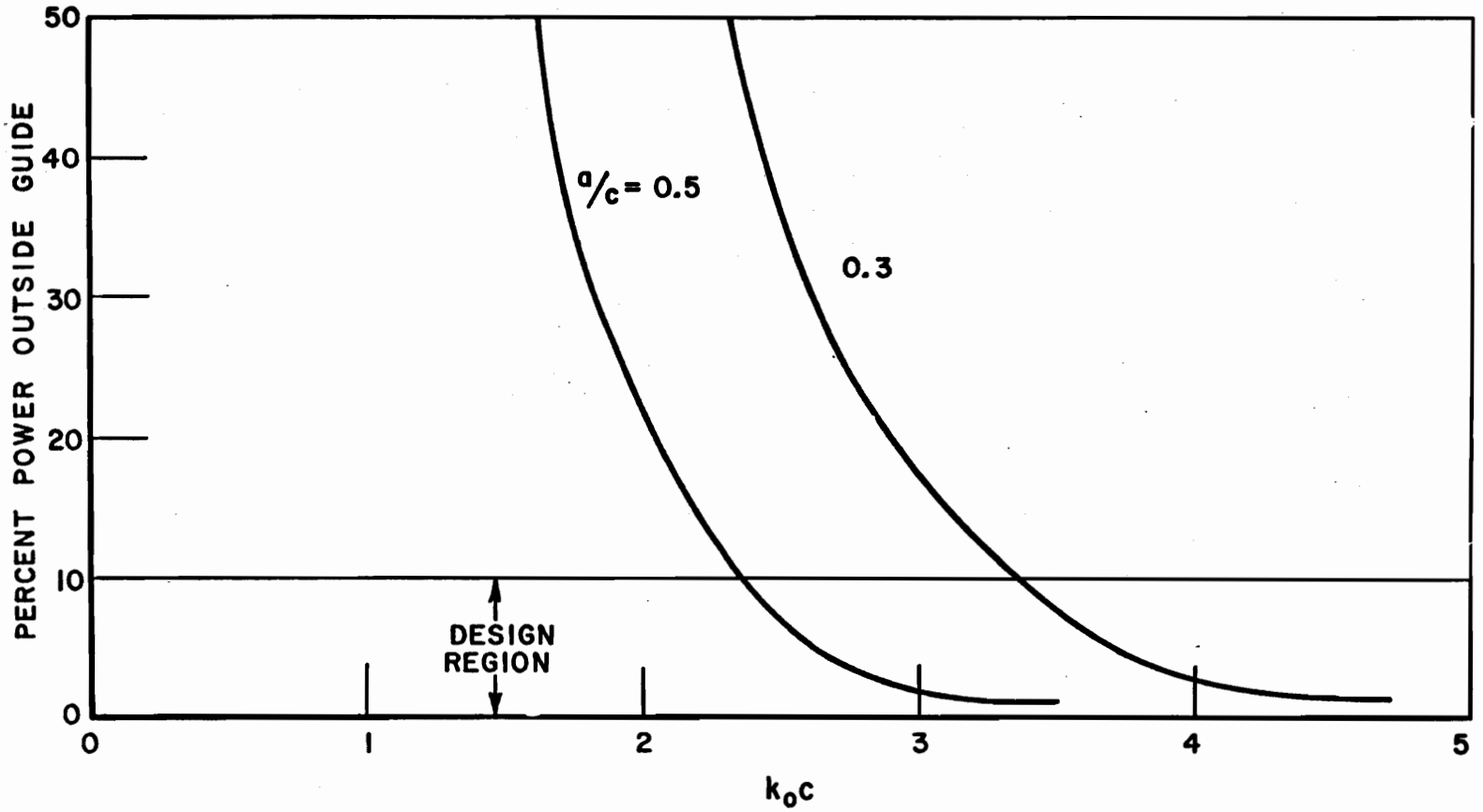

Fig. 11.--Percentage of power outside the guide over the appropriate wavenumber operating range for the dielectric coaxial waveguide with $\epsilon_1=\epsilon_3=2.55$, $\epsilon_2=1.03$ and radii ratio b/c=.95.

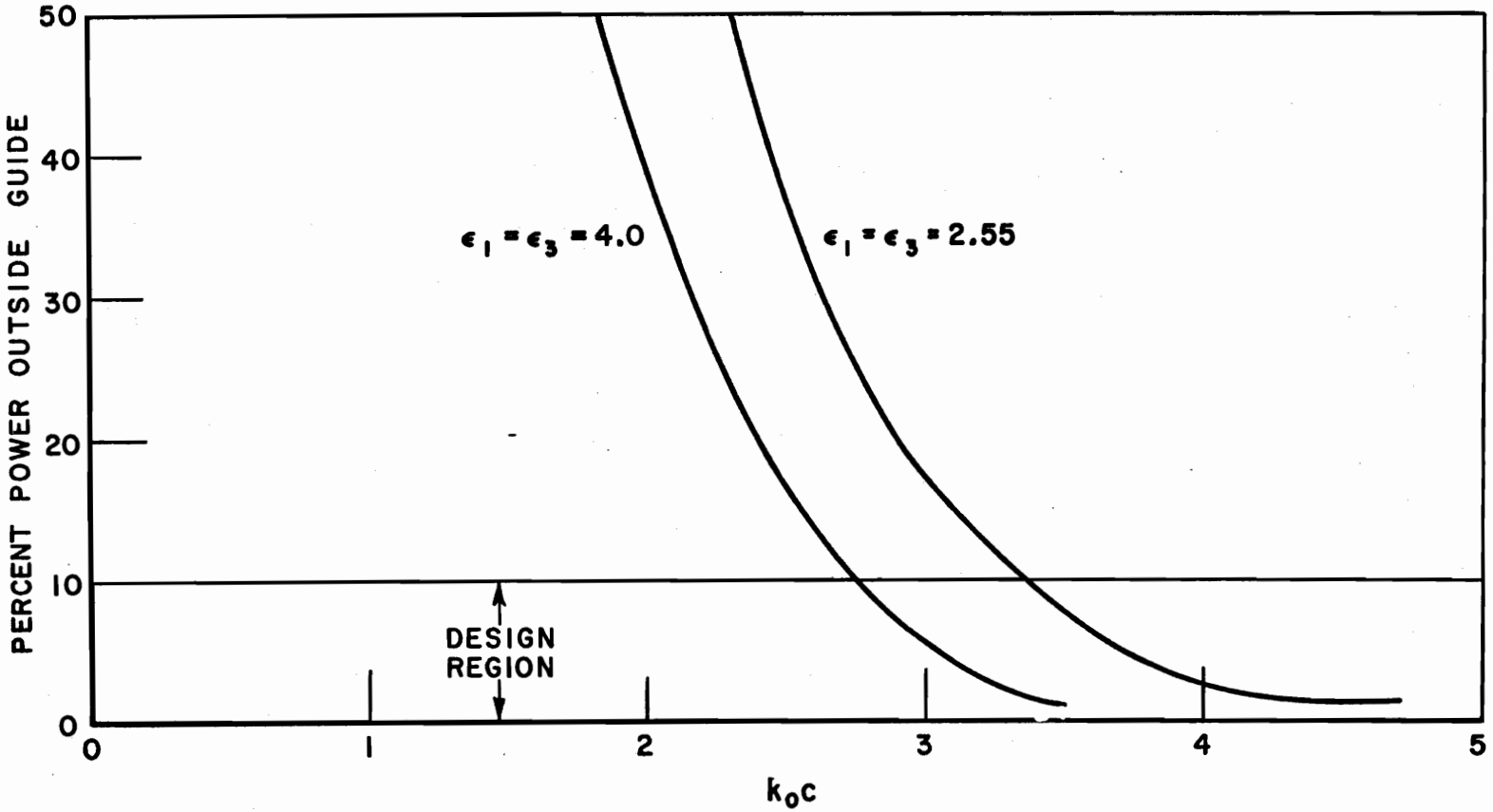

Fig. 12.--Percentage of power outside the guide over the appropriate wavenumber operating range for the dielectric coaxial waveguide with ϵ_2=1.03, a/c=.3 and b/c=.95.

The launching of a wave and the introduction of curvature or bends require tight binding of the wave to the guide. Setting a limit of 10% of the power that can be transported externally as the transport criterion, a near optimum configuration may be obtained. As alternative power criteria one might use the rate of field decay in the external medium or simply the normalized field amplitudes at the external boundary. This affects very little savings from a computational standpoint. At a minimum the four normalized field components and/or their derivatives must be evaluated at least at one point on the external boundary in order to formulate an alternate standard. From the power percentage curves in Fig. 10, it is apparent that larger operating ranges are obtained as the radii ratio b/c approaches unity. As seen from the b/c = .95 curve in Fig. 10, in order to obtain a significant operating range, a b/c ratio very near unity is essential. Figure 11 shows the effect of changes in the radii ratio a/c. Increasing the a/c ratio has the effect of reducing the operating range that satisfies the design criteria. The right terminal point of each of the curves in Figs. 10-12 denotes the onset of the H_{01} mode.

Changes in the relative dielectric constant of the inner rod region (r<a) also affect the allowable operating range. A comparison of similar coaxial waveguide configurations differing only in relative dielectric constant is shown in Fig. 12. The higher dielectric constant structure shows a smaller allowable operating range. It will also be remembered that lower dielectric constant

material is favorable because of lower attenuation factors and more nearly linear phase characteristics.

Thus far, in designing a coaxial waveguide, the power consideration has proved that small dielectric constant material, large values of b/c and small values of a/c are beneficial. If the relative dielectric constant is made too near unity, the size must be made significantly larger or most of the energy will travel outside the guide. The value of b/c cannot be set equal to one for this would result in a configuration made of a dielectric rod surrounded by a polyfoam tube. Although this would increase the operating range, the attenuation would become susceptible to environmental effects. The dielectric properties of polyfoam may be considerably affected by environmental changes. Even a small amount of moisture absorption can greatly increase the loss tangent of polyfoam in the microwave range[9]. This would greatly increase the attenuation factor for that range. For this reason, it is important to have some protective outer layer to separate the polyfoam from the surroundings. This thin outer dielectric shell can be made from some type of glaze or varnish sealer. There are also limits on how small the a/c ratio can be made. If the dielectric rod ($r<a$) crossectional area and the outer tube ($b<r<c$) crossectional area are comparable, the energy will be split between them with a relatively large amount outside the guide similar to the condition existing for the tube configuration.

C. Design Criteria

Although no rigid optimization criteria have been established, general criteria for the design of a coaxial dielectric waveguide which will perform satisfactorily can be stated. The trade-offs in energy, attenuation and linearity of phase are numerous and depend on the particular application. Using a general engineering approach, the design considerations are summarized:

1. Excitation of the HE_{11} mode in the range of wavenumbers below the H_{01} cutoff frequency is essential to avoid multimode operation.
2. All dielectric material should be chosen with low loss tangents for small absorption. The inner dielectric tube ($a<r<b$) should be made with a relative dielectric constant near unity and the inner rod ($r<a$) and outer tube ($b<r<c$) should have small relative dielectric constants.
3. A b/c radii ratio near unity is essential and a small value of a/c is preferable for obtaining large allowable operating ranges.
4. An operating range with a limit of 10% of the power transported outside the guide is necessary to eliminate the effects of the surroundings.
5. The pulse dispersion criteria as described in Section E should be considered from the standpoint of overall system performance.

D. Example: X-Band Waveguide

The problem is to design a dielectric coaxial waveguide to be used in the X-band frequency range. The following system requirements are assumed:

1. Excitation of the HE_{11} mode alone
2. Operation in the X-band frequency range with center frequency 10 GHz and a substantial operating range
3. Allowable power outside the guide <10%
4. Transmission of signal pulses with lengths varying from 1 microsecond to 100 nanoseconds and a bandwidth of 100 MHz.

Following the design criteria presented in Chapter I.C, the following design configuration is obtained; a/c = .3, b/c = .95, $\varepsilon_1 = \varepsilon_3 = 2.55$ and $\varepsilon_2 = 1.03$. For this configuration, the energy criterion allows for a wavenumber operating range of $k_o c$ from 3.35 to 4.7 from Fig. 10. Thus, the center frequency 10 GHz corresponds to the center of this allowable wavenumber range ($k_o c = 4$). The freespace wavelength λ_o at 10 GHz is three centimeters. Therefore, at 10 GHz;

$$k_o c = \frac{2\pi c}{\lambda_o} = 4.0, \tag{7}$$

from which the outer radius of the circular coaxial guide can be determined. The radii of the different layers are shown in Table 1.

TABLE 1
RADII OF DESIGN CONFIGURATION

RADIUS	PHYSICAL SIZE
a	.57 cm
b	1.81 cm
c	1.91 cm

The freespace wavelengths of the upper and lower frequency limits of the operating range can be found by employing the limits of the wavenumber operating range as follows:

(8a) $$\lambda_{o\ up} = \frac{2\pi c}{4.7} = 2.56 \text{ cm}$$

and

(8b) $$\lambda_{o\ low} = \frac{2\pi c}{3.35} = 3.56 \text{ cm.}$$

From their freespace wavelengths, the upper and lower limits of the frequency band are obtained as 11.7 GHz and 8.4 GHz, respectively. This represents a 1.4:1.0 operating frequency range. The physical size of this designed dielectric waveguide for the X-band region is comparable to the size of a metal waveguide designed for X-band operation. The operating frequency range is also similar to that theoretically determined for a metal guide.

The loss tangents of the dielectric material should be chosen as small as availability allows. A typical dielectric material with relative dielectric constant 2.55 is Styron C-176 which has a loss tangent of .0002. A polyfoam material with relative dielectric

constant 1.03 is styrofoam which also has a loss tangent of .0002. Using these materials for construction, the phase velocity and attenuation can be calculated from the normalized propagation constant obtained from the appropriate dispersion and attenuation curves. For the center frequency 10 GHz, the phase velocity is .924 times the speed of light, and the attenuation is .1009 dB/m. The fields for the HE_{11} mode in the design configuration at 10 GHz are shown in Figs. 13a to 13f. Comparing the field plots of the coaxial design configuration with those for the rod, tube and coaxial guides shown in Figs. 3, 5 and 9, respectively, one can deduce that there is less external energy transported in this configuration.

The dielectric rod waveguide is seen from Fig. 10 to have a small range of wavenumbers which satisfies the energy criterion. Choosing the center of this range to correspond to 10 GHz as was done for the design configuration, an operating range of 1.1:1.0 is obtained. This is considerably smaller than the operating range of the design configuration. The phase velocity and attenuation factor can also be calculated at 10 GHz as before. Using a Styron C-176 dielectric rod, the phase velocity was found to be .784 times the speed of light and the attenuation factor is .262 dB/m. This shows the coaxial configuration transmits relatively fast waves over a much wider operating range with less than half the attenuation of a comparable dielectric rod waveguide.

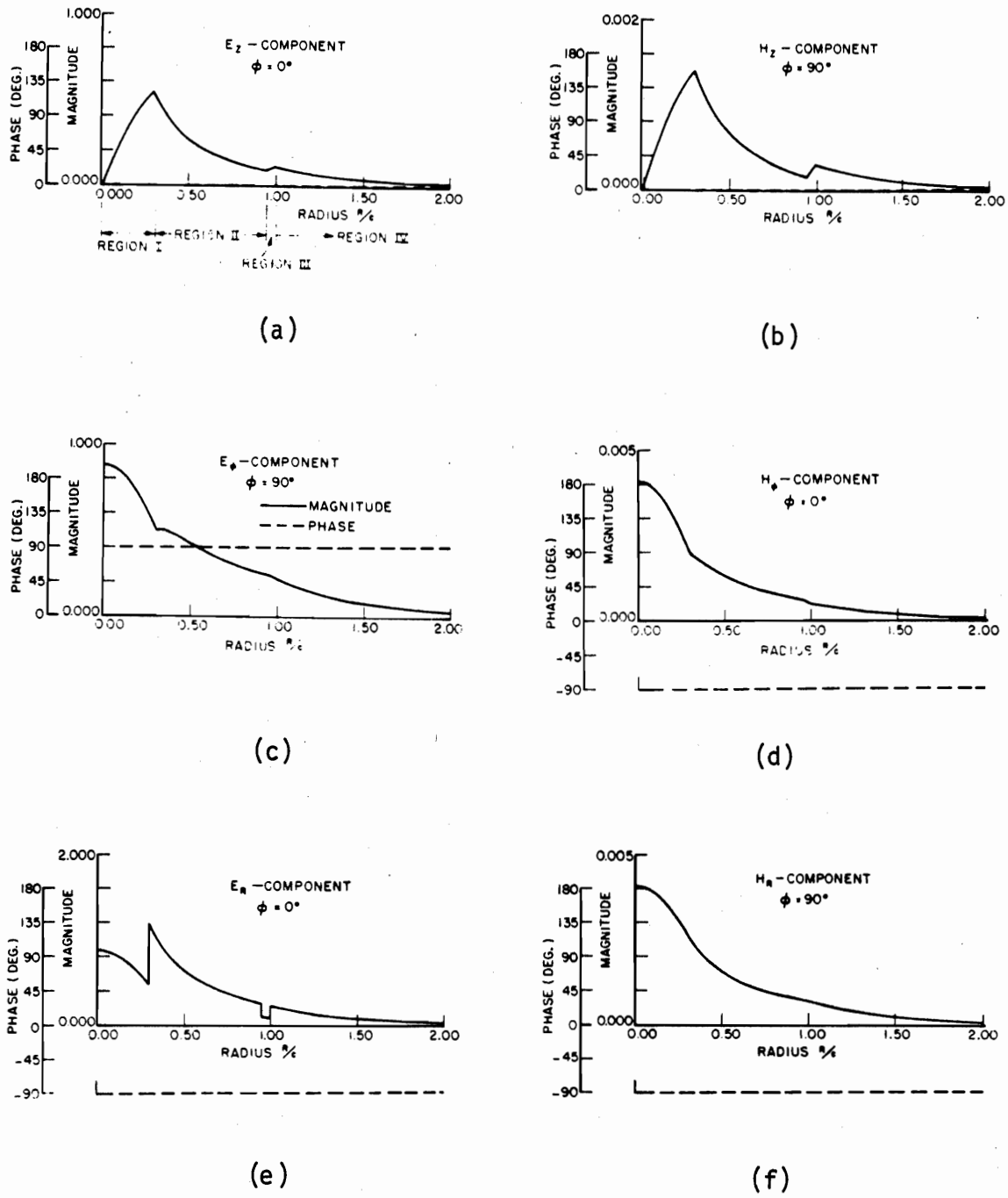

Fig. 13.--Field components of the X-band design configuration for the HE_{11} mode with $\epsilon_1=\epsilon_3=2.55$, $\epsilon_2=1.03$, a/c=.3, b/c=.95 and $Re(\gamma/k_0)=1.082$ (transverse plane).

E. Dispersion of Pulses

Accurate transmission of video pulse detail is a consideration in the design of a transmission system. S. Goldman[10] has established criteria for determining the amount of loss in pulse detail from the transmission phase characteristics.

1. If the variation from a linear phase characteristic is as much as 1 radian in a frequency range of

$$\frac{1}{3 \times \text{pulse length}},$$

a complete loss of signal detail can be expected.

2. If the variation from a linear phase characteristic is no more than half a radian in a frequency range

$$\frac{1}{3 \times \text{pulse length}},$$

there probably will be no serious loss of signal detail.

The above criteria can be applied to the dispersion curves of the dielectric waveguide configurations which essentially contain the phase characteristics of the guides.

A further consideration is the determination of the shortest time detail that can be resolved on a pulse modulated carier, i.e., the resolution of the shortest rise time of a pulse propagating on a dispersive system. A convenient way of approaching the problem is to evaluate a rectangular pulse of length 2T as a function of position on the dispersive and slightly absorbing waveguide. The waveguide system (transfer) function is $H(\omega) = \epsilon^{-jz\gamma(\omega)}$. The pulse, as a function of position on the guide, is specified by

$$(9) \qquad g(z,t) = \frac{1}{2\pi} \int_{-\infty} F(\omega) \epsilon^{z \text{ Re } \gamma(\omega)} \epsilon^{j[\omega t - z \text{ Im } \gamma(\omega)]} d\omega$$

where $F(\omega)$ is the Fourier transform of the rectangular pulse

$$f(t) = [u(t+T) - u(t-T)] \cos \omega_o t$$

and ω_o is the carrier angular frequency. This pulse may be made more realistic by introducing a finite rise and decay time.

For simplicity of computation the pulse f(t) was taken as trapezoidal with a 1 nsec initial and final slope and a 23 nsec length. The transmitted pulse along the guide is specified by the Fourier inversion (9). To define the initial rise or slope of the transmitted pulse, one point (t_o) is taken as the onset zero amplitude of the resultant waveform (envelope). The second point (t_{ss}) is taken as the intersection of the steady state amplitude of the pulse with the initial rise of the waveform as shown in Fig. 14.

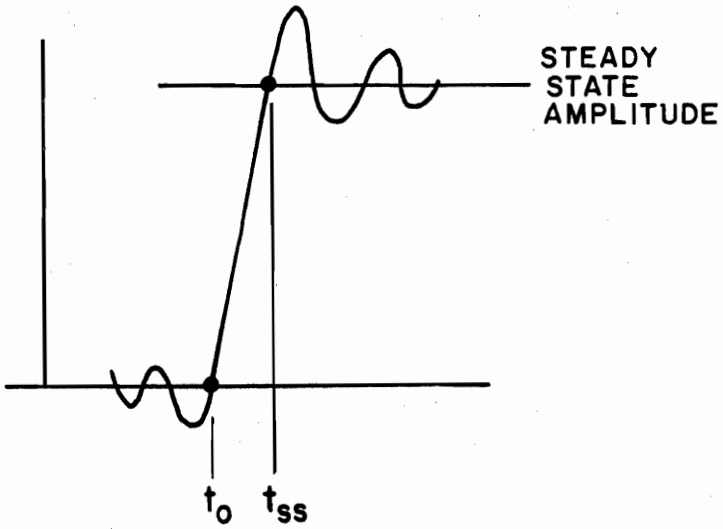

Fig. 14.--Definition of pulse rise.

This, or a similar definition, is required because of the amplitude oscillation introduced by the inversion. The initial pulse slopes so defined are shown in Fig. 15. The ordinate is pulse amplitude and the abscissa is nsec time units. The temporal pulse spreading per meter is defined by

$$\frac{\Delta t}{L} = \frac{(t_{ss} - t_o) - 1}{L} \left(\frac{\text{nsec}}{\text{m}}\right) \tag{10}$$

where all times are in nsec and L is the path length in meters. For this particular coaxial waveguide, the data show $\frac{\Delta t}{L} \approx .002 \frac{\text{nsec}}{\text{m}}$ At all stations the pulse form detail was similar. The attenuation of the higher frequencies rather than dispersion apparently accounts for the pulse spreading.

Since it is inconvenient to perform these calculations for every design, an estimate of pulse dispersion is quite desirable. The transit time t for a signal of angular frequency ω to travel a distance L is

$$t = \frac{L}{v_g(\omega)} = L \frac{d[\text{Re } \gamma(\omega)]}{d\omega}$$

where $v_g(\omega)$ is the group velocity (velocity of energy propagation) evaluated at ω. Thus

$$\frac{t_\ell - t_u}{L} = \frac{\Delta t}{L} = [\text{Re } \gamma(\omega_\ell)]' - [\text{Re } \gamma(\omega_u)]' = [\text{Re } \gamma(\omega_o)]'' \, \Delta\omega \tag{11}$$

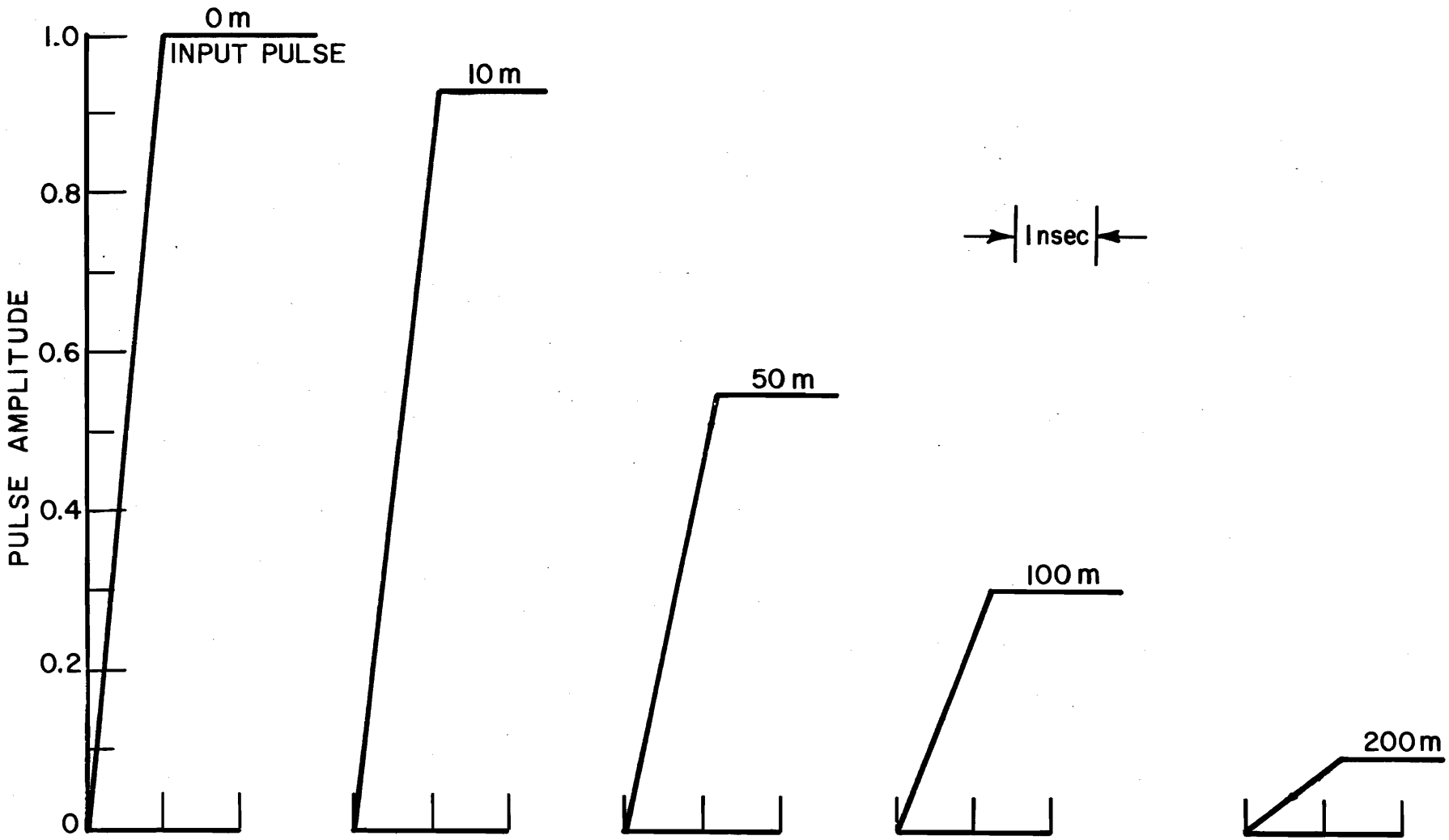

Fig. 15.--Leading edge of pulse at indicated positions along coaxial dielectric guide.

where $\omega_\ell - \omega_u$ is the system bandwidth, ω_o is the carrier angular frequency and the primes denote differentiation with respect to ω. For the designed coaxial waveguide $[\text{Re } \gamma(\omega_o)]'' \approx 3 \times 10^{-20}$ so for a 100 m guide with a permitted pulse spreading of 0.1 nsec a bandwidth 5 MHz or less is required. Evaluation of Eq. (11) for a metal rectangular X-band guide gives a maximum bandwidth of 3 MHz for the same conditions.

CHAPTER II
DETERMINATION OF MODAL CUTOFF FREQUENCIES FOR DIELECTRIC WAVEGUIDES

The modal cutoff frequencies of the coaxial dielectric waveguide are necessary for the physical design. To show the general method of determining the expressions for cutoff, the dielectric tube (ℓ=2), the simplest general case, is treated in detail. The results for the rod (ℓ=1) and coaxial (ℓ=3) configurations are summarized.

Cutoff of a dielectric waveguide mode occurs when the phase velocity of the guided wave becomes equal to the phase velocity of a plane wave in the surrounding medium. When the surrounding medium is vacuum, cutoff is obtained when the phase velocity of the guide mode equals the speed of light c. The phase velocity in terms of the normalized propagation factor (γ/k_o) is:

$$(12) \qquad v = \frac{\omega}{\mathrm{Re}\gamma} = \frac{c}{\mathrm{Re}[\gamma/k_o]} .$$

This indicates that as $v \to c$, cutoff requires $\mathrm{Re}(\gamma/k_o) \to 1$. The radial wavenumber h_n is defined by;

$$(13) \qquad \frac{h_n}{k_o} = \sqrt{\varepsilon_n - (\gamma/k_o)^2}$$

where ε_n is the relative permittivity of region n.

$$\epsilon_n = \left(\frac{\epsilon_n}{\epsilon_o}\right)(1 - j \tan\delta_n) \tag{14}$$

where ϵ_n is the dielectric constant and $\tan\delta_n$ is the loss tangent of region n. The relative permittivity ϵ_{ext} of the exterior medium (freespace) is equal to unity thus by Eq. (13), (h_{ext}/k_o) approaches zero at cutoff. This condition is utilized to determine the cutoff value for any mode of an ℓ-layer coaxial type dielectric waveguide from appropriately determined dispersion relations. The expressions for three coaxial-type configurations (ℓ = 1, 2 and 3) are given in Appendix II.

The general procedure is to define the quantity $h_{ext}\, r_{ext}$ (product of the external wavenumber and the outer radius of the guide) equal to a variable q and to consider the limiting expression of the appropriate dispersion relation as $q \to 0$. The elements of the determinant in the dispersion relation will be expressed as functions of q. The resulting determinant must still vanish since it is the limiting case of the dispersion equation. The cutoff relation is obtained by equating to zero the coefficient (determinant) of the lowest order q-term whose coefficient is not identically zero. The first few q-terms may be listed in ascending order as follows: $1, q^2\ell nq, q^2, (q^2\ell nq)^2, q^2(q^2\ell nq), q^4, q^2(q^2\ell nq)^2, q^4(q^2\ell nq)$. In the remainder of this section, the lowest order q-term with nonvanishing coefficient will be shown to have a determinant representation of which the zeros determine the mode cutoff values. The order of the required determinant is the same as the order of the dispersion

determinants given in Appendix II. The order of the cutoff determinants for the hybrid modes will be

$$(15) \qquad \text{Order of } D = \begin{cases} 2 & \text{if } \ell=1 \\ 4\ell-4 & \text{if } \ell>1 \end{cases}$$

and the H and E modes will follow:

$$(16) \qquad \text{Order of } D = \begin{cases} 1 & \text{if } \ell=1 \\ 2\ell-2 & \text{if } \ell>1 \end{cases}$$

The dielectric tube waveguide ($\ell=2$) is first characterized by three dielectric regions $\varepsilon_1 \neq 1$, $\varepsilon_2 \neq 1$ and $\varepsilon_3 = 1$. In this case $h_3 b = q$. Upon substitution of q for $h_3 b$ in the hybrid mode (HE_{nm} and EH_{nm}) dispersion determinant Eq. (II-34), the result is shown in Eq. (17)*.

The quantity $\left\{ q \dfrac{H_n^{(2)'}(q)}{H_n^{(2)}(q)} \right\}$ in rows 2 and 4 of the determinant can be expanded in terms of q as follows:

AS AMENDED

$$(18) \qquad \left\{ q \frac{H_n^{(2)'}(q)}{H_n^{(2)}(q)} \right\} \sim \begin{cases} -[1+q^2 \ell nq + \alpha q^2 + \cdots] & \text{for } n=1 \\ -n + \dfrac{q^2}{2(n-1)} + \cdots & \text{for } n>1 \end{cases}$$

where $\alpha = \gamma - \ell n 2$ and γ is Eulers constant. By substituting the appropriate expressions of Eq. (18) (only the first two terms of either expansion are needed) into the terms of Eq. (17), the two results are obtained from Eqs. (19) and (20).

*On page 34.

(17)

$$
\begin{vmatrix}
\epsilon_1(h_1a)(h_2a)^2J_n'(h_1a)J_n(h_2a) & \epsilon_1(h_1a)(h_2a)^2J_n'(h_1a)N_n(h_2a) & n[(h_2a)^2-(h_1a)^2]J_n(h_1a)J_n(h_2a) & n[(h_2a)^2-(h_1a)^2]J_n(h_1a)N_n(h_2a) \\
-\epsilon_2(h_1a)^2(h_2a)J_n(h_1a)J_n'(h_2a) & -\epsilon_2(h_1a)^2(h_2a)J_n(h_1a)N_n'(h_2a) & -\frac{n}{2(k_ob)^2}[(h_2a)^2-(h_1a)^2]J_n(h_1a)J_n(h_2a)q^2 & -\frac{n}{2(k_ob)^2}[(h_2a)^2-(h_1a)^2]J_n(h_1a)N_n(h_2a)q^2 \\
(h_2b)^2J_n(h_2b)\left\{q\frac{H_n^{(2)'}(q)}{H_n^{(2)}(q)}\right\} & (h_2b)^2N_n(h_2b)\left\{q\frac{H_n^{(2)'}(q)}{H_n^{(2)}(q)}\right\} & n(h_2b)^2J_n(h_2b) & n(h_2b)^2N_n(h_2b) \\
-\epsilon_2(h_2b)J_n'(h_2b)q^2 & -\epsilon_2(h_2b)N_n'(h_2b)q^2 & -n\left(\frac{\epsilon_2+1}{2}\right)J_n(h_2b)q^2 & -n\left(\frac{\epsilon_2+1}{2}\right)N_n(h_2b)q^2 \\
n[(h_2a)^2-(h_1a)^2]J_n(h_1a)J_n(h_2a) & n[(h_2a)^2-(h_1a)^2]J_n(h_1a)N_n(h_2a) & (h_1a)(h_2a)^2J_n'(h_1a)J_n(h_2a) & (h_1a)(h_2a)^2J_n'(h_1a)N_n(h_2a) \\
-\frac{n}{2(k_ob)^2}[(h_2a)^2-(h_1a)^2]J_n(h_1a)J_n(h_2a)q^2 & -\frac{n}{2(k_ob)^2}[(h_2a)^2-(h_1a)^2]J_n(h_1a)N_n(h_2a)q^2 & -(h_1a)^2(h_2a)J_n(h_1a)J_n'(h_2a) & -(h_1a)^2(h_2a)J_n(h_1a)N_n'(h_2a) \\
n(h_2b)^2J_n(h_2b) & n(h_2b)^2N_n(h_2b) & (h_2b)^2J_n(h_2b)\left\{q\frac{H_n^{(2)'}(q)}{H_n^{(2)}(q)}\right\} & (h_2b)^2N_n(h_2b)\left\{q\frac{H_n^{(2)'}(q)}{H_n^{(2)}(q)}\right\} \\
-n\frac{(\epsilon_2+1)}{2}J_n(h_2b)q^2 & -n\frac{(\epsilon_2+1)}{2}N_n(h_2b)q^2 & -(h_2b)J_n'(h_2b)q^2 & -(h_2b)N_n'(h_2b)q^2
\end{vmatrix} = 0
$$

for n=1

(19)

$$\begin{vmatrix}
\epsilon_1(h_1a)(h_2a)^2J_1'(h_1a)J_1(h_2a) & \epsilon_1(h_1a)(h_2a)^2J_1'(h_1a)N_1(h_2a) & [(h_2a)^2-(h_1a)^2]J_1(h_1a)J_1(h_2a) & [(h_2a)^2-(h_1a)^2]J_1(h_1a)N_1(h_2a) \\
\quad -\epsilon_2(h_1a)^2(h_2a)J_1(h_1a)J_1'(h_2a) & \quad -\epsilon_2(h_1a)^2(h_2a)J_1(h_1a)N_1'(h_2a) & \quad -\frac{1}{2(k_0b)^2}[(h_2a)^2-(h_1a)^2]J_1(h_1a)J_1(h_2a)q^2 & \quad -\frac{1}{2(k_0b)^2}[(h_2a)^2-(h_1a)^2]J_1(h_2a)N_1(h_2a)q^2 \\
-(h_2b)^2J_1(h_2b)-q^2\ln q(h_2b)^2J_1(h_2b) & -(h_2b)^2N_1(h_2b)-(h_2b)^2N_1(h_2b)q^2\ln q & (h_2b)^2J_1(h_2b) & (h_2b)^2N_1(h_2b) \\
\quad -[\epsilon_2(h_2b)J_1'(h_2b)+\alpha(h_2b)^2J_1(h_2b)]q^2 & \quad -[\epsilon_2(h_2b)N_1'(h_2b)+\alpha(h_2b)^2N_1(h_2b)]q^2 & \quad -\left(\frac{\epsilon_2+1}{2}\right)J_1(h_2b)q^2 & \quad -\left(\frac{\epsilon_2+1}{2}\right)N_1(h_2b)q^2 \\
[(h_2a)^2-(h_1a)^2]J_1(h_1a)J_1(h_2a) & [(h_2a)^2-(h_1a)^2]J_1(h_1a)N_1(h_2a) & (h_1a)(h_2a)^2J_1'(h_1a)J_1(h_2a) & (h_1a)(h_2a)^2J_1'(h_1a)N_1(h_2a) \\
\quad -\frac{1}{2(k_0b)^2}[(h_2a)^2-(h_1a)^2]J_1(h_1a)J_1(h_2a)q^2 & \quad -\frac{1}{2(k_0b)^2}[(h_2a)^2-(h_1a)^2]J_1(h_1a)N_1(h_2a)q^2 & \quad -(h_1a)^2(h_2a)J_1(h_1a)J_1'(h_2a) & \quad -(h_1a)^2(h_2a)J_1(h_1a)N_1'(h_2a) \\
(h_2b)^2J_1(h_2b) & (h_2b)^2N_1(h_2b) & -(h_2b)^2J_1(h_2b)-(h_2b)^2J_1(h_2b)q^2\ln q & -(h_2b)^2N_1(h_2b)-(h_2b)^2N_1(h_2b)q^2\ln q \\
\quad -\frac{(\epsilon_2+1)}{2}J_1(h_2b)q^2 & \quad -\frac{(\epsilon_2+1)}{2}N_1(h_2b)q^2 & \quad -[(h_2b)J_1'(h_2b)+\alpha(h_2b)^2J_1(h_2b)]q^2 & \quad -[(h_2b)N_1'(h_2b)+\alpha(h_2b)^2N_1(h_2b)]q^2
\end{vmatrix} = 0$$

for n>1

(20)

$$\begin{vmatrix}
\epsilon_1(h_1a)(h_2a)^2J_n'(h_1a)J_n(h_2a) & \epsilon_1(h_1a)(h_2a)^2J_n'(h_1a)N_n(h_2a) & n[(h_2a)^2-(h_1a)^2]J_n(h_1a)J_n(h_2a) & n[(h_2a)^2-(h_1a)^2]J_n(h_1a)N_n(h_2a) \\
\quad -\epsilon_2(h_1a)^2(h_2a)J_n(h_1a)J_n'(h_2a) & \quad -\epsilon_2(h_1a)^2(h_2a)J_n(h_1a)N_n'(h_2a) & \quad -\frac{n}{2(k_0b)^2}[(h_2a)^2-(h_1a)^2]J_n(h_1a)J_n(h_2a)q^2 & \quad -\frac{n}{2(k_0b)^2}[(h_2a)^2-(h_1a)^2]J_n(h_1a)N_n(h_2a)q^2 \\
-n(h_2b)^2J_n(h_2b) & -n(h_2b)^2N_n(h_2b) & n(h_2b)^2J_n(h_2b) & n(h_2b)^2N_n(h_2b) \\
\quad -[\epsilon_2(h_2b)J_n'(h_2b)-\frac{(h_2b)^2}{2(n-1)}J_n(h_2b)]q^2 & \quad -[\epsilon_2(h_2b)N_n'(h_2b)-\frac{(h_2b)^2}{2(n-1)}N_n(h_2b)]q^2 & \quad -n\left(\frac{\epsilon_2+1}{2}\right)J_n(h_2b)q^2 & \quad -n\left(\frac{\epsilon_2+1}{2}\right)N_n(h_2b)q^2 \\
n[(h_2a)^2-(h_1a)^2]J_n(h_1a)J_n(h_2a) & n[(h_2a)^2-(h_1a)^2]J_n(h_1a)N_n(h_2a) & (h_1a)(h_2a)^2J_n'(h_1a)J_n(h_2a) & (h_1a)(h_2a)^2J_n'(h_1a)N_n(h_2a) \\
\quad -\frac{n}{2(k_0b)^2}[(h_2a)^2-(h_1a)^2]J_n(h_1a)J_n(h_2a)q^2 & \quad -\frac{n}{2(k_0b)^2}[(h_2a)^2-(h_1a)^2]J_n(h_1a)N_n(h_2a)q^2 & \quad -(h_1a)^2(h_2a)J_n(h_1a)J_n'(h_2a) & \quad -(h_1a)^2(h_2a)J_n(h_1a)N_n'(h_2a) \\
n(h_2b)^2J_n(h_2b) & n(h_2b)^2N_n(h_2b) & -n(h_2b)^2J_n(h_2b) & -n(h_2b)^2N_n(h_2b) \\
\quad -n\frac{(\epsilon_2+1)}{2}J_n(h_2b)q^2 & \quad -n\frac{(\epsilon_2+1)}{2}N_n(h_2b)q^2 & \quad -[(h_2b)J_n'(h_2b)-\frac{(h_2b)^2}{2(n-1)}J_n(h_2b)]q^2 & \quad -[(h_2b)N_n'(h_2b)-\frac{(h_2b)^2}{2(n-1)}N_n(h_2b)]q^2
\end{vmatrix} = 0.$$

The lowest order q-term in either case may be determined by row-column operations. Considering first the case where n=1, the procedure is to add row 4 to row 2. This produces in row 2 terms with a common factor $q^2 \ell nq$ which may be factored out of the determinant. The lowest order q-term with nonvanishing coefficient must therefore be of order $q^2 \ell nq$ or higher. To show that the coefficient of $q^2 \ell nq$ term does not vanish identically, suppress the remaining q-terms larger than the zeroth order ($q^{(0)}=1$) after factoring the $q^2 \ell nq$ term from row 2. The resulting determinant is indeed not identically zero and the lowest order is $q^2 \ell nq$. The final expression is:

for n=1

$$(21)\quad q^2 \ell nq \begin{vmatrix} \varepsilon_1(h_1a)(h_2a)^2 J_1'(h_1a) J_1(h_2a) & \varepsilon_1(h_1a)(h_2a)^2 J_1'(h_1a) N_1(h_2a) & [(h_2a)^2-(h_1a)^2] J_1(h_1a) J_1(h_2a) & [(h_2a)^2-(h_1a)^2] J_1(h_1a) N_1(h_2a) \\ -\varepsilon_2(h_1a)^2(h_2a) J_1(h_1a) J_1'(h_2a) & -\varepsilon_2(h_1a)^2(h_2a) J_1(h_1a) N_1'(h_2a) & & \\ -J_1(h_2b) & -N_1(h_2b) & -J_1(h_2b) & -N_1(h_2b) \\ [(h_2a)^2-(h_1a)^2] J_1(h_1a) J_1(h_2a) & [(h_2a)^2-(h_1a)^2] J_1(h_1a) N_1(h_2a) & (h_1a)(h_2a)^2 J_1'(h_1a) J_1(h_2a) & (h_1a)(h_2a)^2 J_1'(h_1a) N_1(h_2a) \\ & & -(h_1a)^2(h_2a) J_1(h_1a) J_1'(h_2a) & -(h_1a)^2(h_2a) J_1(h_1a) N_1'(h_2a) \\ J_1(h_2b) & N_1(h_2b) & -J_1(h_2b) & -N_1(h_2b) \end{vmatrix} = 0.$$

AS AMENDED

The zeros of the determinant in Eq. (21) are the cutoff values of the hybrid modes of the dielectric-filled dielectric tube waveguide for n=1.

Substitution of the expansion of $\left\{ q \dfrac{H_n^{(2)'}(q)}{H_n^{(2)}} \right\}$ for n>1 from Eq. (18) into Eq. (20) and then addition of row 4 to row 2 of this determinant results in the terms in row 2 having a common q^2 factor which is factored from the determinant. If the terms containing the

higher orders of q are suppressed, then the lowest order q-term with nonvanishing coefficient is the q^2 term. The cutoff expression obtained is

for n>1

$$(22)\quad q^2 \begin{vmatrix} \epsilon_1(h_1a)(h_2a)^2J_n'(h_1a)J_n(h_2a) & \epsilon_1(h_1a)(h_2a)^2J_n'(h_1a)N_n(h_2a) & n[(h_2a)^2-(h_1a)^2]J_n(h_1a)J_n(h_2a) & n[(h_2a)^2-(h_1a)^2]J_n(h_1a)N_n(h_2a) \\ -\epsilon_2(h_1a)^2(h_2a)J_n(h_1a)J_n'(h_2a) & -\epsilon_2(h_1a)^2(h_2a)J_n(h_1a)N_n'(h_2a) & & \\ -[\epsilon_2(h_2b)J_n'(h_2b)-\frac{(h_2b)^2}{2(n-1)}J_n(h_2b) & -[\epsilon_2(h_2b)N_n'(h_2b)-\frac{(h_2b)^2}{2(n-1)}N_n(h_2b) & -[n\frac{\epsilon_2+1}{2}J_n(h_2b)+(h_2b)J_n'(h_2b) & -[n\frac{\epsilon_2+1}{2}N_n(h_2b)+(h_2b)N_n'(h_2b) \\ +n\frac{(\epsilon_2+1)}{2}J_n(h_2b)] & +n\frac{(\epsilon_2+1)}{2}N_n(h_2b)] & -\frac{(h_2b)^2}{2(n-1)}J_n(h_2b)] & -\frac{(h_2b)^2}{2(n-1)}N_n(h_2b)] \\ n[(h_2a)^2-(h_1a)^2]J_n(h_1a)J_n(h_2a) & n[(h_2a)^2-(h_1a)^2]J_n(h_1a)N_n(h_2a) & (h_1a)(h_2a)^2J_n'(h_1a)J_n(h_2a) & (h_1a)(h_2a)^2J_n'(h_1a)N_n(h_2a) \\ & & -(h_1a)^2(h_2a)J_n(h_1a)J_n'(h_2a) & -(h_1a)^2(h_2a)J_n(h_1a)N_n'(h_2a) \\ J_n(h_2b) & N_n(h_2b) & -J_n(h_2b) & -N_n(h_2b) \end{vmatrix} = 0$$

and the zeros of this determinant are the cutoff wavenumbers for the hybrid modes of the dielectric-filled dielectric tube waveguide for n>1.

In the two preceding cases, the external radial wavenumber was the only wavenumber which was a function of q. If $\epsilon_1 = 1.$, then an internal wavenumber (h_1) is also a function of q indicating the interior medium must also satisfy the cutoff condition. (This situation is not possible in the rod since there is only one dielectric; but for the tube and all other higher ℓ-layer configurations with more than one interface, this condition does arise.) The air-filled dielectric tube configuration is the most simple structure of this type. As in the two preceding examples, $h_3b = q$; but also in this case $h_1a = (a/b)q$. The dispersion relation for the hybrid modes Eq. (II-34) then takes the form

$$
(23)\quad
\begin{vmatrix}
(h_2b)^2 J_n(h_2a)\left\{\frac{(aq/b)J_n'(aq/b)}{J_n(aq/b)}\right\} & (h_2b)^2 N_n(h_2a)\left\{\frac{(aq/b)J_n'(aq/b)}{J_n(aq/b)}\right\} & n(h_2b)^2 J_n(h_2a) & n(h_2b)^2 N_n(h_2a) \\
-\varepsilon_2(h_2a)J_n'(h_2a)q^2 & -\varepsilon_2(h_2a)N_n'(h_2a)q^2 & -n\left(\frac{\varepsilon_2+1}{2}\right)J_n(h_2a)q^2 & -n\left(\frac{\varepsilon_2+1}{2}\right)N_n(h_2a)q^2 \\
(h_2b)^2 J_n(h_2b)\left\{\frac{q\,H_n^{(2)'}(q)}{H_n^{(2)}(q)}\right\} & (h_2b)^2 N_n(h_2b)\left\{\frac{q\,H_n^{(2)'}(q)}{H_n^{(2)}(q)}\right\} & n(h_2b)^2 J_n(h_2b) & n(h_2b)^2 N_n(h_2b) \\
-\varepsilon_2(h_2b)J_n'(h_2b)q^2 & -\varepsilon_2(h_2b)N_n'(h_2b)q^2 & -n\,\frac{(\varepsilon_2+1)}{2}J_n(h_2b)q^2 & -n\,\frac{(\varepsilon_2+1)}{2}N_n(h_2b)q^2 \\
n(h_2b)^2 J_n(h_2a) & n(h_2b)^2 N_n(h_2a) & (h_2b)^2 J_n(h_2a)\left\{\frac{(aq/b)J_n'(aq/b)}{J_n(aq/b)}\right\} & (h_2b)^2 N_n(h_2a)\left\{\frac{(aq/b)J_n'(aq/b)}{J_n(aq/b)}\right\} \\
-n\left(\frac{\varepsilon_2+1}{2}\right)J_n(h_2a)q^2 & -n\left(\frac{\varepsilon_2+1}{2}\right)N_n(h_2a)q^2 & -(h_2a)J_n'(h_2a)q^2 & -(h_2a)N_n'(h_2a)q^2 \\
n(h_2b)^2 J_n(h_2b) & n(h_2b)N_n(h_2b) & (h_2b)^2 J_n(h_2b)\left\{\frac{qH_n^{(2)'}(q)}{H_n^{(2)}(q)}\right\} & (h_2b)^2 N_n(h_2b)\left\{\frac{qH_n^{(2)'}(q)}{H_n^{(2)}(q)}\right\} \\
-n\,\frac{(\varepsilon_2+1)}{2}J_n(h_2b)q^2 & -n\,\frac{(\varepsilon_2+1)}{2}N_n(h_2b)q^2 & -(h_2b)J_n'(h_2b)q^2 & -(h_2b)N_n'(h_2b)q^2
\end{vmatrix} = 0
$$

In addition to the expressions given in Eq. (18) for $\left\{ q\,\frac{H_n^{(2)'}(q)}{H_n^{(2)}(q)} \right\}$ terms in the second and fourth rows, the expansion of $\left\{\frac{(a/b)q\,J_n'(aq/b)}{J_n(aq/b)}\right\}$ appearing in the first and third rows of the determinant in Eq. (23) is given by:

$$
(24)\quad \left\{\frac{(a/b)q\,J_n'(aq/b)}{J_n(aq/b)}\right\} \sim n - \frac{(a/b)^2 q^2}{2(n+1)} - \frac{(a/b)^4 q^4}{8(n+1)^2(n+2)} - \cdots .
$$

Substituting the appropriate expansions involving q into the determinantal Eq. (23), the expressions for the hybrid modes are given in Eqs. (25) and (26). The determinants in these two expressions are slightly more complicated, but the procedure for obtaining the cutoff relation is similar to that described above. Add row 4 to row 2 of the determinant in Eq. (25) and factor $q^2 \ell nq$ from the resulting second row. Subtract row 3 from row 1 obtaining a new row 1 having a common q^2 factor which is then factored. If the remaining terms of order

for n=1

$$
\begin{vmatrix}
(h_{2b})^2 J_1(h_{2a}) & (h_{2b})^2 N_1(h_{2a}) & (h_{2b})^2 J_1(h_{2a}) & (h_{2b})^2 N_1(h_{2a}) \\
-\left[\frac{(h_{2a})^2}{4} J_1(h_{2a}) + \epsilon_2 (h_{2a}) J_1'(h_{2a})\right] q^2 & -\left[\frac{(h_{2a})^2}{4} N_1(h_{2a}) + \epsilon_2 (h_{2a}) N_1'(h_{2a})\right] q^2 & -\left(\frac{\epsilon_2+1}{2}\right) J_1(h_{2a}) q^2 & -\left(\frac{\epsilon_2+1}{2}\right) N_1(h_{2a}) q^2 \\
-(h_{2b})^2 J_1(h_{2b}) - q_2 \ln q (h_{2b})^2 J_1(h_{2b}) & -(h_{2b})^2 N_1(h_{2b}) - (h_{2b})^2 N_1(h_{2b}) q^2 \ln q & (h_{2b})^2 J_1(h_{2b}) & (h_{2b})^2 N_1(h_{2b}) \\
-\left[\epsilon_2 (h_{2b}) J_1'(h_{2b}) + \alpha (h_{2b})^2 J_1(h_{2b})\right] q^2 & -\left[\epsilon_2 (h_{2b}) N_1'(h_{2b}) + \alpha (h_{2b})^2 N_1(h_{2b})\right] q^2 & -\frac{(\epsilon_2+1)}{2} J_1(h_{2b}) q^2 & -\frac{(\epsilon_2+1)}{2} N_1(h_{2b}) q^2 \\
(h_{2b})^2 J_1(h_{2a}) & (h_{2b})^2 N_1(h_{2a}) & (h_{2b})^2 J_1(h_{2a}) & (h_{2b})^2 N_1(h_{2a}) \\
-\left(\frac{\epsilon_2+1}{2}\right) J_1(h_{2a}) q^2 & -\left(\frac{\epsilon_2+1}{2}\right) N_1(h_{2a}) q^2 & -\left[\frac{(h_{2a})^2}{4} J_1(h_{2a}) + (h_{2a}) J_1'(h_{2a})\right] q^2 & -\left[\frac{(h_{2a})^2}{4} N_1(h_{2a}) + (h_{2a}) N_1'(h_{2a})\right] q^2 \\
(h_{2b})^2 J_1(h_{2b}) & (h_{2b}) N_1(h_{2b}) & (h_{2b})^2 J_1(h_{2b}) - (h_{2b})^2 J_1(h_{2b}) q^2 \ln q & -(h_{2b})^2 N_1(h_{2b}) - (h_{2b})^2 N_1(h_{2b}) q^2 \ln q \\
-\frac{(\epsilon_2+1)}{2} J_1(h_{2b}) q^2 & -\frac{(\epsilon_2+1)}{2} N_1(h_{2b}) q^2 & -\left[(h_{2b}) J_1'(h_{2b}) + \alpha (h_{2b})^2 J_1(h_{2b})\right] q^2 & -\left[(h_{2b}) N_1'(h_{2b}) + \alpha (h_{2b})^2 N_1(h_{2b})\right] q^2
\end{vmatrix} = 0 \qquad (25)
$$

and for $n>1$

$$
(26)\quad
\begin{vmatrix}
n(h_{2b})^2 J_n(h_{2a}) & n(h_{2b})^2 N_n(h_{2a}) & n(h_{2b})^2 J_n(h_{2a}) & n(h_{2b})^2 N_n(h_{2a}) \\
-\left[\frac{(h_{2a})^2}{2(n+1)} J_n(h_{2a}) + \epsilon_2 (h_{2a}) J_n'(h_{2a})\right] q^2 & -\left[\frac{(h_{2a})^2}{2(n+1)} N_n(h_{2a}) + \epsilon_2 (h_{2a}) N_n'(h_{2a})\right] q^2 & -n\left(\frac{\epsilon_2+1}{2}\right) J_n(h_{2a}) q^2 & -n\left(\frac{\epsilon_2+1}{2}\right) N_n(h_{2a}) q^2 \\
-n(h_{2b})^2 J_n(h_{2b}) & -n(h_{2b})^2 N_n(h_{2b}) & n(h_{2b})^2 J_n(h_{2b}) & n(h_{2b})^2 N_n(h_{2b}) \\
-\left[\epsilon_2 (h_{2b}) J_n'(h_{2b}) - \frac{(h_{2b})^2}{2(n-1)} J_n(h_{2b})\right] q^2 & -\left[\epsilon_2 (h_{2b}) N_n'(h_{2b}) - \frac{(h_{2b})^2}{2(n-1)} N_n(h_{2b})\right] q^2 & -n\frac{(\epsilon_2+1)}{2} J_n(h_{2b}) q^2 & -n\frac{(\epsilon_2+1)}{2} N_n(h_{2b}) q^2 \\
n(h_{2b})^2 J_n(h_{2a}) & n(h_{2b})^2 N_n(h_{2a}) & n(h_{2b})^2 J_n(h_{2a}) & n(h_{2b})^2 N_n(h_{2a}) \\
-n\left(\frac{\epsilon_2+1}{2}\right) J_n(h_{2a}) q^2 & -n\left(\frac{\epsilon_2+1}{2}\right) N_n(h_{2a}) q^2 & -\left[\frac{(h_{2a})^2}{2(n+1)} J_n(h_{2a}) + (h_{2a}) J_n'(h_{2a})\right] q^2 & -\left[\frac{(h_{2a})^2}{2(n+1)} N_n(h_{2a}) + (h_{2a}) N_n'(h_{2a})\right] q^2 \\
n(h_{2b})^2 J_n(h_{2b}) & n(h_{2b}) N_n(h_{2b}) & -n(h_{2b})^2 J_n(h_{2b}) & -n(h_{2b})^2 N_n(h_{2b}) \\
-n\frac{(\epsilon_2+1)}{2} J_n(h_{2b}) q^2 & -n\frac{(\epsilon_2+1)}{2} N_n(h_{2b}) q^2 & -\left[(h_{2b}) J_n'(h_{2b}) - \frac{(h_{2b})^2}{2(n-1)} J_n(h_{2b})\right] q^2 & -\left[(h_{2b}) N_n'(h_{2b}) - \frac{(h_{2b})^2}{2(n-1)} N_n(h_{2b})\right] q^2
\end{vmatrix} = 0.
$$

greater than $q^{(o)}$ are suppressed, the resulting determinant is not identically zero. Thus, the $q^2(q^2 \ell nq)$ term is the lowest order with a nonvanishing coefficient. The final expression is given in Eq. (27). The zeros of the determinant in Eq. (27) produce the cutoff wavenumbers for the n=1 hybrid modes for an air-filled dielectric tube.

In the determinant of Eq. (26), add row 4 to row 2 and from the new row 2 factor q^2. Subtract row 3 from row 1, and from the new row 1 factor out another q^2. Suppression of higher q terms reduces the determinant to the coefficient of the q^4 term which is not identically vanishing. The resulting determinantal expression is given in Eq. (28). This is the determinant whose zeros define the cutoff wavenumbers for the n>1 hybrid modes of an air-filled dielectric tube waveguide.

The procedure illustrated above with only slight modification can be used for any mode of an ℓ-layer coaxial type dielectric waveguide. As shown in the preceding examples, the first step is to obtain the dispersion determinant which, for the configurations involved in this report, are given in Appendix II. Substitution of the appropriate expansions in terms of the variable q, which is introduced by the exterior (and interior, if applicable) cutoff condition, is performed. Any common row or column q-term is factored from the determinant after the required row-column operations are performed. After the lowest order q-term is removed from the determinant, the q-terms of higher order than $q^{(o)}$ in all the elements of the determinant are suppressed; and the coefficient of the lowest order q-term is

for n=1

(27)

$$q^2(q^2 1nq)\begin{vmatrix} -\left[\frac{(h_2a)^2}{4}J_1(h_2a)+\varepsilon_2(h_2a)J_1'(h_2a) & -\left[\frac{(h_2a)^2}{4}N_1(h_2a)+\varepsilon_2(h_2a)N_1'(h_2a) & -\left[\left(\frac{\varepsilon_2+1}{2}\right)J_1(h_2a)-\frac{(h_2a)^2}{4}J_1(h_2a) & -\left[\left(\frac{\varepsilon_2+1}{2}\right)N_1(h_2a)-\frac{(h_2a)^2}{4}N_1(h_2a)\right. \\ \quad -\left(\frac{\varepsilon_2+1}{2}\right)J_1(h_2a)\right] & \quad -\left(\frac{\varepsilon_2+1}{2}\right)N_1(h_2a)\right] & \quad -(h_2a)J_1'(h_2a)\right] & \quad \left.-(h_2a)N_1'(h_2a)\right] \\ -(h_2b)^2J_1(h_2b) & -(h_2b)^2N_1(h_2b) & -(h_2b)^2J_1(h_2b) & -(h_2b)^2N_1(h_2b) \\ (h_2b)^2J_1(h_2a) & (h_2b)^2N_1(h_2a) & [(h_2b)^2J_1(h_2a)-(h_2a)J_1'(h_2a)] & [(h_2b)^2N_1(h_2a)-(h_2a)N_n'(h_2a)] \\ (h_2b)^2J_1(h_2b) & (h_2b)N_1(h_2b) & -(h_2b)^2J_1(h_2b) & -(h_2b)^2N_1(h_2b) \end{vmatrix}=0$$

for n>1

(28)

$$q^4\begin{vmatrix} -\left[\frac{(h_2a)^2}{2(n+1)}J_n(h_2a)+\varepsilon_2(h_2a)J_n'(h_2a)\right. & -\left[\frac{(h_2a)^2}{2(n+1)}N_n(h_2a)+\varepsilon_2(h_2a)N_n'(h_2a)\right. & -\left[n\left(\frac{\varepsilon_2+1}{2}\right)J_n(h_2a)-\frac{(h_2a)^2}{2(n+1)}J_n(h_2a)\right. & -\left[n\left(\frac{\varepsilon_2+1}{2}\right)N_n(h_2a)-\frac{(h_2a)^2}{2(n+1)}N_n(h_2a)\right. \\ \quad \left.-n\left(\frac{\varepsilon_2+1}{2}\right)J_n(h_2a)\right] & \quad \left.-n\left(\frac{\varepsilon_2+1}{2}\right)N_n(h_2a)\right] & \quad \left.-(h_2a)J_n'(h_2a)\right] & \quad \left.-(h_2a)N_n'(h_2a)\right] \\ -\left[\varepsilon_2(h_2b)J_n'(h_2b)-\frac{(h_2b)^2}{2(n-1)}J_n(h_2b)\right. & -\left[\varepsilon_2(h_2b)N_n'(h_2b)-\frac{(h_2b)^2}{2(n-1)}N_n(h_2b)\right. & -\left[n\left(\frac{\varepsilon_2+1}{2}\right)J_n(h_2b)+(h_2b)J_n'(h_2b)\right. & -\left[n\left(\frac{\varepsilon_2+1}{2}\right)N_n(h_2b)+(h_2b)N_n'(h_2b)\right. \\ \quad \left.+n\frac{(\varepsilon_2+1)}{2}J_n(h_2b)\right] & \quad \left.+n\frac{\varepsilon_2+1}{2}N_n(h_2b)\right] & \quad \left.-\frac{(h_2b)^2}{2(n-1)}J_n(h_2b)\right] & \quad \left.-\frac{(h_2b)^2}{2(n-1)}N_n(h_2b)\right] \\ n(h_2b)^2J_n(h_2a) & n(h_2b)^2N_n(h_2a) & [n(h_2b)^2J_n(h_2a)-(h_2a)J_n'(h_2a)] & [n(h_2b)^2N_n(h_2a)-(h_2a)N_n'(h_2a)] \\ n(h_2b)^2J_n(h_2b) & n(h_2b)N_n(h_2b) & -n(h_2b)^2J_n(h_2b) & -n(h_2b)^2N_n(h_2b) \end{vmatrix}=0$$

obtained. The zeros of the resulting determinant are the cutoff wavenumbers of the configuration and mode involved. Table 2 summarizes the lowest order q-terms with non-identically vanishing coefficients and the next higher order of q-term which is suppressed for each mode and configuration treated in this report.

To complete the dielectric tube, the resultant cutoff determinants for the E_{om} and H_{om} modes are found from Eqs. (II-23) and (II-27) for the dielectric-filled and air-filled cases.

Dielectric-Filled Tube ($\varepsilon_1 > 1.$)

H_{om} modes:

$$(29)\quad q^{(o)} \begin{vmatrix} (h_2a)\, J_0'(h_1a)J_0(h_2a) - (h_1a)J_0(h_1a)J_0'(h_2a) & (h_2a)J_0'(h_1a)N_0(h_2a) - (h_1a)J_0(h_1a)N_0'(h_2a) \\ J_0(h_2b) & N_0(h_2b) \end{vmatrix} = 0$$

E_{om} modes:

$$(30)\quad q^{(o)} \begin{vmatrix} -\frac{(h_2a)}{2} J_0(h_2a) + J_1(h_2a) & -\frac{h_2a}{2} N_0(h_2a) + N_1(h_2a) \\ J_0(h_2b) & N_0(h_2b) \end{vmatrix} = 0$$

AS AMENDED ($\varepsilon_1 = 1$)

E_{om} ($\varepsilon_1 > 1$) AS AMENDED

SWITCH EQUATIONS

Air-Filled Tube ($\varepsilon_1 = 1.$)

H_{om} modes:

$$(31)\quad q^{(o)} \begin{vmatrix} \varepsilon_1(h_2a)\, J_0'(h_1a)J_0(h_2a) - \varepsilon_2(h_1a)J_0(h_1a)J_0'(h_2a) & \varepsilon_1(h_2a)J_0'(h_1a)N_0(h_2a) - \varepsilon_2(h_1a)J_0(h_1a)N_0'(h_2a) \\ J_0(h_2b) & N_0(h_2b) \end{vmatrix} = 0$$

E_{om} modes:

$$(32)\quad q^{(o)} \begin{vmatrix} -\varepsilon_1 \frac{(h_2a)}{2} J_0(h_2a) + \varepsilon_2 J_1(h_2a) & -\varepsilon_1 \left(\frac{h_2a}{2}\right) N_0(h_2a) + \varepsilon_2 N_1(h_2a) \\ J_0(h_2b) & J_0(h_2b) \end{vmatrix} = 0$$

TABLE 2
CUTOFF SUMMARY

modes	Lowest order q-term with nonvanishing coefficient	Order of next higher q-term which must be suppressed
CONFIGURATIONS WITH NO INTERIOR REGION CUTOFF		
E_{om}	$q^{(o)}$	$q^2 \ell nq$
H_{om}	$q^{(o)}$	$q^2 \ell nq$
HE_{1m}	$q^2 \ell nq$	q^2
HE_{nm} $(n>1)$	q^2	q^4
CONFIGURATIONS WITH ONE INTERIOR REGION CUTOFF		
E_{om}	$q^{(o)}$	$q^2 \ell nq$
H_{om}	$q^{(o)}$	$q^2 \ell nq$
HE_{1m}	$q^4 \ell nq$	q^4
HE_{nm} $(n>1)$	q^4	$q^4(q^2 \ell nq)$

The cutoff wavenumbers for the various modes of the coaxial dielectric waveguide configuration can be obtained from the zeros of the cutoff determinants listed in Eqs. (33) to (36) when none of the interior dielectrics have unit relative permittivity. In each case, the lowest order q-term for which the remaining determinant is nonvanishing is indicated.

Coaxial Dielectric Waveguides ($\ell=3$)

$h_4 c = q \to 0$ $\quad \varepsilon_1 \neq 1.$ $\varepsilon_2 \neq 1.$ and $\varepsilon_3 \neq 1.$

H_{om} modes [Eq. (II-42)]:

(33)

$$q(o) \begin{vmatrix} -(h_3b)J_1(h_2b) & -(h_3b)N_1(h_2b) & (h_2b)J_1(h_3b) & (h_2b)N_1(h_3b) \\ -(h_2a)J_1(h_1a)J_o(h_2a) & -(h_2a)J_1(h_1a)N_o(h_2a) & 0 & 0 \\ +(h_1a)J_o(h_1a)J_1(h_2a) & +(h_1a)J_o(h_1a)N_1(h_2a) & & \\ J_o(h_2b) & N_o(h_2b) & -J_o(h_3b) & -N_o(h_3b) \\ 0 & 0 & J_o(h_3c) & N_o(h_3c) \end{vmatrix} = 0$$

E_{om} modes [Eq. (II-38)]:

(34)

$$q(o) \begin{vmatrix} -\varepsilon_1(h_2a)J_1(h_1a)J_o(h_2a) & -\varepsilon_1(h_2a)J_1(h_1a)N_o(h_2a) & 0 & 0 \\ +\varepsilon_2(h_1a)J_o(h_1a)J_1(h_2a) & +\varepsilon_1(h_1a)J_o(h_1a)N_1(h_2a) & & \\ J_o(h_2b) & N_o(h_2b) & -J_o(h_3b) & -N_o(h_3b) \\ -\varepsilon_2(h_3b)J_1(h_2b) & -\varepsilon_2(h_3b)N_1(h_2b) & \varepsilon_3(h_2b)J_1(h_3b) & \varepsilon_3(h_2b)N_1(h_3b) \\ 0 & 0 & J_o(h_3c) & N_o(h_3c) \end{vmatrix} = 0$$

Hybrid modes [HE_{nm} and EH_{nm}, from Eq. (II-49)]:

(35)

$$q^2 \ln q \begin{vmatrix} \text{COLUMN 1} & \text{COLUMN 2} & \text{COLUMN 3} & \text{COLUMN 4} \\ \varepsilon_1(h_1a)(h_2a)^2J_1'(h_1a)J_1(h_2a) & \varepsilon_1(h_1a)(h_2a)^2J_1'(h_1a)N_1(h_2a) & [(h_2a)^2-(h_1a)^2]J_1(h_1a)J_1(h_2a) & [(h_2a)^2-(h_1a)^2]J_1(h_1a)N_1(h_2a) \\ -\varepsilon_2(h_1a)^2(h_2a)J_1(h_1a)J_1'(h_2a) & -\varepsilon_2(h_1a)^2(h_2a)J_1(h_1a)N_1'(h_2a) & & \\ 0 & 0 & 0 & 0 \\ \varepsilon_2(h_2b)(h_3b)^2J_1'(h_2b) & \varepsilon_2(h_2b)(h_3b)^2N_1'(h_2b) & (h_3b)^2J_1(h_2b) & (h_3b)^2N_n(h_2b) \\ J_1(h_2b) & N_1(h_2b), & 0 & 0 \\ 0 & 0 & J_1(h_2b) & N_1(h_2b) \\ (h_3b)^2J_1(h_2b) & (h_3b)^2N_1(h_2b) & (h_2b)(h_3b)^2J_1'(h_2b) & (h_2b)(h_3b)^2N_1'(h_2b) \\ [(h_2a)^2-(h_1a)^2]J_1(h_1a)J_1(h_2a) & [(h_2a)^2-(h_1a)^2]J_1(h_1a)N_1(h_2a) & (h_1a)(h_2a)^2J_1'(h_1a)J_1(h_2a) & (h_1a)(h_2a)^2J_1'(h_1a)N_1(h_2a) \\ & & -(h_1a)^2(h_2a)J_1(h_1a)J_1'(h_2a) & -(h_1a)^2(h_2a)J_1(h_1a)N_1'(h_2a) \\ 0 & 0 & 0 & 0 \end{vmatrix}$$

$$\begin{vmatrix} \text{COLUMN 5} & \text{COLUMN 6} & \text{COLUMN 7} & \text{COLUMN 8} \\ 0 & 0 & 0 & 0 \\ -(h_3c)^2J_1(h_3c) & -(h_3c)^2N_1(h_3c) & -(h_3c)^2J_1(h_3c) & -(h_3c)^2N_1(h_3c) \\ -\varepsilon_3(h_2b)^2(h_3b)J_1'(h_3b) & -\varepsilon_3(h_2b)^2(h_3b)N_1'(h_3b) & -(h_2b)^2J_1(h_3b) & -(h_2b)^2N_1(h_3b) \\ -J_1(h_3b) & -N_1(h_3b) & 0 & 0 \\ 0 & 0 & -J_1(h_3b) & -N_1(h_3b) \\ -(h_2b)^2J_1(h_3b) & -(h_2b)^2N_1(h_3b) & -(h_2b)^2(h_3b)J_1'(h_3b) & -(h_2b)^2(h_3b)N_1'(h_3b) \\ 0 & 0 & 0 & 0 \\ (h_3c)^2J_1(h_3c) & (h_3c)^2N_1(h_3c) & -(h_3c)^2J_1(h_3c) & -(h_3c)^2N_1(h_3c) \end{vmatrix} = 0 \quad \text{for } n=1$$

and

for $n>1$

(36)

$$
q^2
\begin{vmatrix}
\text{COLUMN 1} & \text{COLUMN 2} & \text{COLUMN 3} & \text{COLUMN 4} \\
\varepsilon_1(h_1a)(h_2a)^2J_n'(h_1a)J_n(h_2a) & \varepsilon_1(h_1a)(h_2a)^2J_n'(h_1a)N_n(h_2a) & n[(h_2a)^2-(h_1a)^2]J_n(h_1a)J_n(h_2a) & n[(h_2a)^2-(h_1a)^2]J_n(h_1a)N_n(h_2a) \\
-\varepsilon_2(h_1a)^2(h_2a)J_n(h_1a)J_n'(h_2a) & -\varepsilon_2(h_1a)^2(h_2a)J_n(h_1a)N_n'(h_2a) & & \\
0 & 0 & 0 & 0 \\
\varepsilon_2(h_2b)(h_3b)^2J_n'(h_2b) & \varepsilon_2(h_2b)(h_3b)^2N_n'(h_2b) & n(h_3b)^2J_n(h_2b) & n(h_3b)^2N_n(h_2b) \\
J_n(h_2b) & N_n(h_2b) & 0 & 0 \\
0 & 0 & J_n(h_2b) & N_n(h_2b) \\
n(h_3b)^2J_n(h_2b) & n(h_3b)^2N_n(h_2b) & (h_2b)(h_3b)^2J_n'(h_2b) & (h_2b)(h_3b)^2N_n'(h_2b) \\
n[(h_2a)^2-(h_1a)^2]J_n(h_1a)J_n(h_2a) & n[(h_2a)^2-(h_1a)^2]J_n(h_1a)N_n(h_2a) & (h_1a)(h_2a)^2J_n'(h_1a)J_n(h_2a) & (h_1a)(h_2a)^2J_n'(h_1a)N_n(h_2a) \\
 & & -(h_1a)^2(h_2a)J_n(h_1a)J_n'(h_2a) & -(h_1a)^2(h_2a)J_n(h_1a)N_n'(h_2a) \\
0 & 0 & 0 & 0
\end{vmatrix}
$$

$$
\begin{vmatrix}
\text{COLUMN 5} & \text{COLUMN 6} & \text{COLUMN 7} & \text{COLUMN 8} \\
0 & 0 & 0 & 0 \\
\left[\frac{(h_3c)^2}{2(n-1)}J_n(h_3c)-\varepsilon_3(h_3c)J_n'(h_3c) & \left[\frac{(h_3c)^2}{2(n-1)}N_n(h_3c)-\varepsilon_3(h_3c)N_n'(h_3c)\right. & \left[-n\left(\frac{\varepsilon_3+1}{2}\right)J_n(h_3c)+\frac{(h_3c)^2}{2(n-1)}J_n(h_3c)\right. & \left[-n\left(\frac{\varepsilon_3+1}{2}\right)N_n(h_3c)+\frac{(h_3c)^2}{2(n-1)}N_n(h_3c)\right. \\
\left.-n\left(\frac{\varepsilon_3+1}{2}\right)J_n(h_3c)\right] & \left.-n\left(\frac{\varepsilon_3+1}{2}\right)N_n(h_3c)\right] & \left.-(h_3c)J_n'(h_3c)\right] & \left.-(h_3c)N_n'(h_3c)\right] \\
-\varepsilon_3(h_2b)^2(h_3b)J_n'(h_3b) & -\varepsilon_3(h_2b)^2(h_3b)N_n'(h_3b) & -n(h_2b)^2J_n(h_3b) & -n(h_2b)^2N_n(h_3b) \\
-J_n(h_3b) & -N_n(h_3b) & 0 & 0 \\
0 & 0 & -J_n(h_3b) & -N_n(h_3b) \\
-n(h_2b)^2J_n(h_3b) & -n(h_2b)^2N_n(h_3b) & -(h_2b)^2(h_3b)J_n'(h_3b) & -(h_2b)^2(h_3b)N_n'(h_3b) \\
0 & 0 & 0 & 0 \\
n(h_3c)^2J_n(h_3c) & n(h_3c)^2N_n(h_3c) & -n(h_3c)^2J_n(h_3c) & -n(h_3c)^2N_n(h_3c)
\end{vmatrix}
=0
$$

The relatively simple case of the dielectric rod waveguide can be solved by this procedure to produce the following determinantal expressions and lowest order q-terms.

Dielectric Rod Waveguide ($\ell=1$)

$h_2 a = q \to 0 \quad \varepsilon_1 \neq 1.$

H_{om} [Eq. (II-12)] and E_{om} [Eq. (II-8)] modes:

$$(37) \quad q^{(o)} \begin{vmatrix} J_o(h_1 a) & 0 \\ 0 & 1 \end{vmatrix} = 0$$

Hybrid modes [HE_{nm} and EH_{nm} from Eq. (II-19)]:

$$(38) \quad q^2 \ell n q \begin{vmatrix} J_1(h_1 a) & J_1(h_1 a) \\ -J_1(h_1 a) & J_1(h_1 a) \end{vmatrix} = 0 \qquad \text{for } n=1$$

and

$$(39) \quad q^2 \begin{vmatrix} \left[(h_1 a)\varepsilon_1 J_n(h_1 a) - \frac{(h_1 a)^2}{2(n-1)} J_n(h_1 a) + n\left(\frac{\varepsilon_1+1}{2}\right) J_n(h_1 a)\right] & \left[n \frac{(\varepsilon_1+1)}{2} J_n(h_1 a) + (h_1 a) J_n'(h_1 a) - \frac{(h_1 a)^2}{2(n-1)} J_n(h_1 a)\right] \\ -J_n(h_1 a) & J_n(h_1 a) \end{vmatrix} = 0 \quad \text{for } n>1.$$

It will be noted that the determinants in Eqs. (37) to (39) are easily expanded to obtain the well known cutoff equations for the rod modes:

H_{om} and E_{om} cutoff equation:

(40) $J_o(h_1 a) = 0$

Hybrid mode cutoff equations (HE_{nm} and EH_{nm}):

(41) $J_1^2(h_1 a) = 0$ for n=1

and

(42) $$J_n(h_1 a)\left[(\varepsilon_2+1)J_{n-1}(h_1 a) - \frac{(h_1 a)J_n(h_1 a)}{(n-1)}\right] = 0 \quad \text{for } n>1,$$

which agree with the expressions derived by S.A. Schelkunoff[2] and S.P. Schlesinger[3] for the dielectric rod waveguide modes.

Expansions of the determinants obtained for the dielectric tube cutoff wavenumbers agree with the expressions obtained by V.H. Unger[5] for the E_{om}, H_{om} and principal hybrid mode HE_{11}. The above is probably the first formulation of the cutoff relation for the n>1 hybrid modes of the dielectric tube.

In his dissertation, R.I. Barnett[6] found equations for calculating the cutoff wavenumbers for the E_{om} and H_{om} modes of the dielectric coaxial configuration. The expressions obtained by expanding the determinants in Eqs. (33) and (34) agree with those given by Barnett. The hybrid mode cutoff relations for the coaxial dielectric waveguide have not been reported elsewhere.

The zeros of the determinants given in any of the above cutoff relations can be found from a simple iterative procedure assuming lossless dielectric media. For a given n, the cutoff

wavenumbers of all m modes can be calculated from the appropriate cutoff determinant. These cutoff wavenumbers are obtained by starting with the wavenumber equal to zero, incrementing by 0.1 and evaluating the determinant until there is a change in sign of the value of the determinant. The sign change indicates a zero of the determinant has been crossed. By decreasing the increment successively by powers of ten as the iteration across the sign change is accomplished, the zero can be determined to any degree of accuracy. The first zero pertains to the m=1 mode. If the same procedure is continued at larger wavenumbers, the subsequently determined zeros will correspond to the m=2,3,··· modes.

The results are shown in Figs. I-32 to I-60 of Appendix I. An examination of the determinants of the hybrid modes for any of the configurations will show that for the principal hybrid mode HE_{11}, the cutoff wavenumber is always zero. It will be noted from the graphs for the dielectric tube that the limiting cutoff wavenumber (as $a/b \to 0$) of the tube is equal to that of the corresponding dielectric rod wavenumber. Likewise, there are two such limiting cases for the graphs of the coaxial dielectric waveguide. As $a/c \to 0$, the limiting value of the cutoff wavenumber is equal to the corresponding dielectric tube value. Also, as ~~(a/b)~~ $(a/c) \to (b/c)$, the limiting case of the coaxial dielectric waveguide is the dielectric rod and again the cutoff wavenumbers concur.

AS AMENDED

CHAPTER III
SUMMARY

The cutoff, dispersion and attenuation characteristics for the lower order modes are presented for the dielectric rod, tube and coaxial waveguides. Based on these data and energy transporting capabilities, the coaxial guide is shown to be suitable for transmission over moderate distances and a set of design criteria has been formulated. An example of a X-band dielectric coaxial configuration is presented and its transmission properties calculated.

The dielectric coaxial waveguide shows certain advantages over the simple dielectric rod waveguide. The design configuration has been constrained such that less than 10% of the energy is transported outside the guide with all energy transport in the dominant mode. The maximum allowable frequency range satisfying this energy criterion for the X-band dielectric coaxial waveguide was shown to be 8.4 GHz to 11.7 GHz. Imposing such energy restrictions on the rod waveguide greatly reduces the allowable operating frequency range. The coaxial waveguide considered also exhibits lower attenuation over the entire operating band. At the center frequency of 10 GHz, the rod waveguide attenuation was larger than the coaxial configuration attenuation by a factor of more than two and a half. The phase was linear over a larger band for the coaxial guide indicating better transmission

of video pulse detail. The pulse dispersion of the coaxial guide is comparable to that of a metal waveguide.

The construction of long lengths of dielectric rod waveguide presents problems which can be easily overcome in the coaxial configuration. Some simple methods of construction of the coaxial guide have been suggested. The coaxial waveguide has the benefit of a thin outer dielectric shell which can be made of a weather resistant (sealer) material. This would greatly reduce the affect of environment on the dielectric properties (especially the loss tangent) of the waveguide.

The physical size of the coaxial guide designed for the X-band region is comparable to that of a metal guide designed for operation with the same central frequency. The operating frequency band of 1.4:1 is also similar, and the attenuation is small enough in this range to make transmission over moderate distances feasible.

APPENDIX I
DISPERSION AND CUTOFF PROPERTIES OF DIELECTRIC COAXIAL CONFIGURATIONS

LIST OF ILLUSTRATIONS

LIST OF ILLUSTRATIONS (Continued)

CUTOFF WAVENUMBER DATA

Dielectric Rod Waveguide

LIST OF ILLUSTRATIONS (Continued)

LIST OF ILLUSTRATIONS (Continued)

The data obtained for the three cylindrical dielectric coaxial-type waveguides (ℓ=1,2 and 3) of circular cross-section are shown in the following figures. Three types of graphs are presented for each configuration; the dispersion and the corresponding attenuation curves (explained in Appendix II) and the cutoff wavenumbers of some of the lower modes (modal cutoff expressions given in Chapter II).

Modal dispersion and attenuation data are presented for the dielectric rod, tube, and coaxial waveguides in Figs. I-1 to I-31. The equation numbers of the appropriate expressions given in Appendix II used to determine the curves are indicated. Data for the rod configuration are shown in Figs. I-1 to I-3 for dielectric rods with relative dielectric constants 2.55, 4 and 9. Air-filled tube configuration data are plotted in Figs. I-4 and I-5 for a tube with relative dielectric constant 2.55. Figures I-6 to I-31 present the data for the coaxial configurations. The inner tubular dielectric region ($a<r<b$) is always made of material with relative dielectric constant 1.03. In each case, the inner dielectric region ($r<a$) and the outer tubular region ($b<r<c$) are made of material with one of the following relative dielectric constants: 2.55, 4, 9 or 90.

The cutoff wavenumber data of the lower modes are shown in Figs. I-32 to I-60 for configurations with various geometrical and dielectric properties. The appropriate cutoff expression from Chapter II is indicated on the figure. Rod data are plotted in Figs. I-32 and I-33. Air-filled tube data are presented in Figs. I-34 to I-41, and data for the coaxial configurations are shown in Figs. I-42 to I-60.

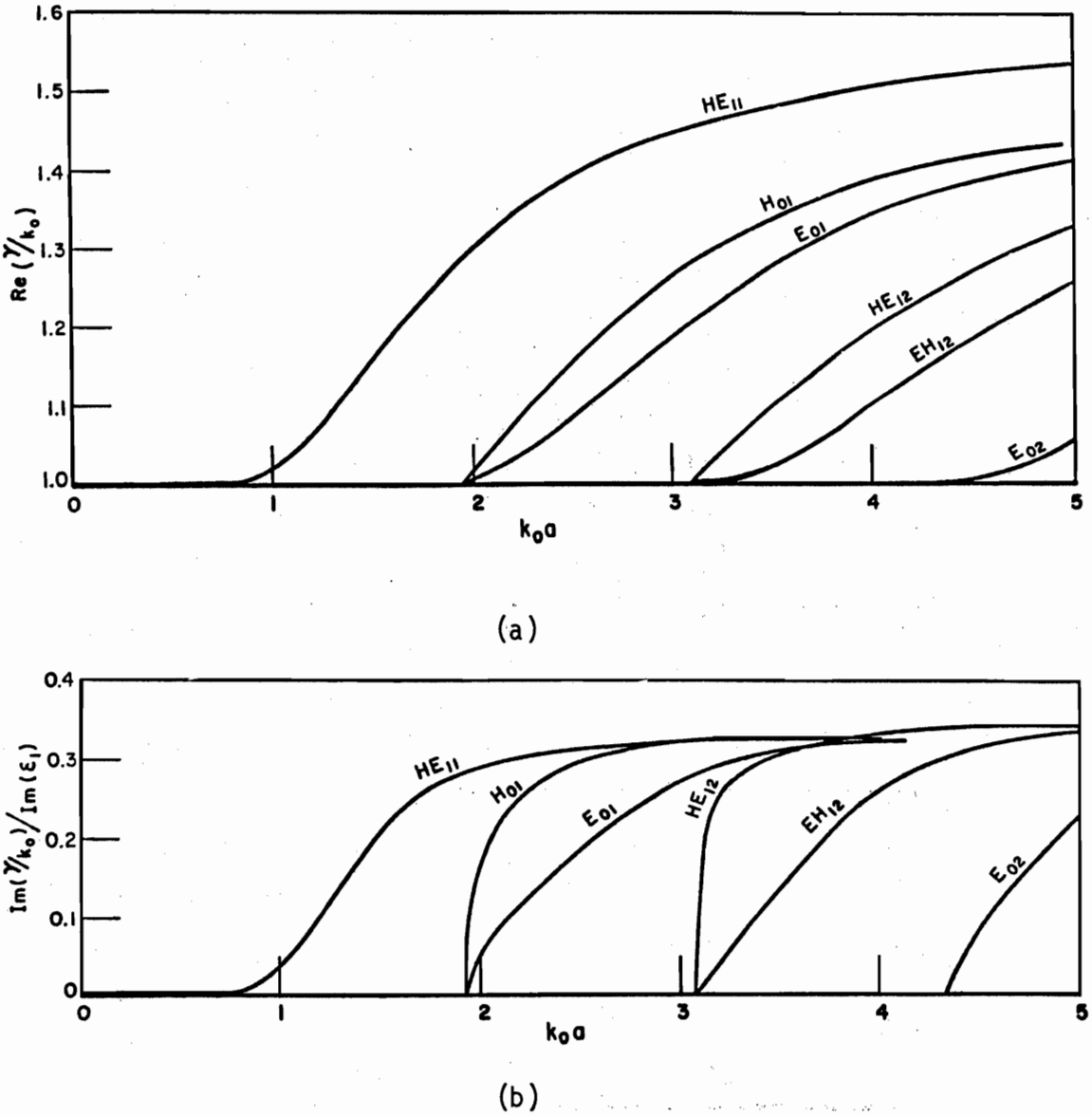

Fig. I-1.--Modal (a) dispersion and (b) attenuation characteristics for dielectric rod waveguide: ϵ_1=2.55 (Eqs. (II-8), (II-12) and (II-19)).

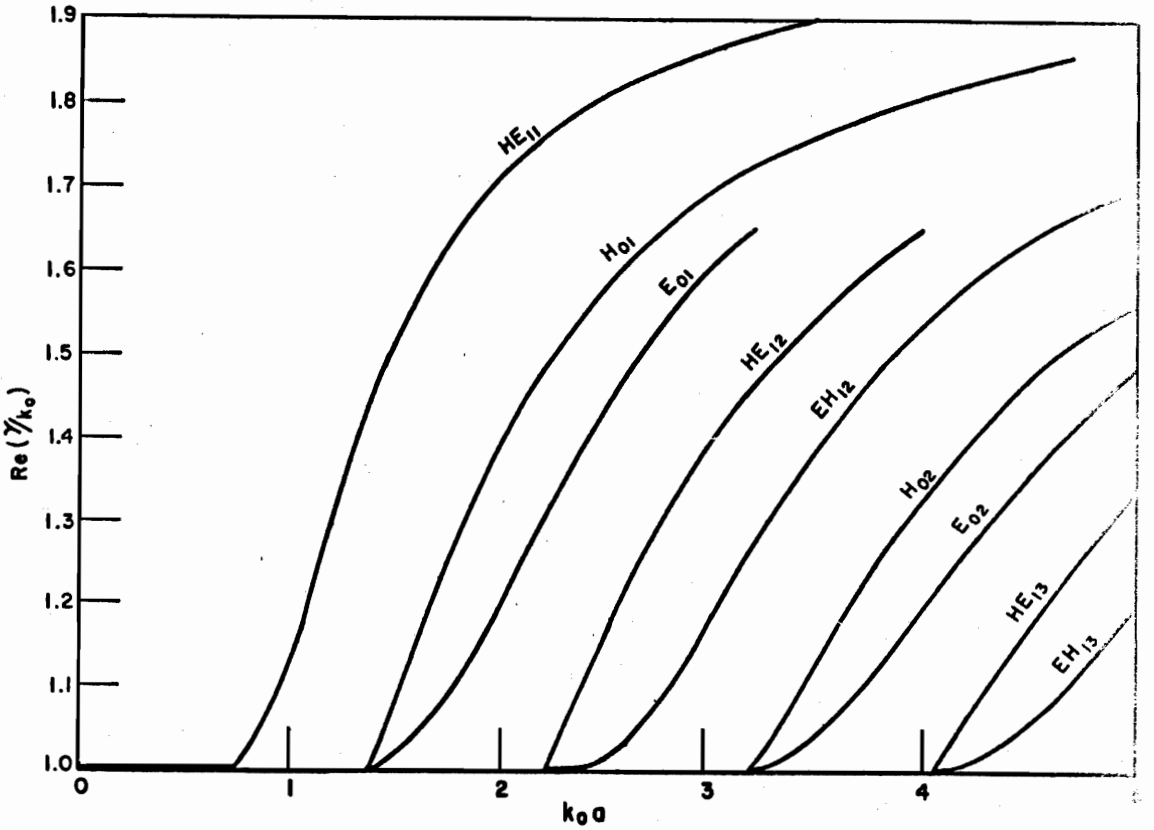

(a)

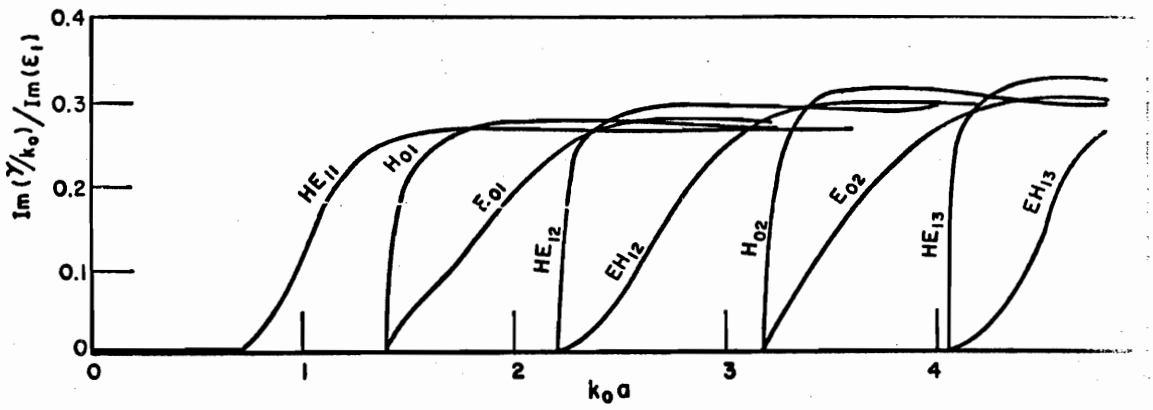

(b)

Fig. I-2.--Modal (a) dispersion and (b) attenuation characteristics for dielectric rod waveguide: ϵ_1=4.0 (Eqs. (II-8), (II-12) and (II-19)).

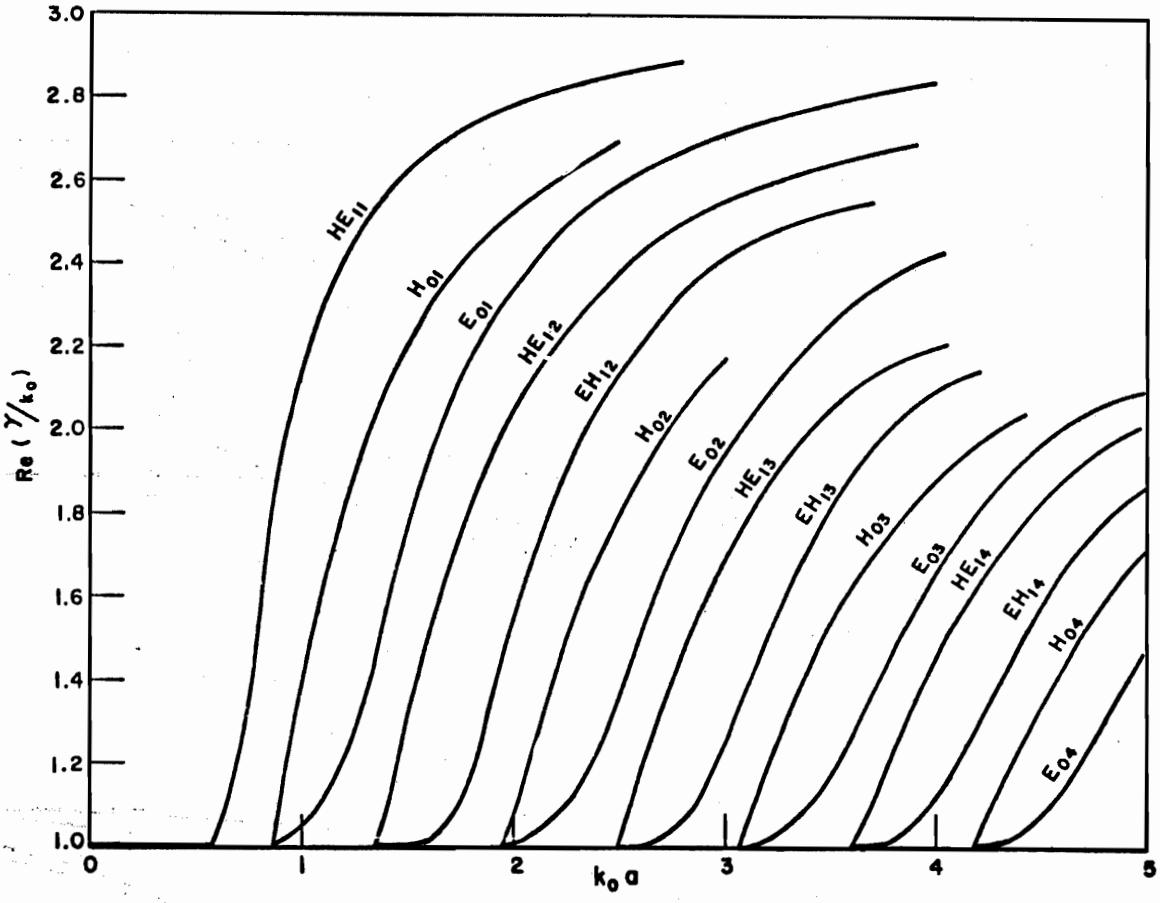

(a)

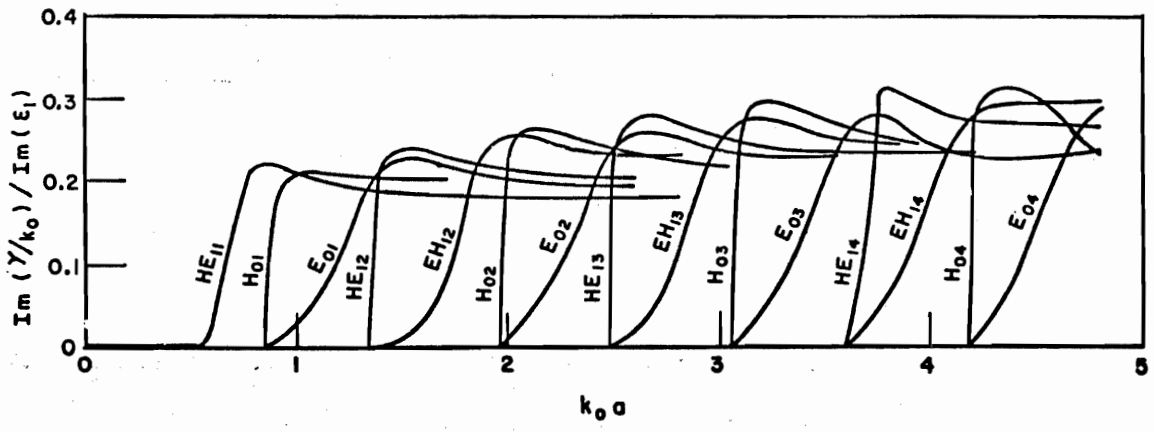

(b)

Fig. I-3.--Modal (a) dispersion and (b) attenuation characteristics for dielectric rod waveguide: ϵ_1=9.0 (Eqs. (II-8), (II-12) and (II-19)).

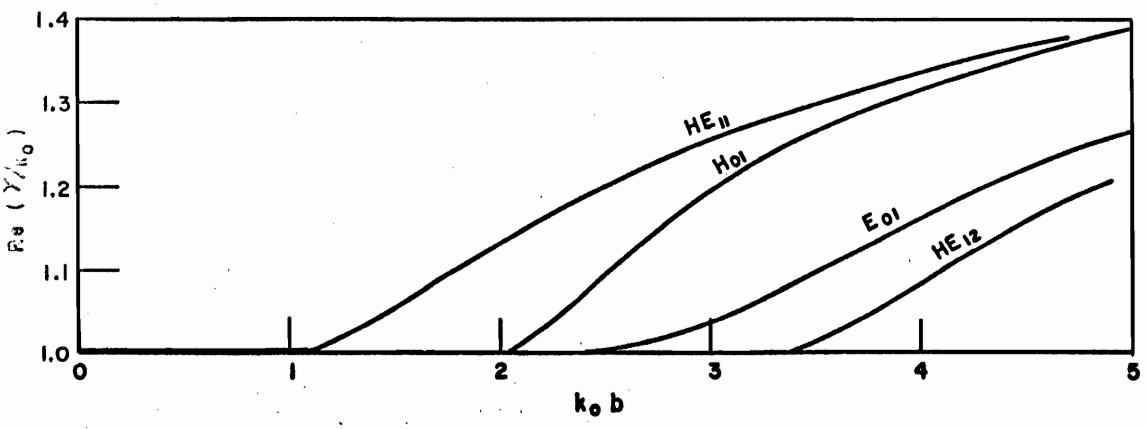

(a)

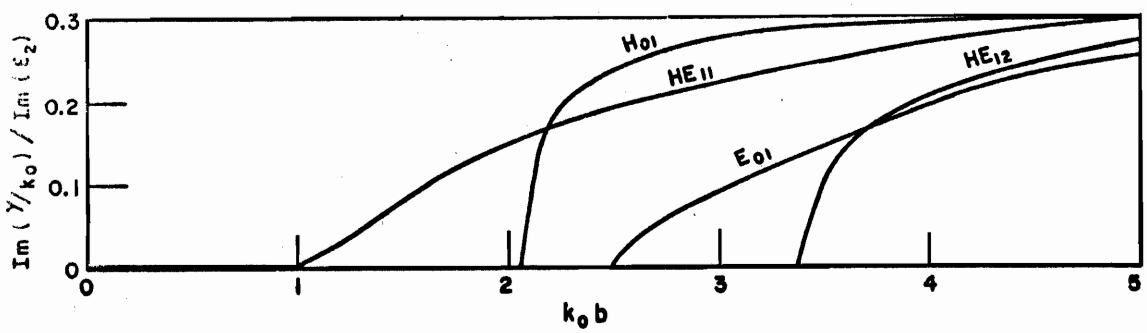

(b)

Fig. I-4.--Modal (a) dispersion and (b) attenuation characteristics for airfilled dielectric tube waveguide: ϵ_1=2.55, a/b=.5 (Eqs. (II-23), (II-27) and (II-34)).

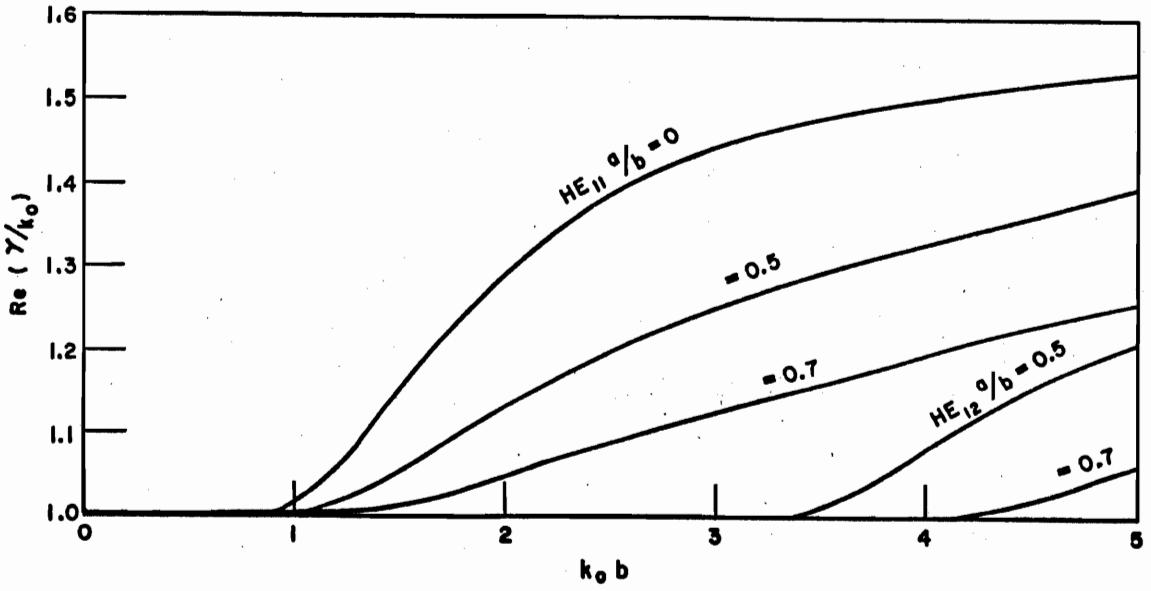

(a)

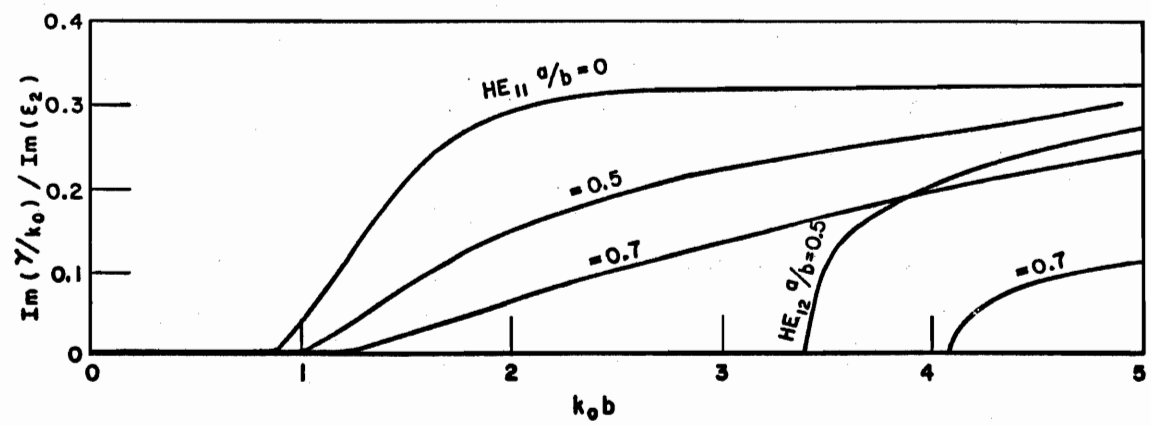

(b)

Fig. I-5.--Modal (a) dispersion and (b) attenuation characteristics for airfilled dielectric tube waveguide: ϵ_2=2.55 (Eq. (II-34)).

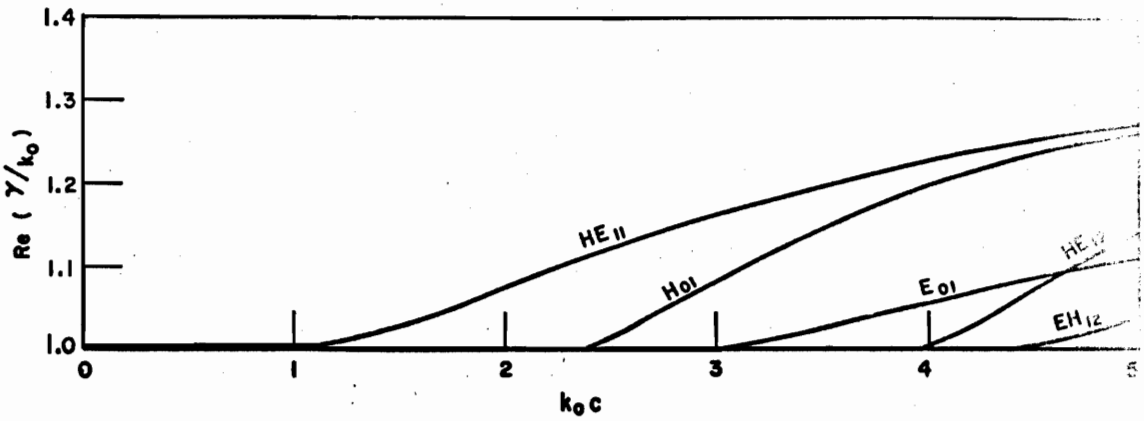

(a)

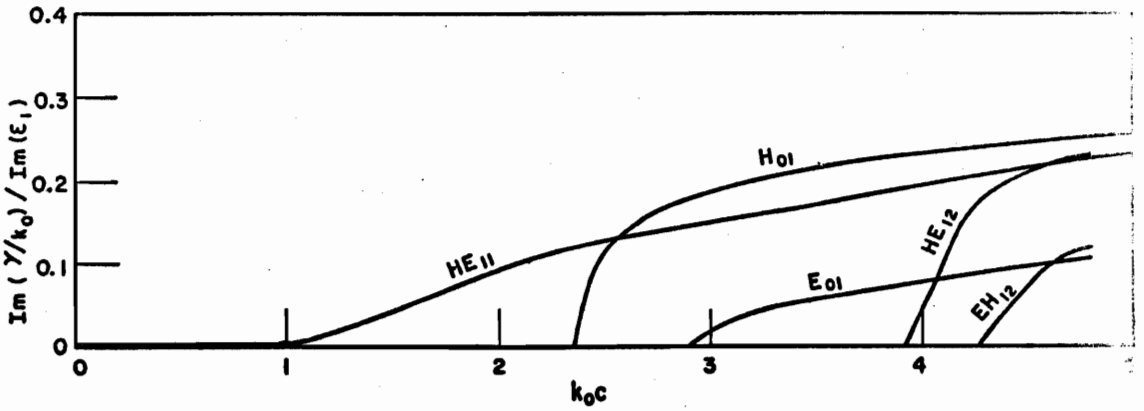

(b)

Fig. I-6.--Modal (a) dispersion and (b) attenuation characteristics for dielectric coaxial waveguide: $\epsilon_1=\epsilon_3=2.55$, $\epsilon_2=1.03$, $a/c=.3$, $b/c=.7$ (Eqs. II-38), (II-42) and (II-49)).

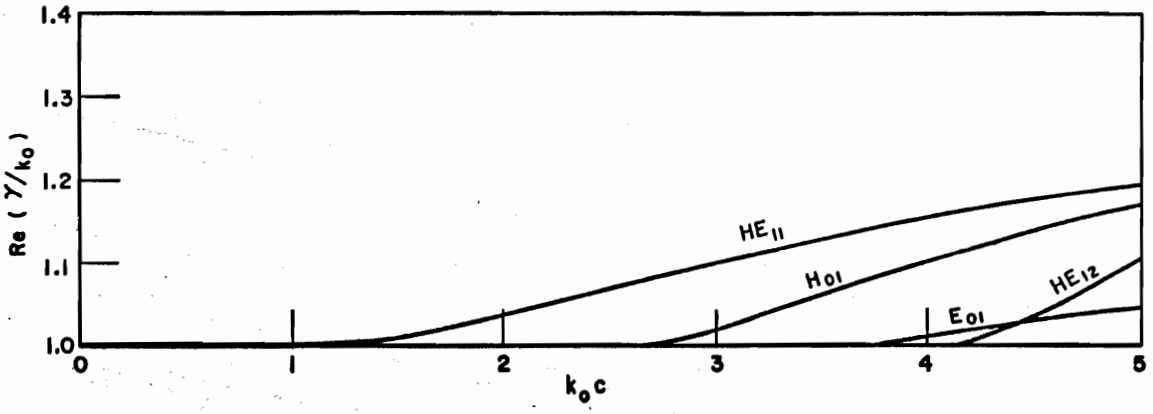

(a)

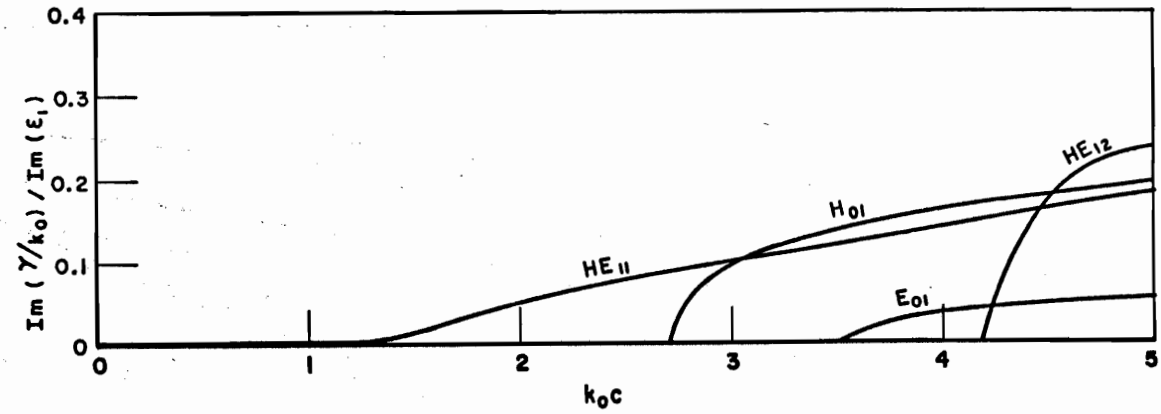

(b)

Fig. I-7.--Modal (a) dispersion and (b) attenuation characteristics for dielectric coaxial waveguide: $\epsilon_1=\epsilon_3=2.55$, $\epsilon_2=1.03$, $a/c=.3$, $b/c=.8$
(Eqs. (II-38), (II-42) and (II-49)).

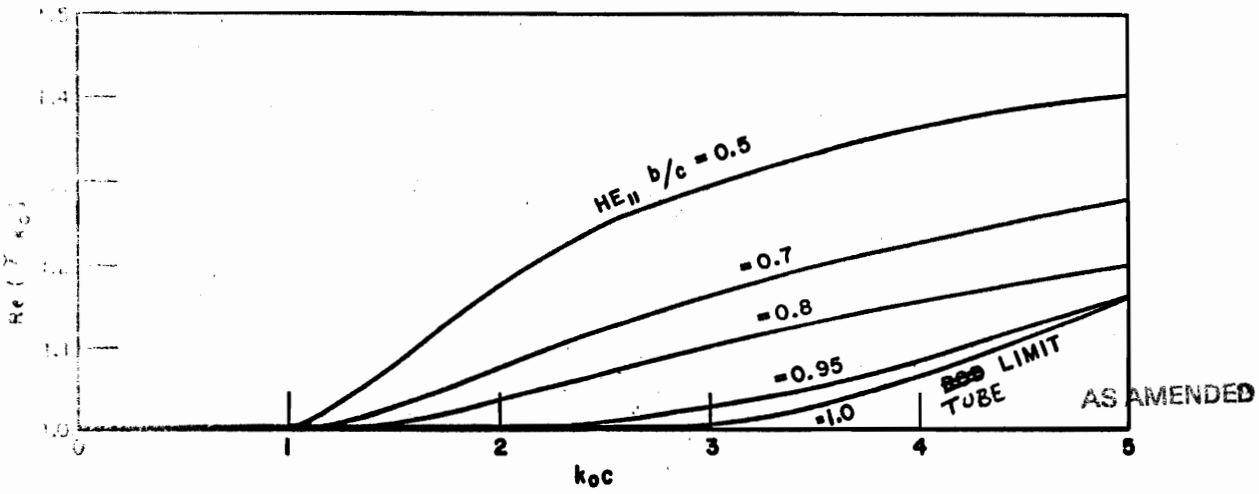

(a)

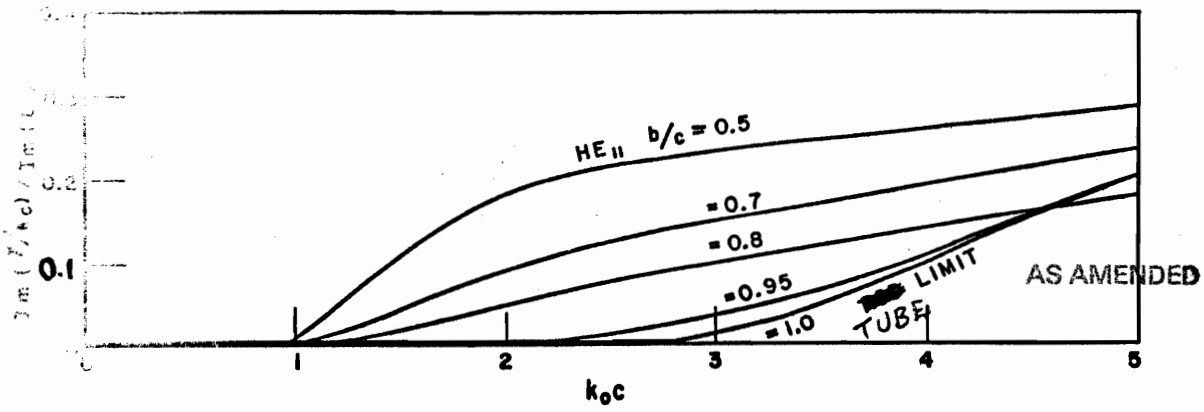

(b)

HE_{11} mode (a) dispersion and (b) attenuation characteristics for dielectric coaxial waveguide: $\epsilon_1 = \epsilon_3 = 2.55$, $\epsilon_2 = 1.03$, $a/c = .3$ (Eq. (II-49)).

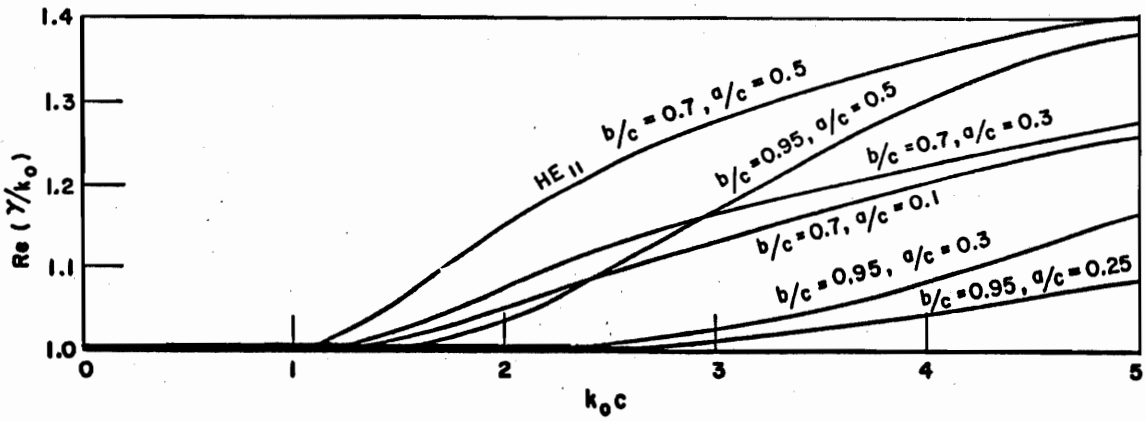

(a)

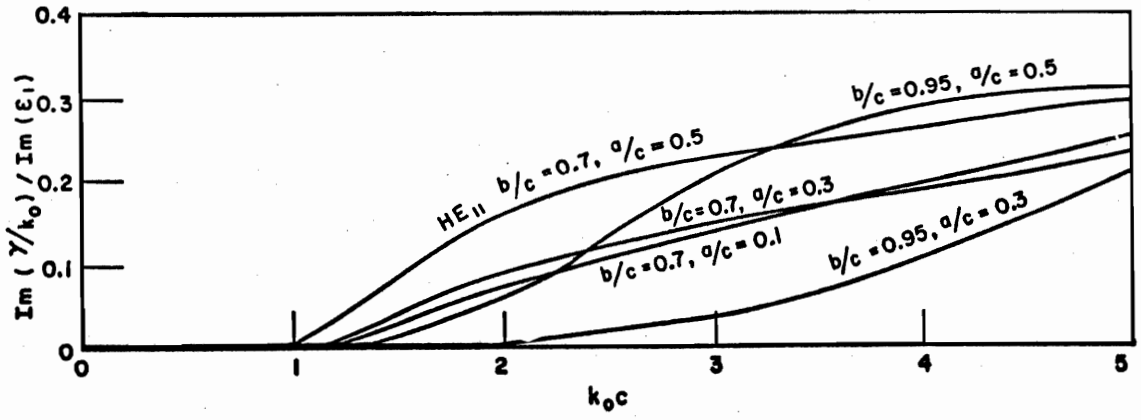

(b)

Fig. I-9.--HE_{11} mode (a) dispersion and (b) attenuation characteristics for dielectric coaxial waveguide: $\epsilon_1=\epsilon_3=2.55$, $\epsilon_2=1.03$ (Eq. (II-49)).

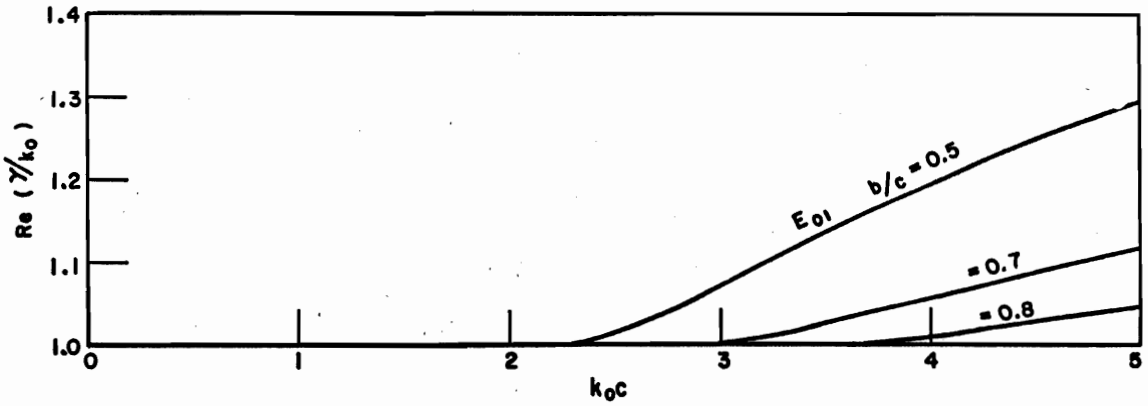

(a)

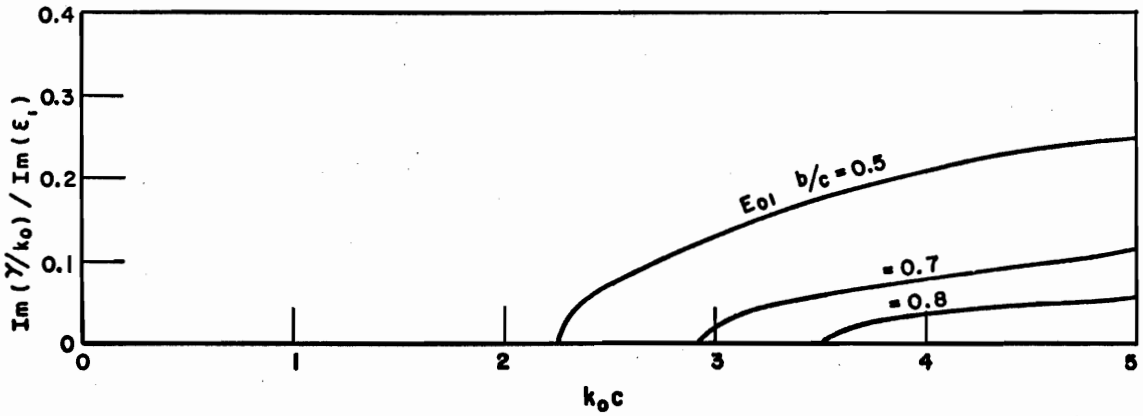

(b)

Fig. I-10.--E_{01} mode (a) dispersion and (b) attenuation characteristics for dielectric coaxial waveguide: $\epsilon_1=\epsilon_3=2.55$, $\epsilon_2=1.03$, a/c=.3 (Eq. (II-38)).

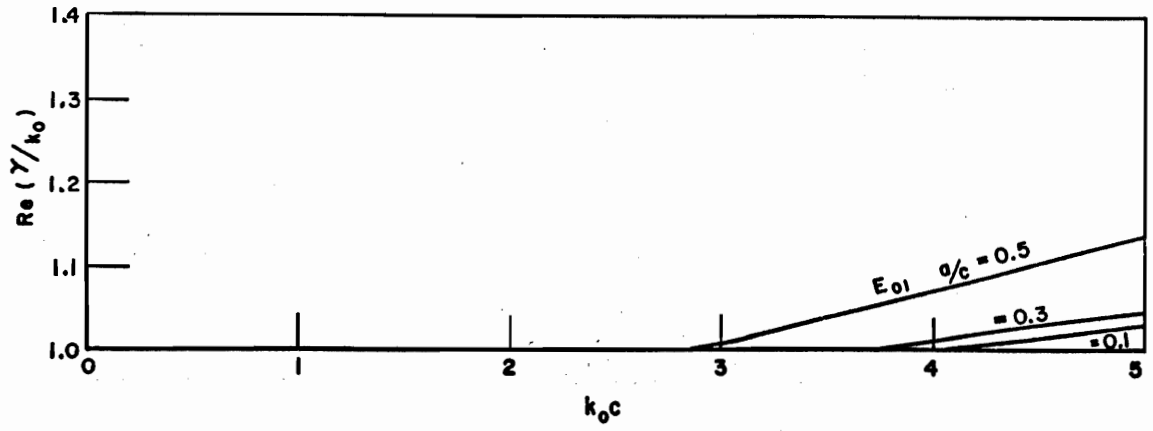

(a)

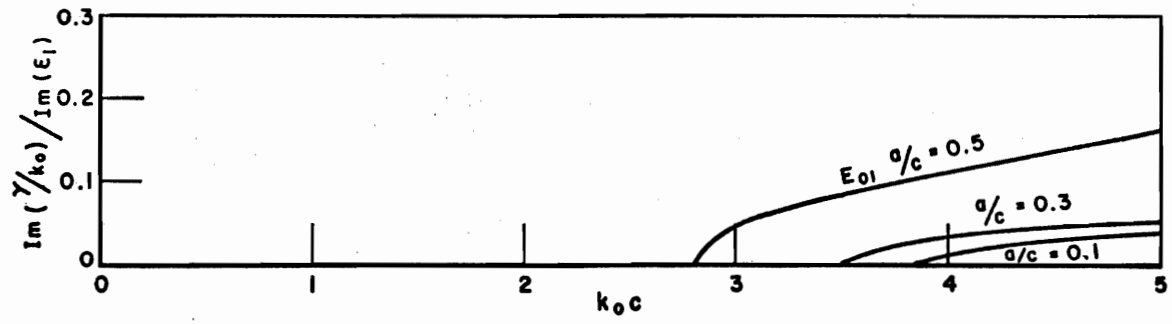

(b)

Fig. I-11.--E_{01} mode (a) dispersion and (b) attenuation characteristics for dielectric coaxial waveguide: $\epsilon_1=\epsilon_3=2.55$, $\epsilon_2=1.03$, b/c=.8 (Eq. (II-38)).

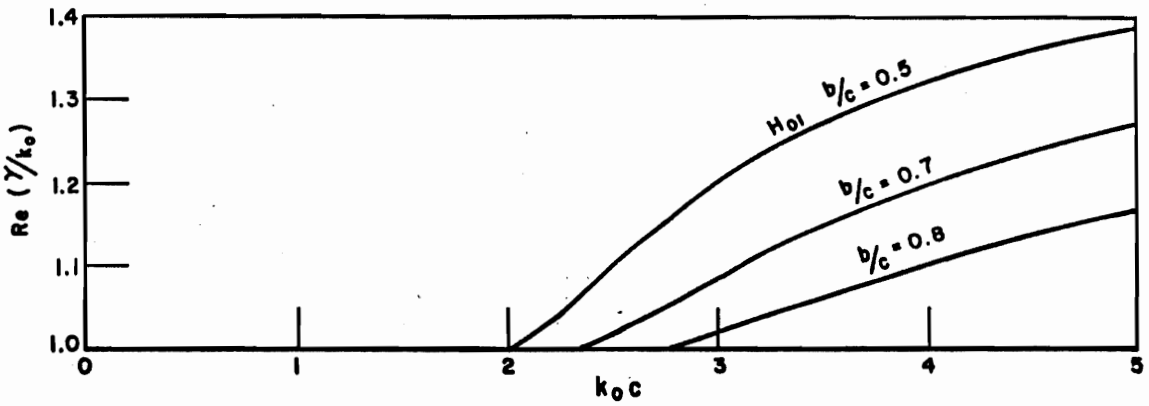

(a)

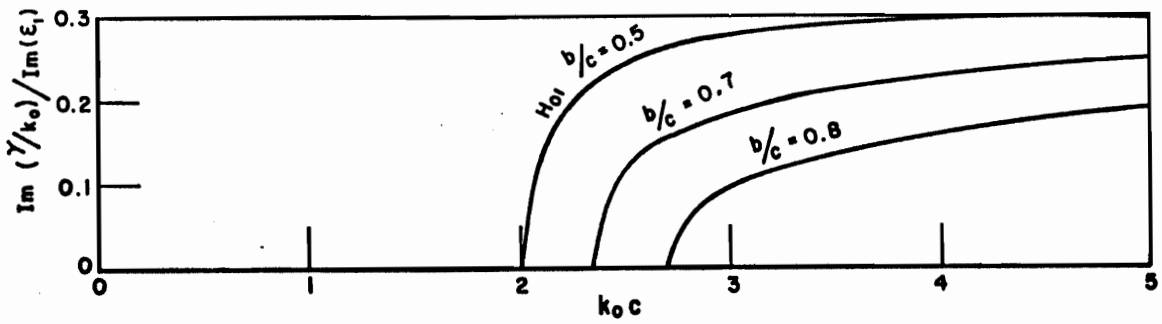

(b)

Fig. I-12.--H_{01} mode (a) dispersion and (b) attenuation characteristics for dielectric coaxial waveguide: $\epsilon_1=\epsilon_3=2.55$, $\epsilon_2=1.03$, a/c=.3 (Eq. (II-42)).

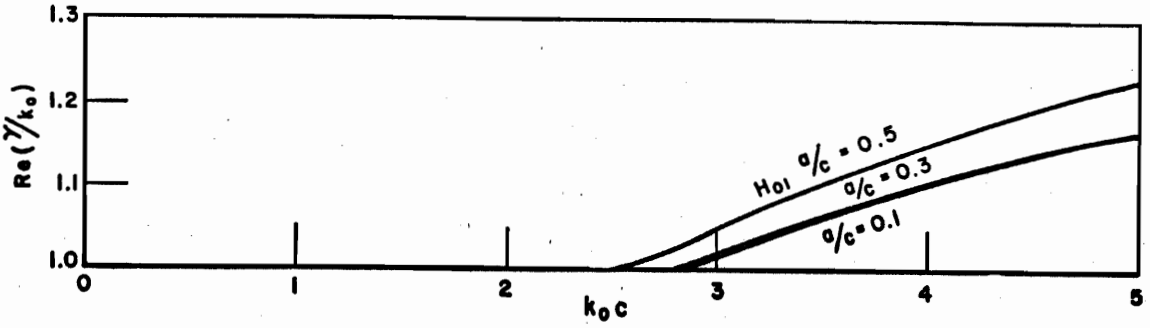

(a)

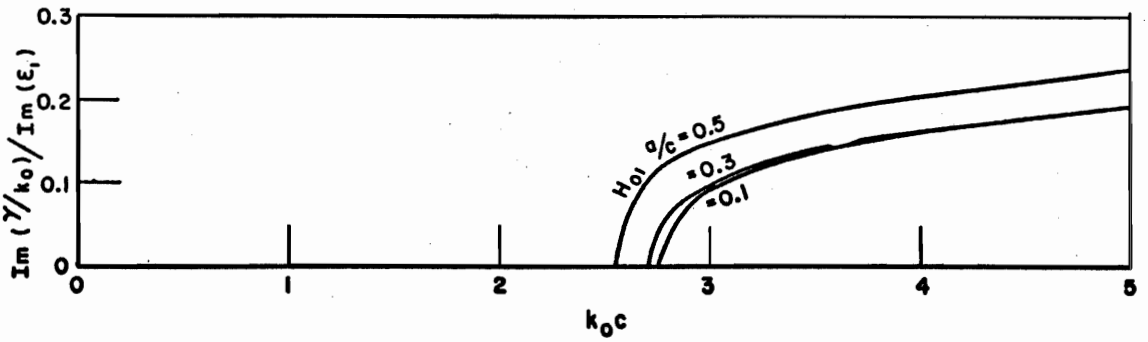

(b)

Fig. I-13.--H_{01} mode (a) dispersion and (b) attenuation characteristics for dielectric coaxial waveguide: $\epsilon_1=\epsilon_3=2.55$, $\epsilon_2=1.03$, b/c=.8 (Eq. (II-42)).

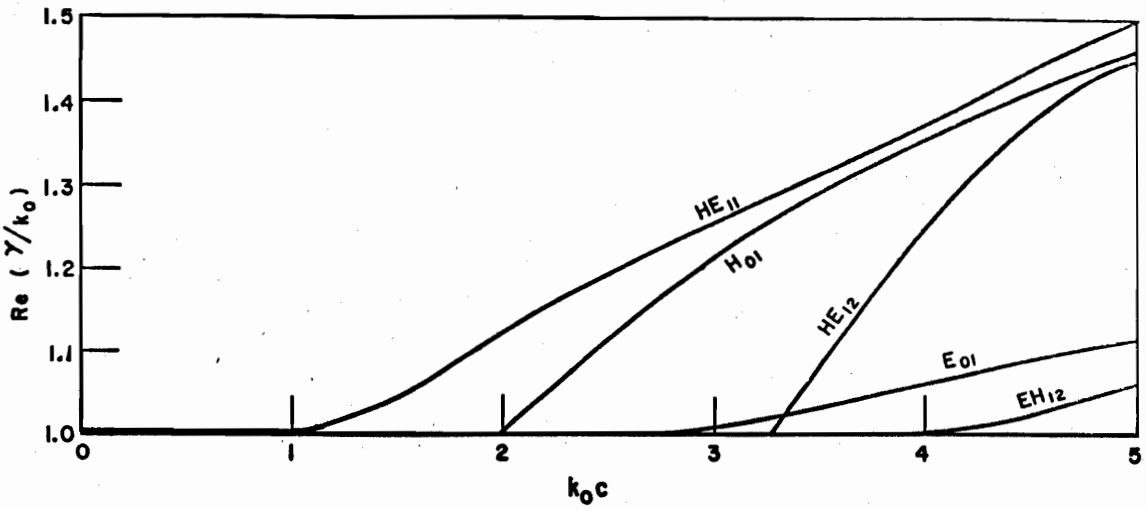

(a)

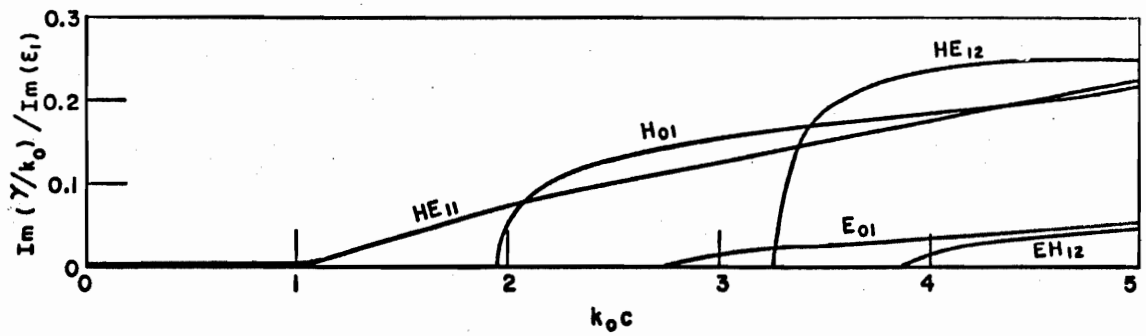

(b)

Fig. I-14.--Modal (a) dispersion and (b) attenuation characteristics for dielectric coaxial waveguide: $\epsilon_1=\epsilon_3=4.0$, $\epsilon_2=1.03$, a/c=.3, b/c=.8 (Eqs. (II-38), (II-42) and (II-49)).

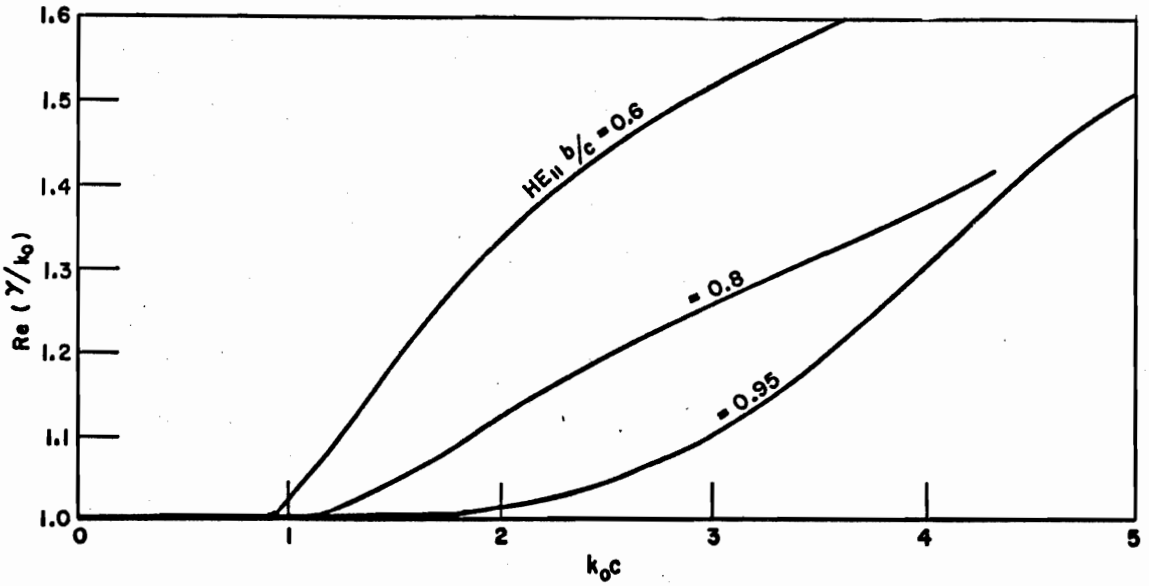

(a)

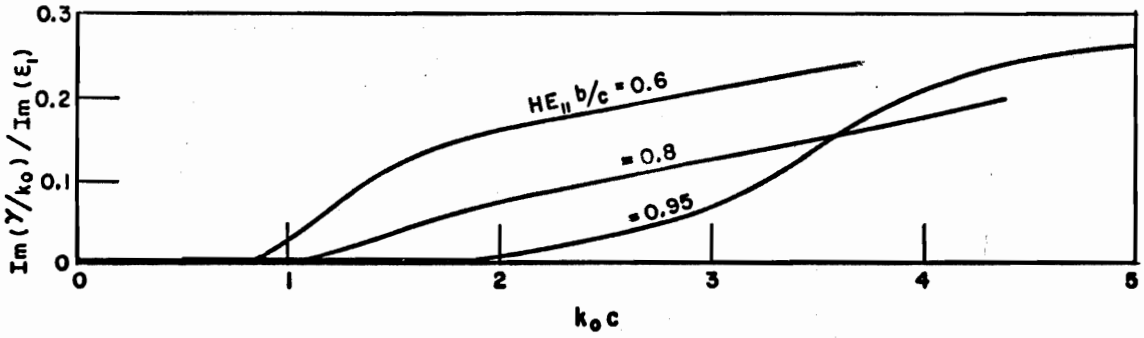

(b)

Fig. I-15.--HE_{11} mode (a) dispersion and (b) attenuation characteristics for dielectric coaxial waveguide: $\epsilon_1 = \epsilon_3 = 4.0$, $\epsilon_2 = 1.03$, a/c=.3 (Eq. (II-49)).

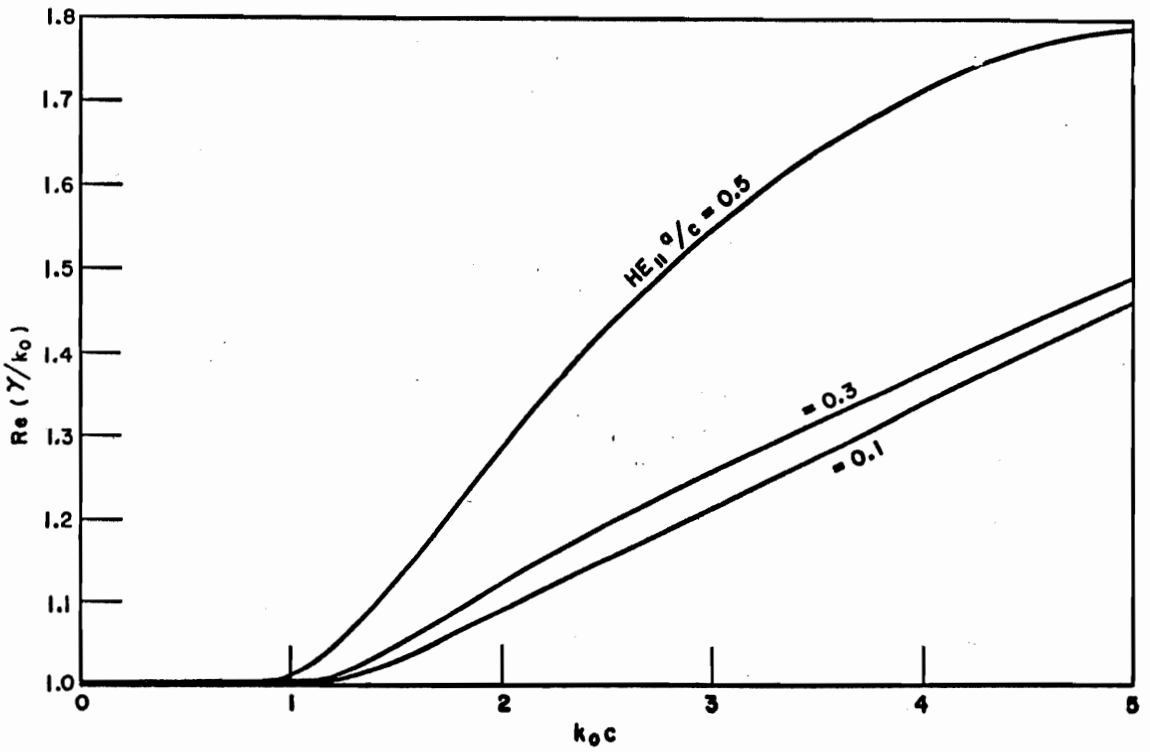

(a)

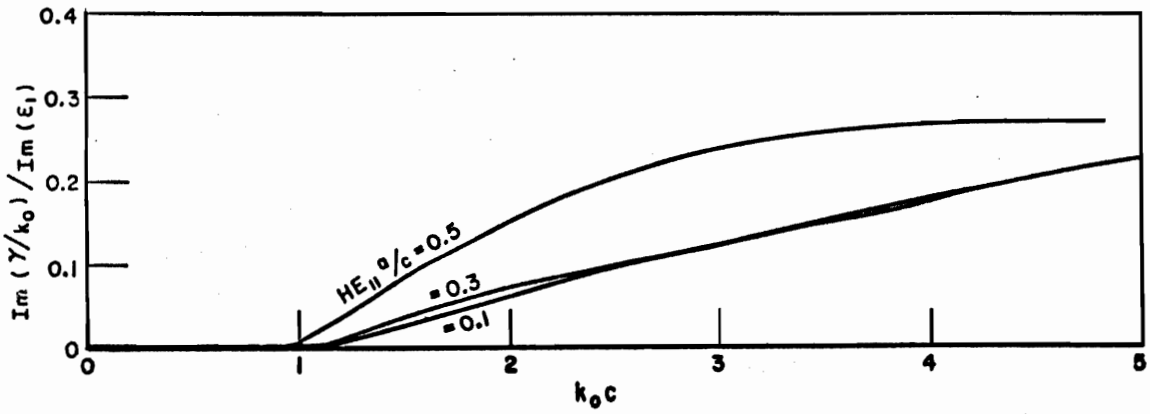

(b)

Fig. I-16.--HE_{11} mode (a) dispersion and (b) attenuation characteristics for dielectric coaxial waveguide: $\epsilon_1=\epsilon_3=4.0$, $\epsilon_2=1.03$, b/c=.8 (Eq. (II-49)).

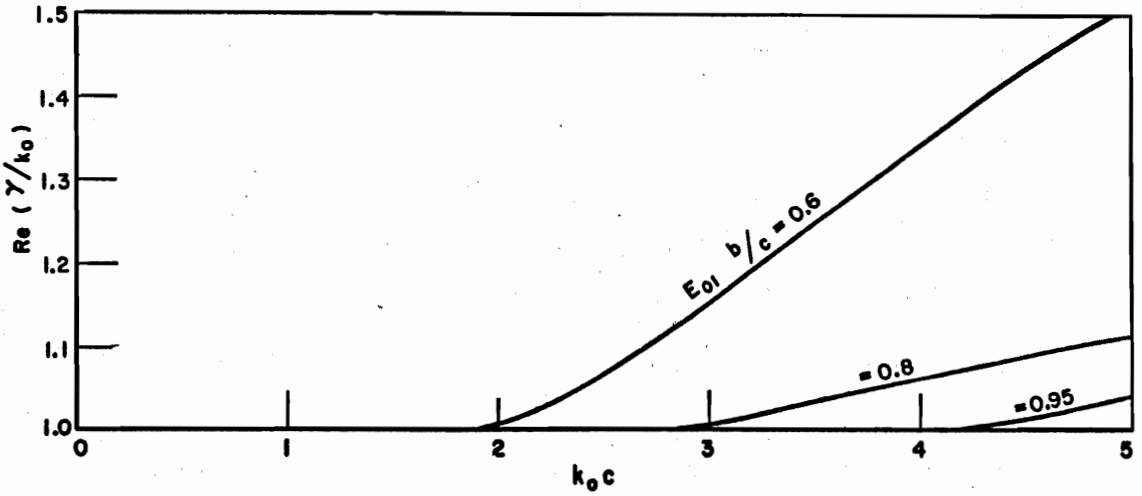

(a)

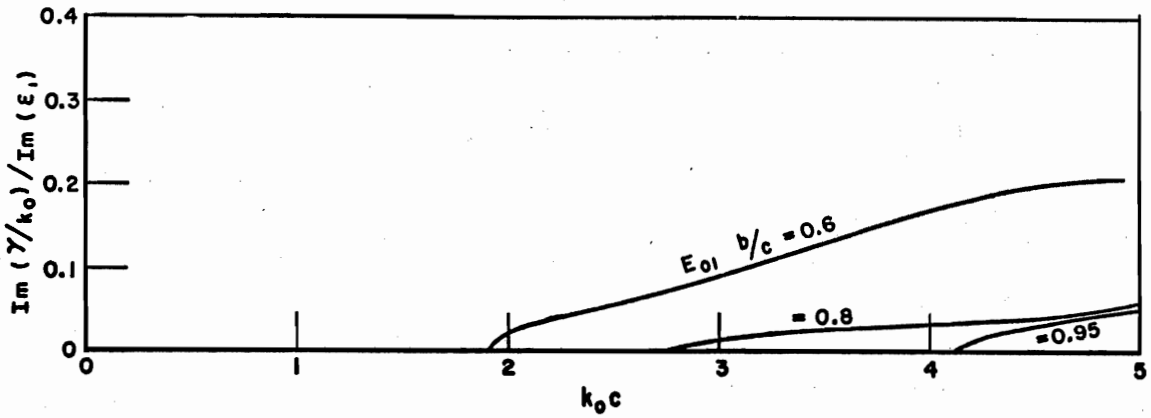

(b)

Fig. I-17.--E_{01} mode (a) dispersion and (b) attenuation characteristics for dielectric coaxial waveguide: $\epsilon_1=\epsilon_3=4.0$, $\epsilon_2=1.03$, a/c=.3 (Eq. (II-38)).

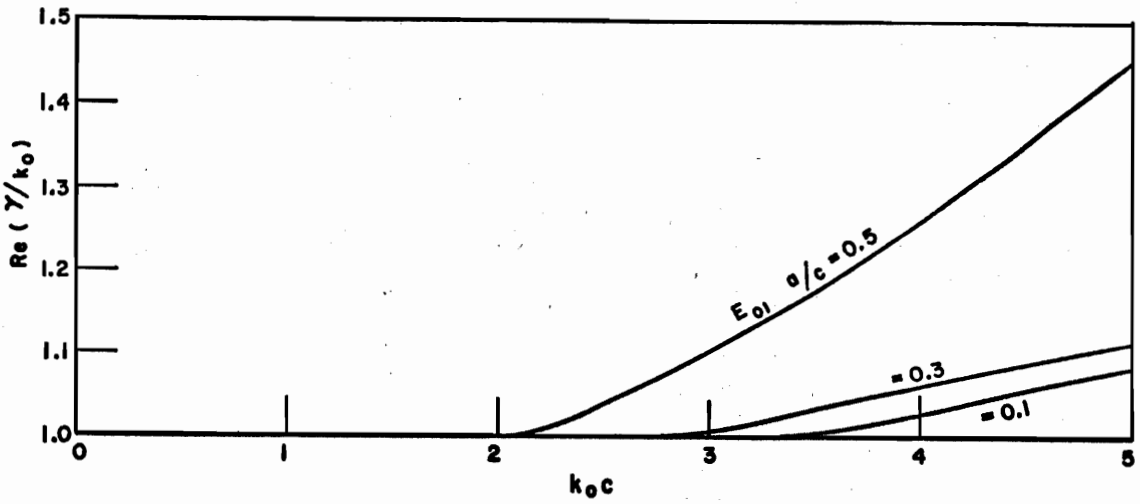

(a)

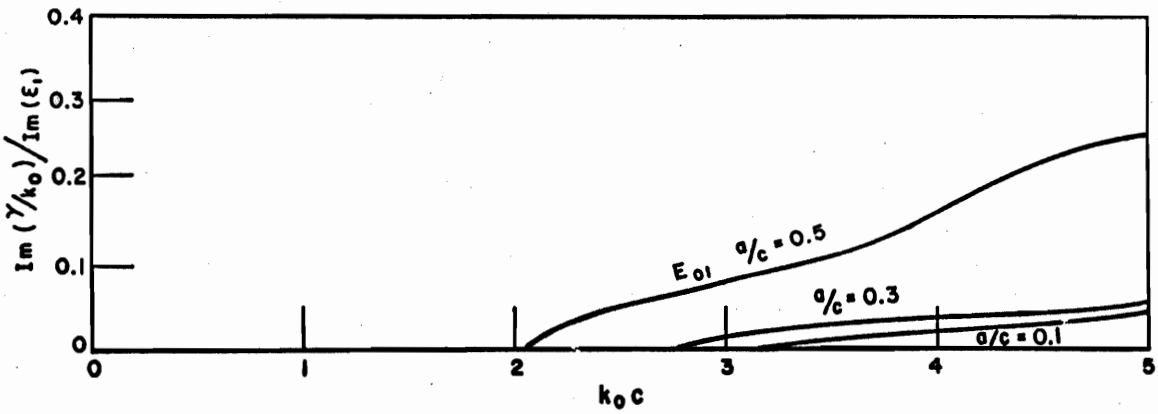

(b)

Fig. I-18.--E_{01} mode (a) dispersion and (b) attenuation characteristics for dielectric coaxial waveguide: $\epsilon_1=\epsilon_3=4.0$, $\epsilon_2=1.03$, b/c=.8 (Eq. (II-38)).

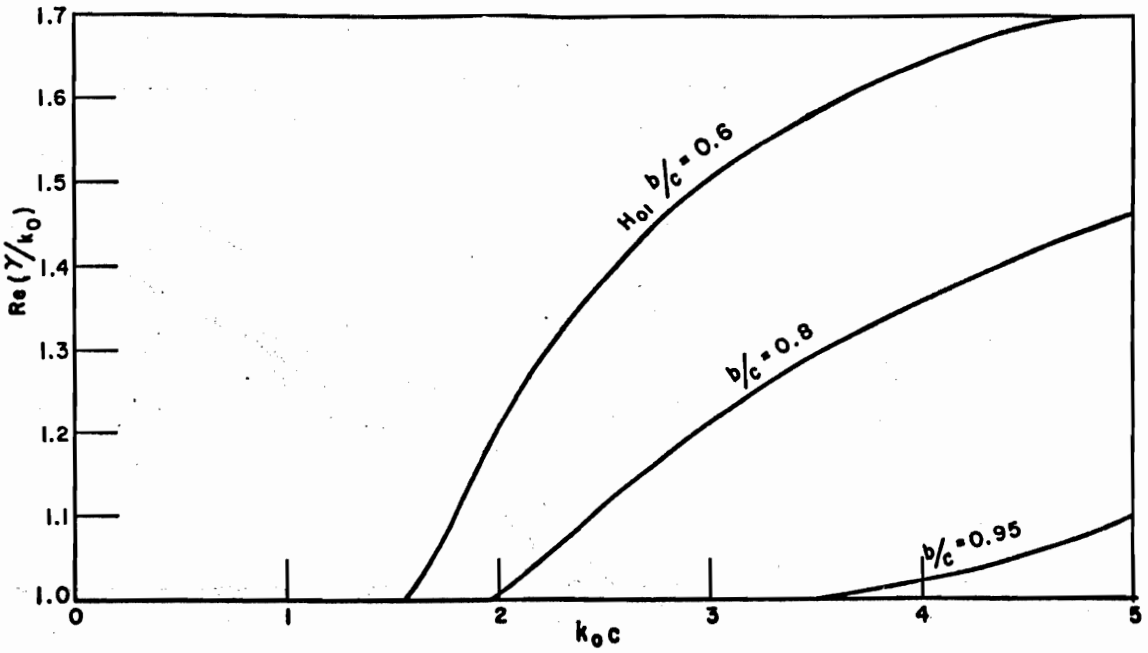

(a)

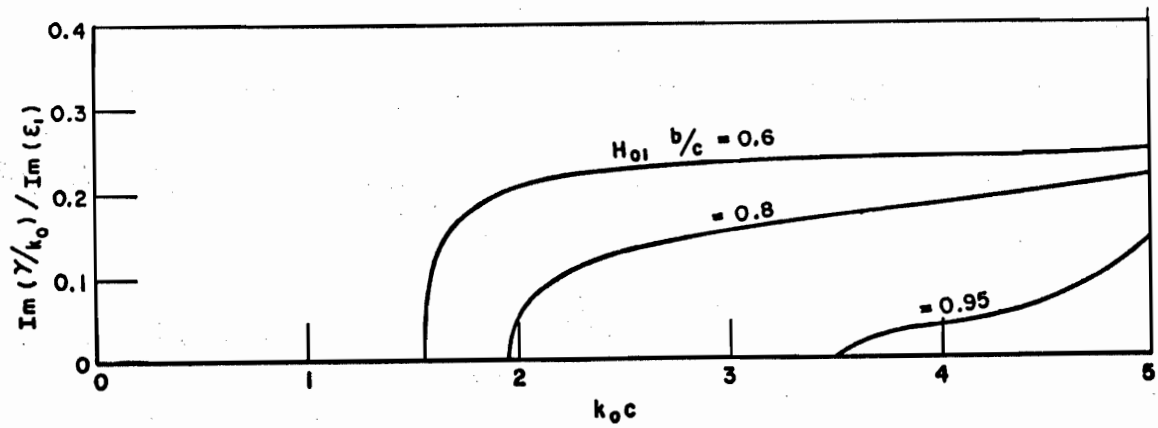

(b)

Fig. I-19.--H_{01} mode (a) dispersion and (b) attenuation characteristics for dielectric coaxial waveguide: $\epsilon_1=\epsilon_3=4.0$, $\epsilon_2=1.03$, a/c=.3 (Eq. (II-42)).

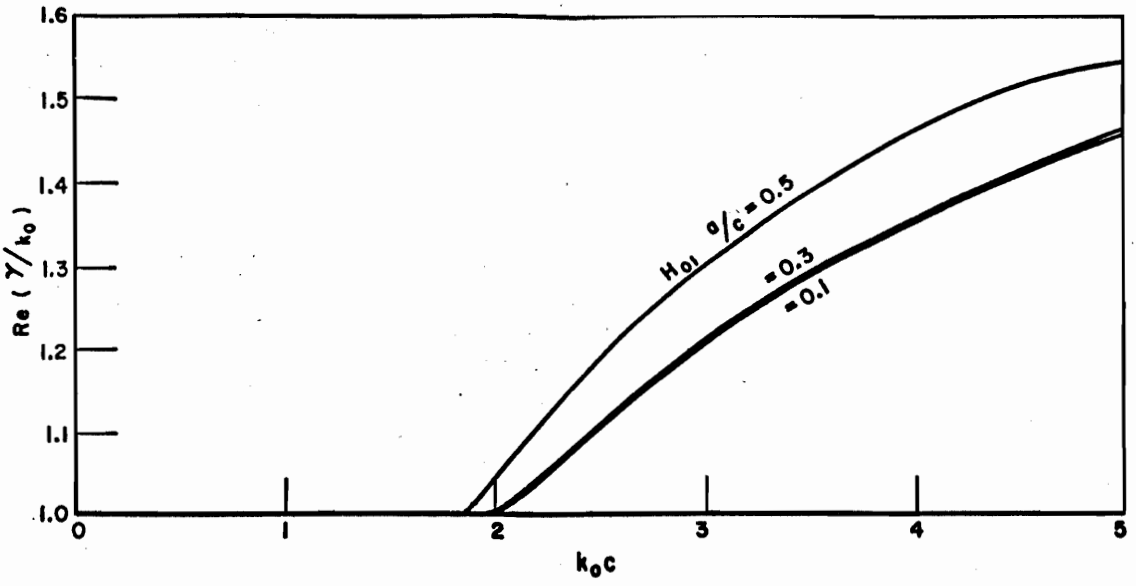

(a)

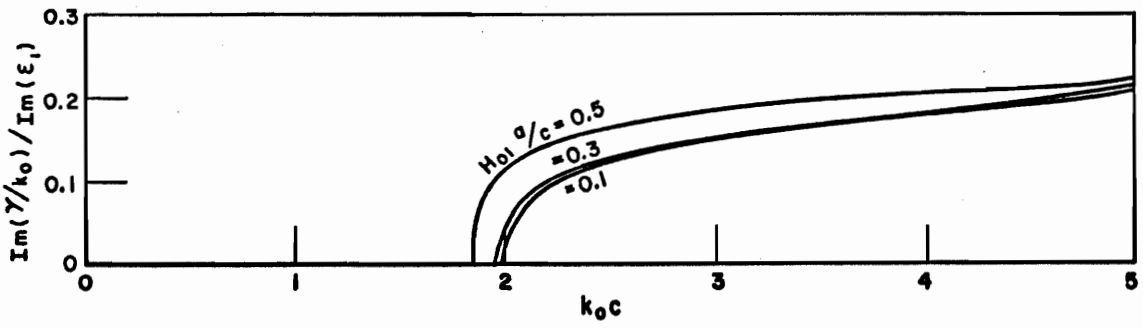

(b)

Fig. I-20.--H_{01} mode (a) dispersion and (b) attenuation characteristics for dielectric coaxial waveguide: $\epsilon_1=\epsilon_3=4.0$, $\epsilon_2=1.03$, b/c=.8 (Eq. (II-42)).

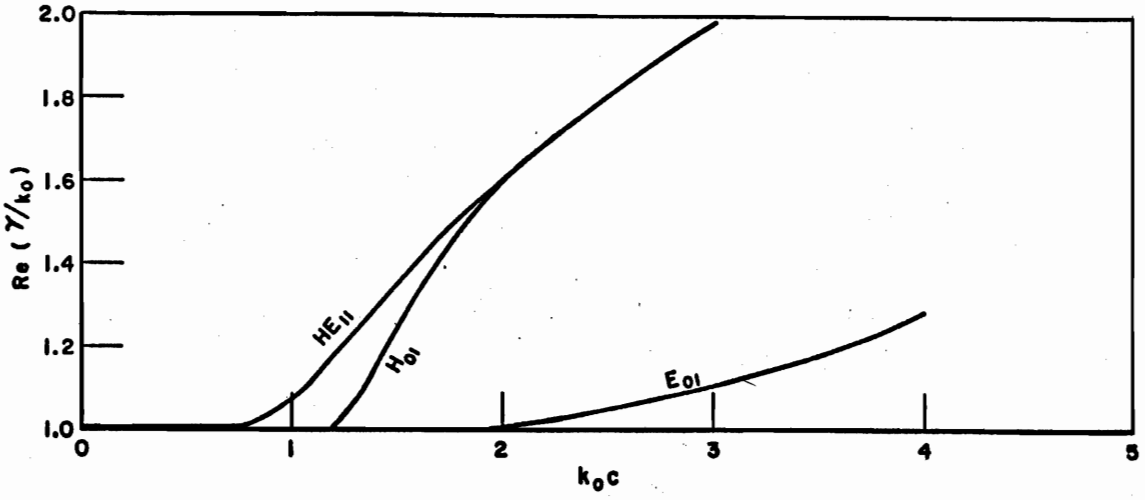

(a)

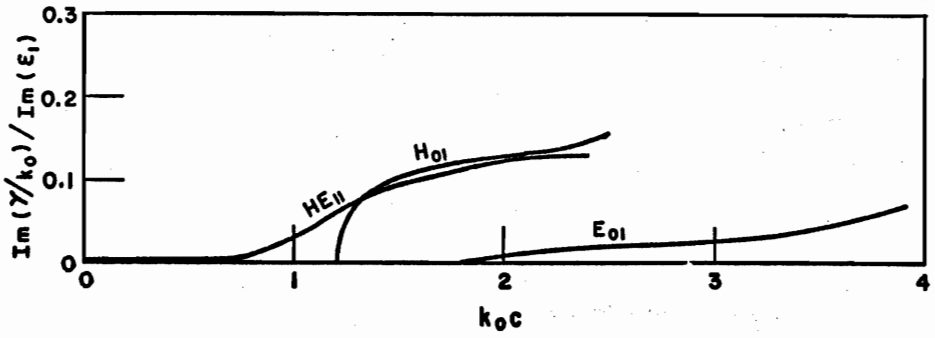

(b)

Fig. I-21.--Modal (a) dispersion and (b) attenuation characteristics for dielectric coaxial waveguide: $\epsilon_1=\epsilon_3=9.0$, $\epsilon_2=1.03$, a/c=.3, b/c=.8
(Eqs. (II-38), (II-42) and (II-49)).

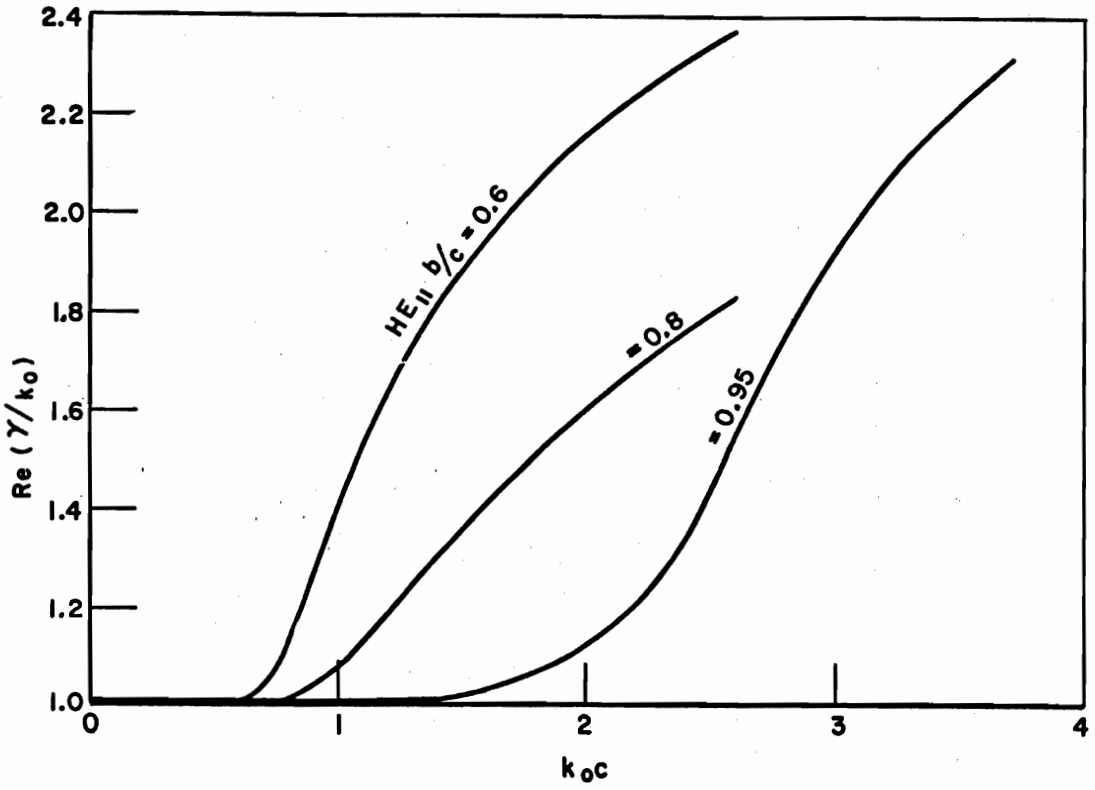

(a)

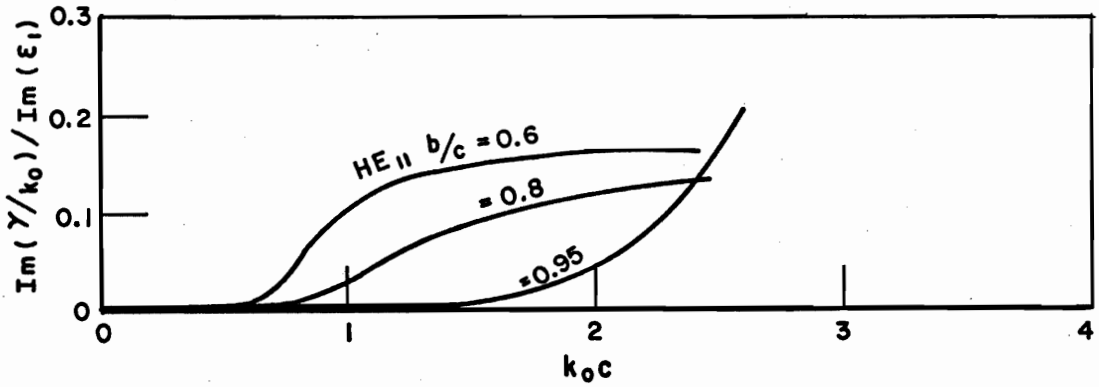

(b)

Fig. I-22.--HE_{11} mode (a) dispersion and (b) attenuation characteristics for dielectric coaxial waveguide: $\epsilon_1=\epsilon_3=9.0$, $\epsilon_2=1.03$, a/c=.3 (Eq. (II-49)).

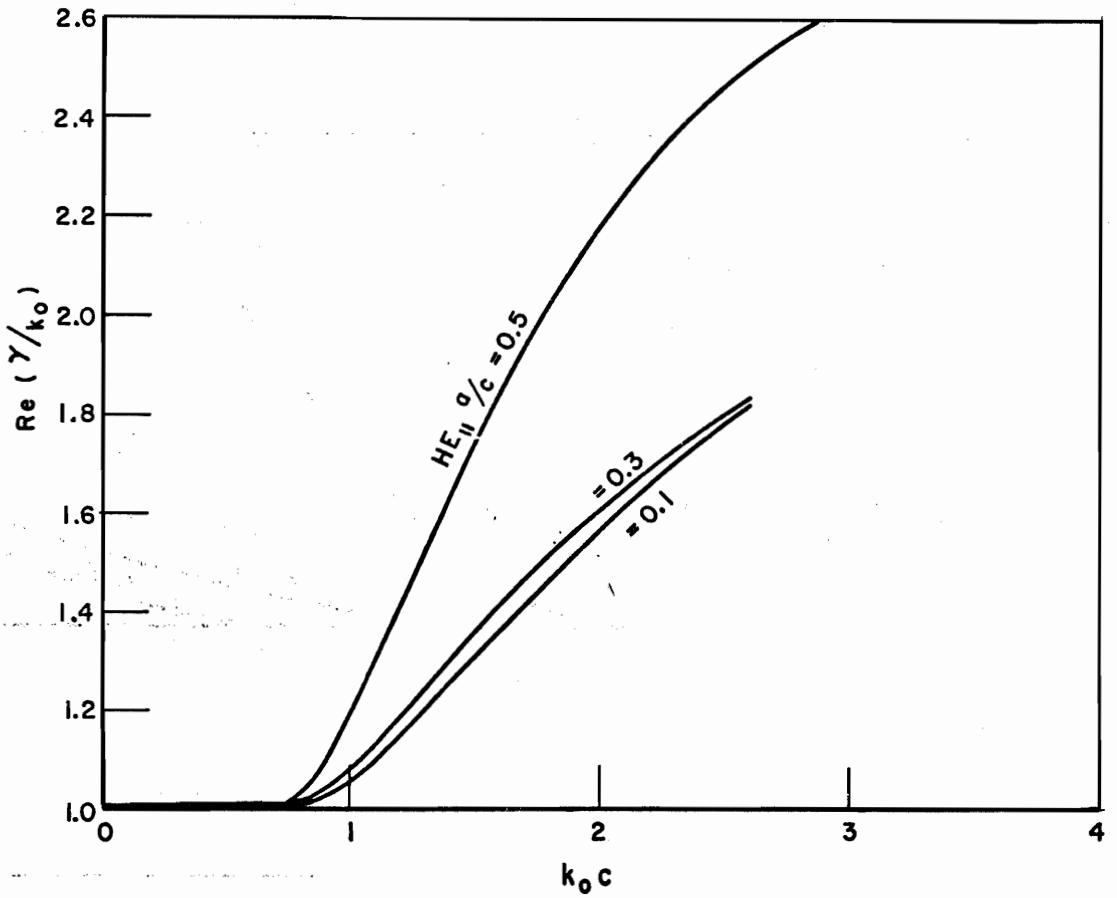

(a)

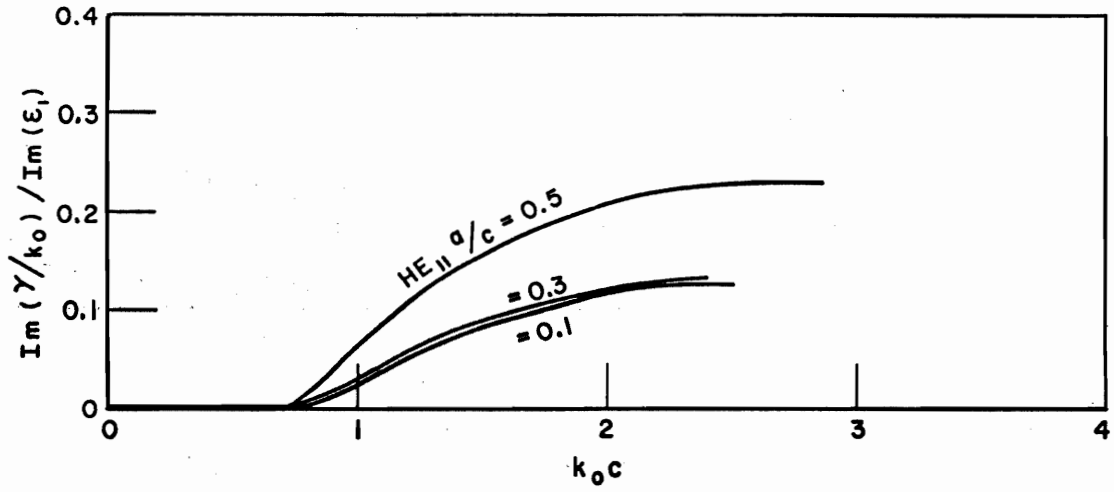

(b)

Fig. I-23.--HE_{11} mode (a) dispersion and (b) attenuation characteristics for dielectric coaxial waveguide: $\epsilon_1=\epsilon_3=9.0$, $\epsilon_2=1.03$, b/c=.8 (Eq. (II-49)).

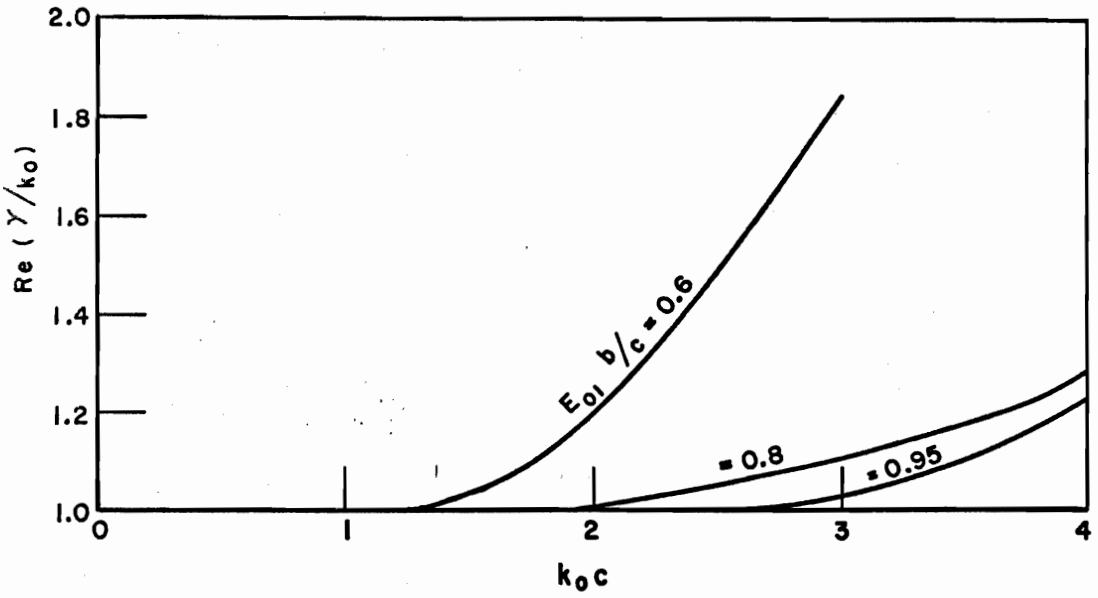

(a)

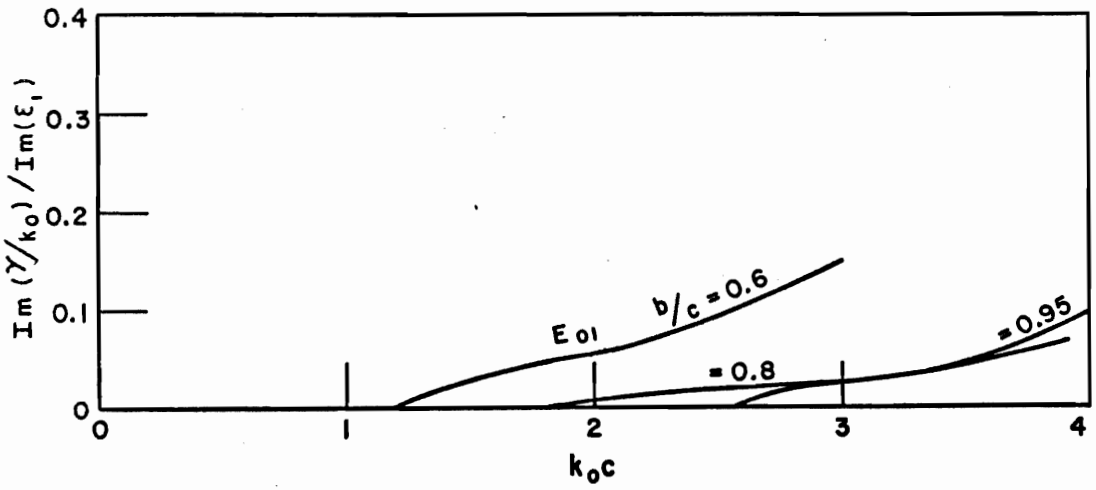

(b)

Fig. I-24.--E_{01} mode (a) dispersion and (b) attenuation characteristics for dielectric coaxial waveguide: $\epsilon_1=\epsilon_3=9.0$, $\epsilon_2=1.03$, $a/c=.3$ (Eq. (II-38)).

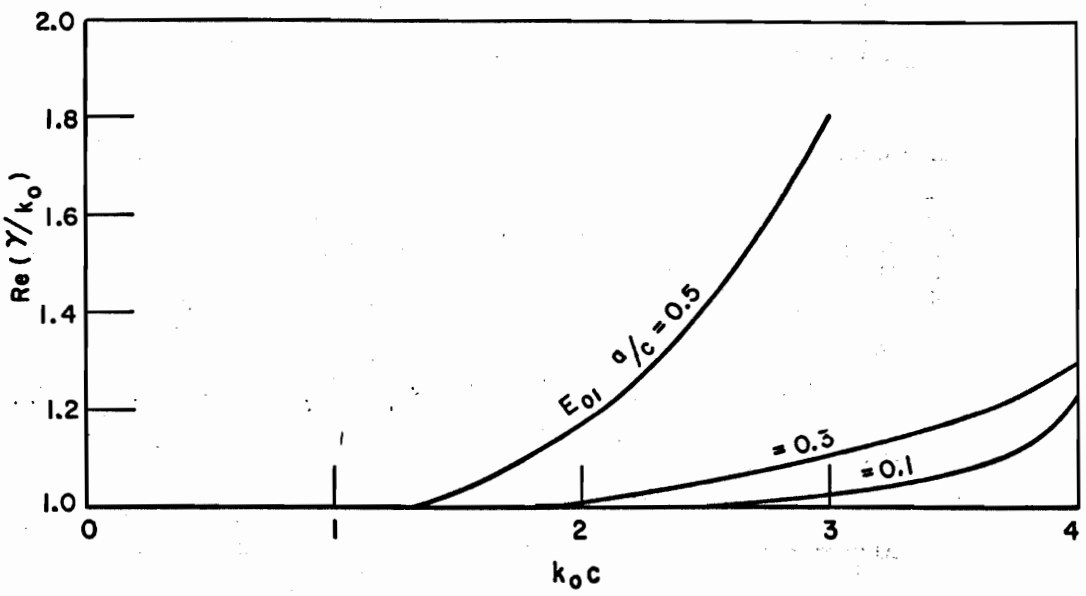

(a)

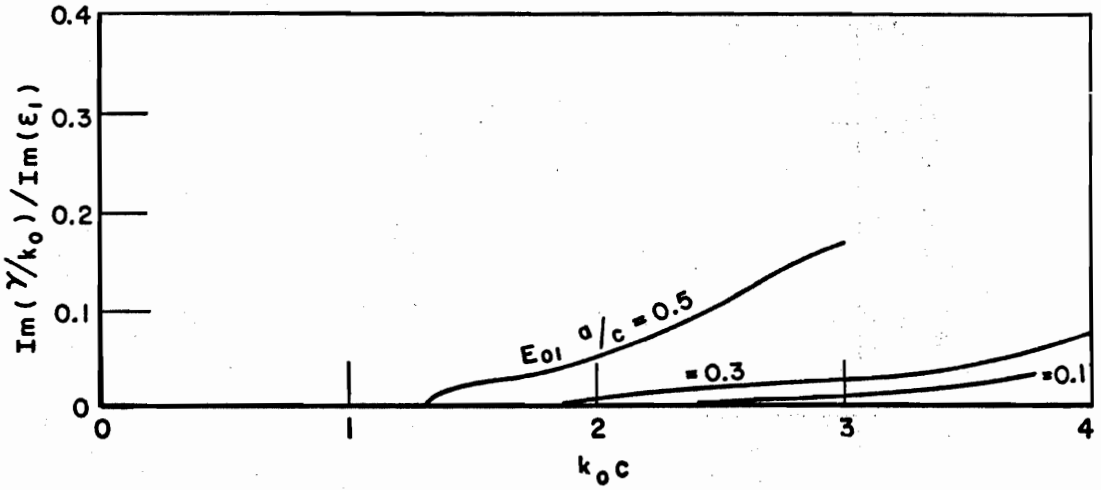

(b)

Fig. I-25.--E_{01} mode (a) dispersion and (b) attenuation characteristics for dielectric coaxial waveguide: $\epsilon_1=\epsilon_3=9.0$, $\epsilon_2=1.03$, b/c=.8 Eq. (II-38)).

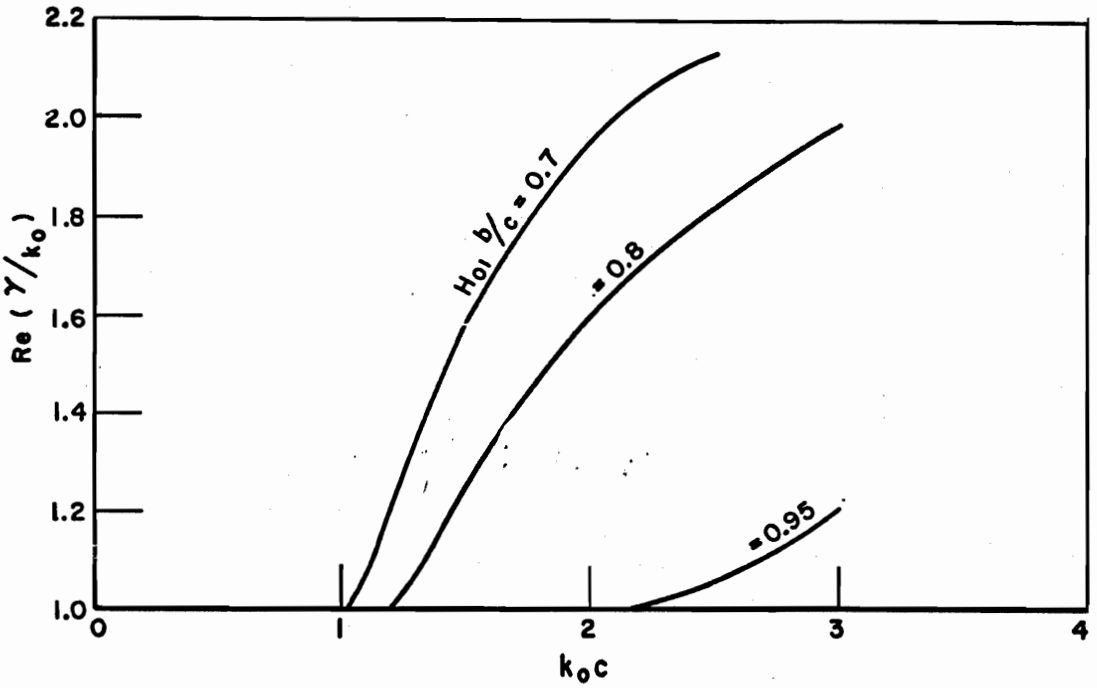

(a)

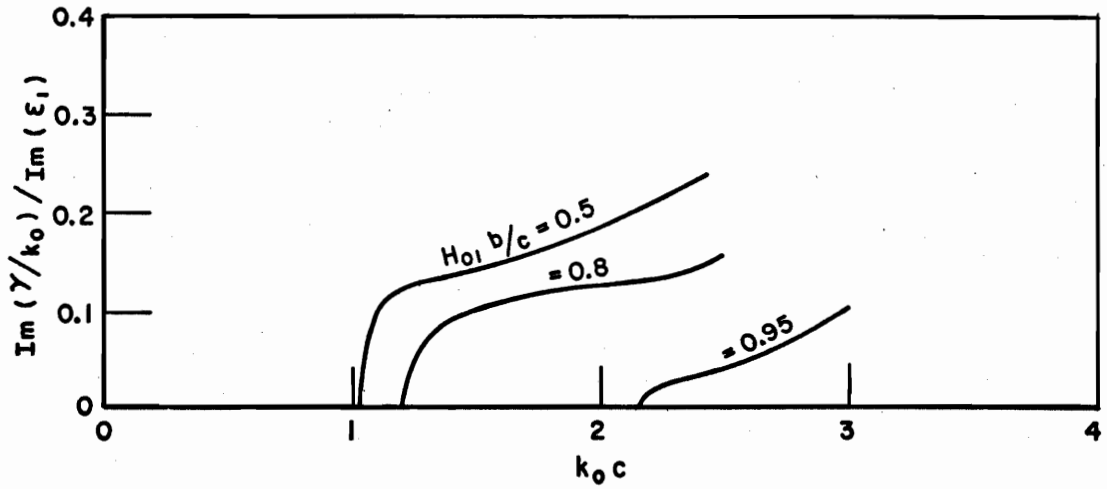

(b)

Fig. I-26.--H_{01} mode (a) dispersion and (b) attenuation characteristics for dielectric coaxial waveguide: $\epsilon_1=\epsilon_3=9.0$, $\epsilon_2=1.03$, a/c=.3 (Eq. (II-42)).

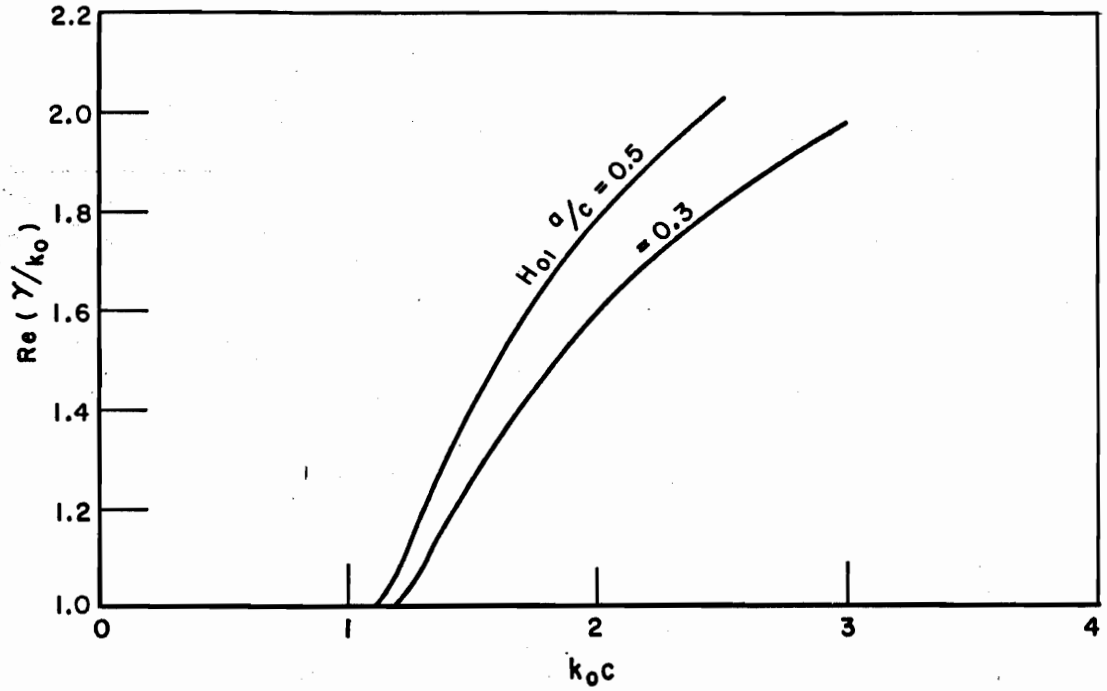

(a)

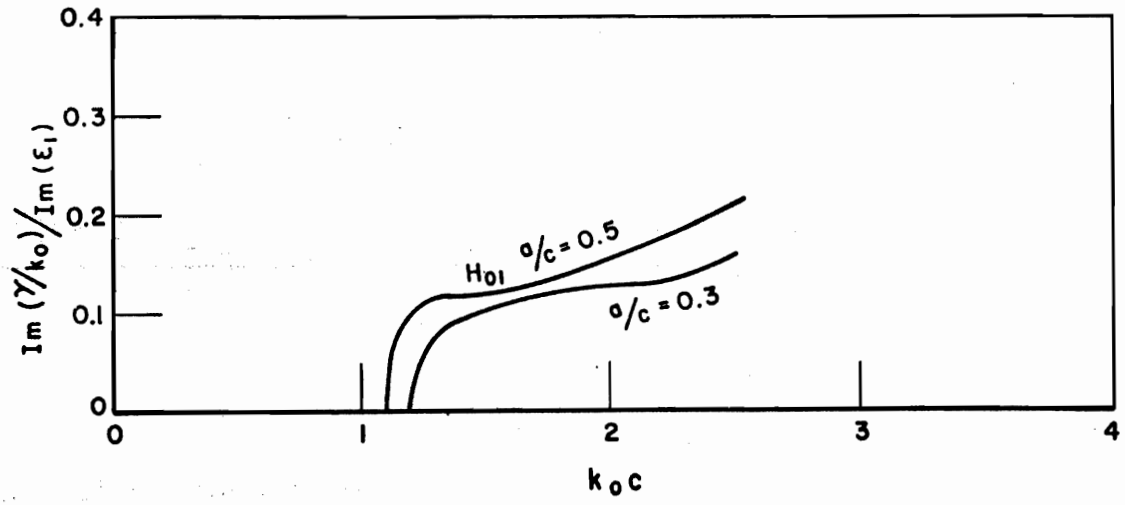

(b)

Fig. I-27.--H_{01} mode (a) dispersion and (b) attenuation characteristics for dielectric coaxial waveguide: $\epsilon_1=\epsilon_3=9.0$, $\epsilon_2=1.03$, b/c=.8 (Eq. (II-42)).

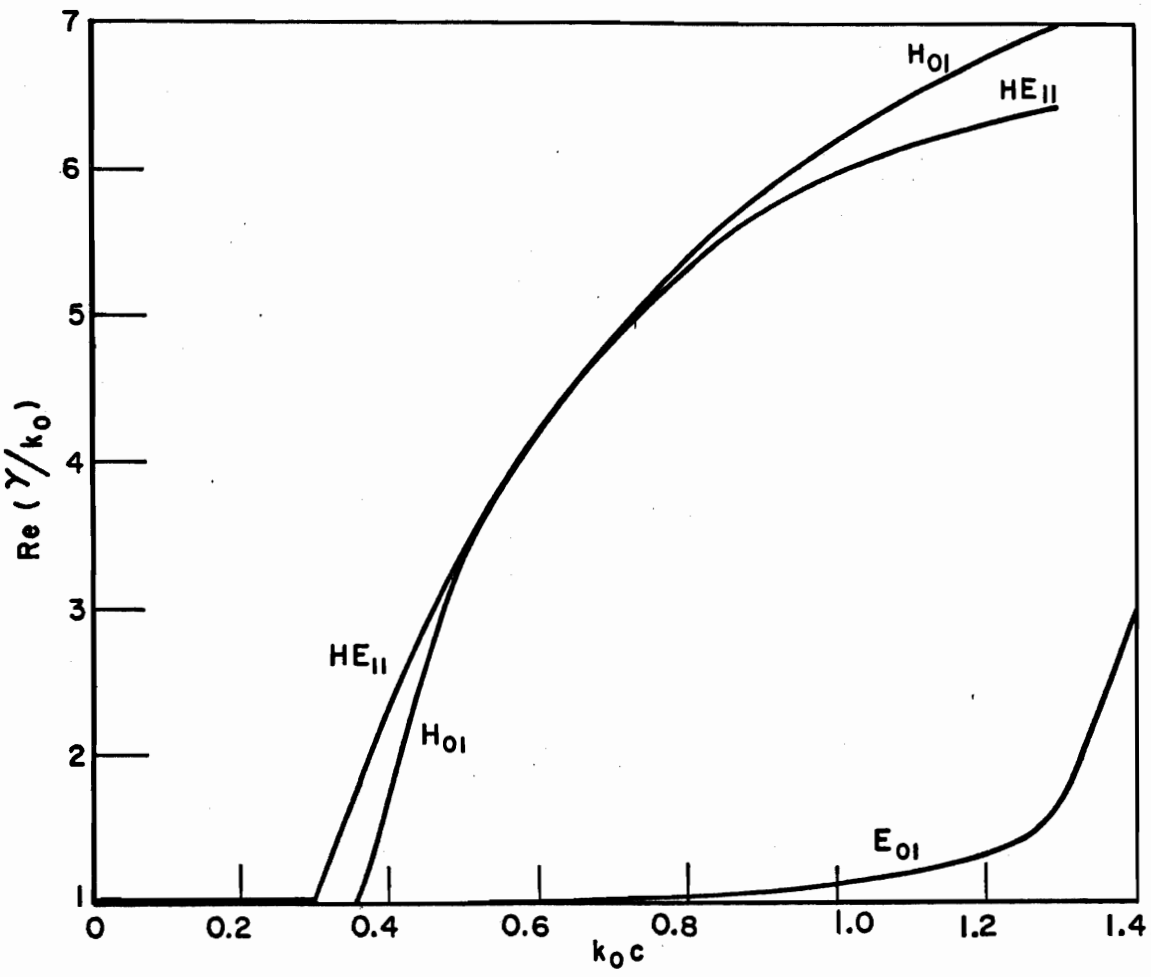

Fig. I-28.--Modal dispersion characteristics for dielectric coaxial waveguide: $\epsilon_1=\epsilon_3=90.$, $\epsilon_2=1.03$, a/c=.3, b/c=.8 (Eqs. (II-38), (II-42) and (II-49)).

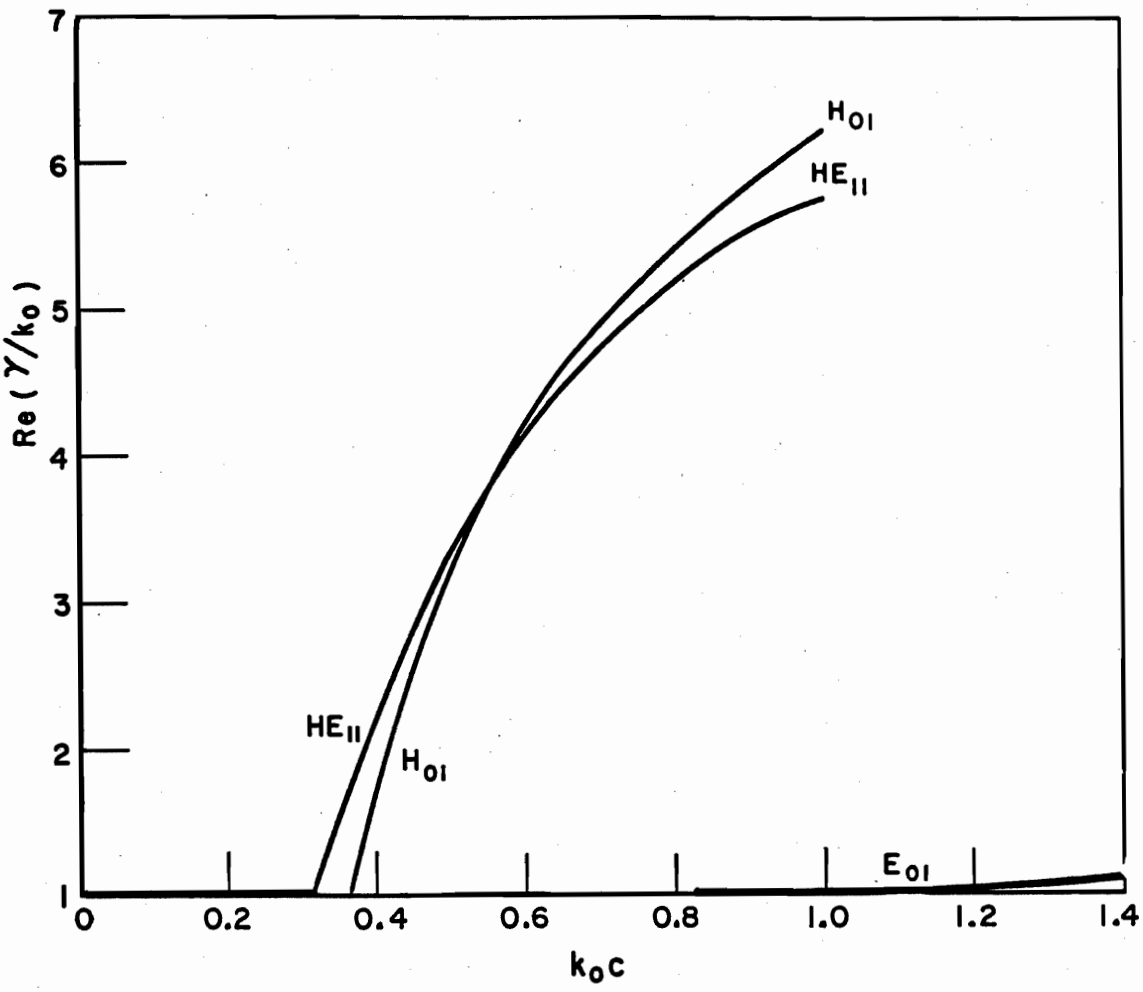

Fig. I-29.--Modal dispersion characteristics for dielectric coaxial waveguide: $\epsilon_1=\epsilon_3=90.$, $\epsilon_2=1.03$, a/c=.1, b/c=.8 (Eqs. (II-38), (II-42) and (II-49)).

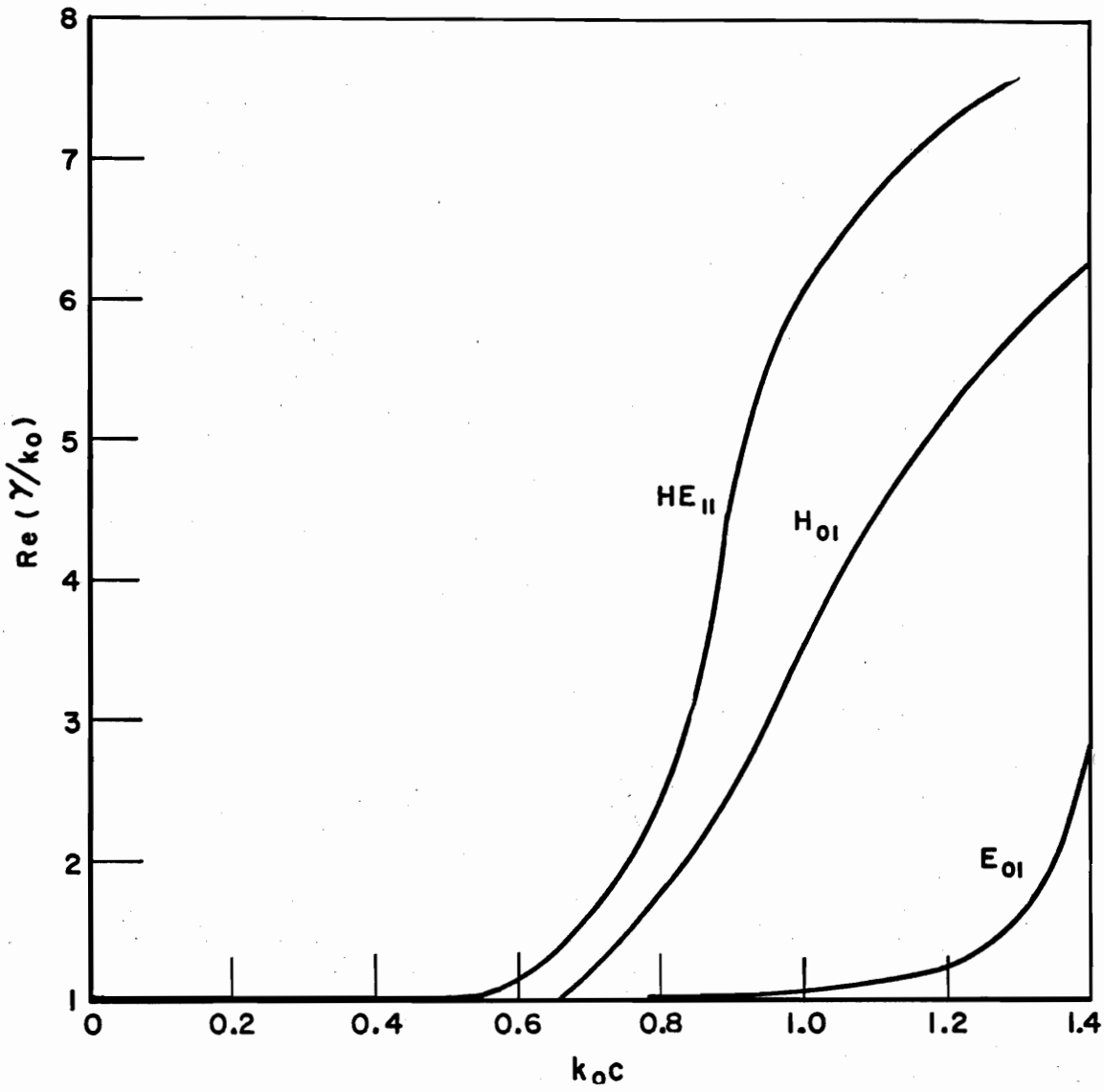

Fig. I-30.--Modal dispersion characteristics for dielectric coaxial waveguide: $\epsilon_1=\epsilon_3=90.$, $\epsilon_2=1.03$, a/c=.3, b/c=.95 (Eqs. (II-38), (II-42) and (II-49)).

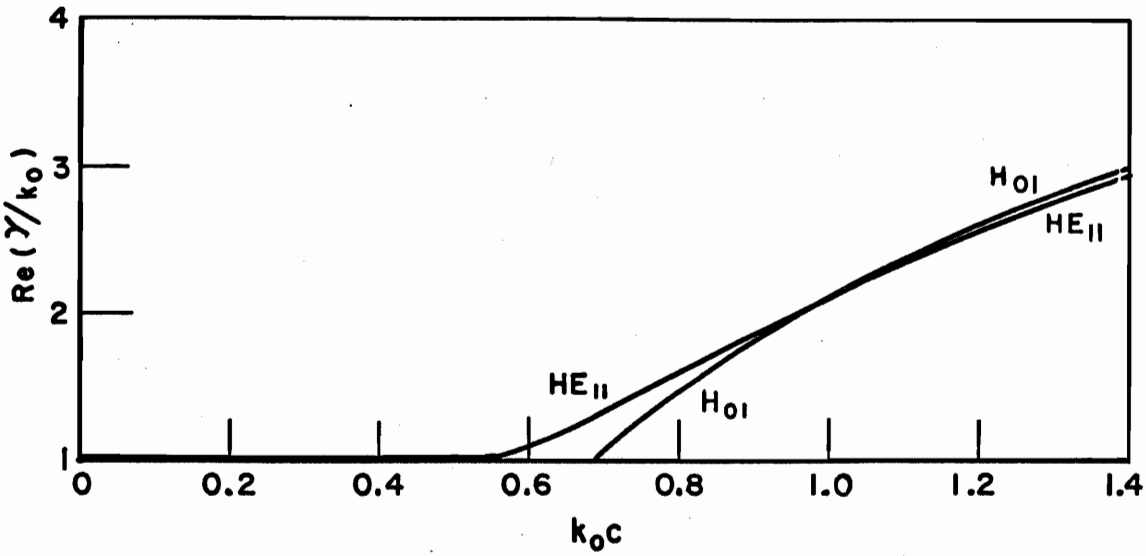

Fig. I-31.--Modal dispersion characteristics for dielectric coaxial waveguide: $\epsilon_1 = \epsilon_3 = 90.$, $\epsilon_2 = 1.03$, $a/c = .1$, $b/c = .95$ (Eqs. (II-42) and (II-49)).

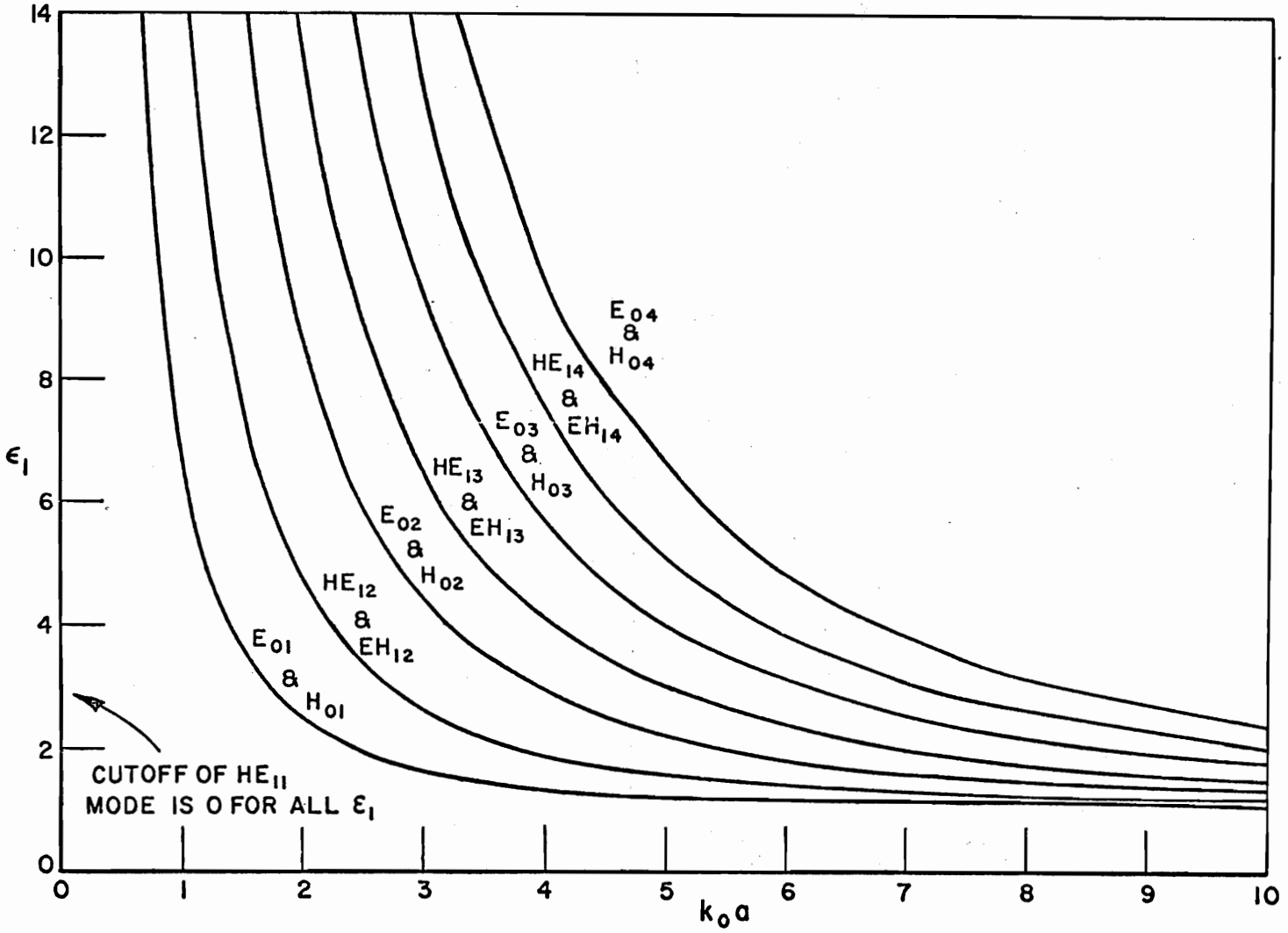

Fig. I-32.--Permittivity versus modal cutoff wavenumbers for dielectric rod waveguide (Eqs. (40) and (41)).

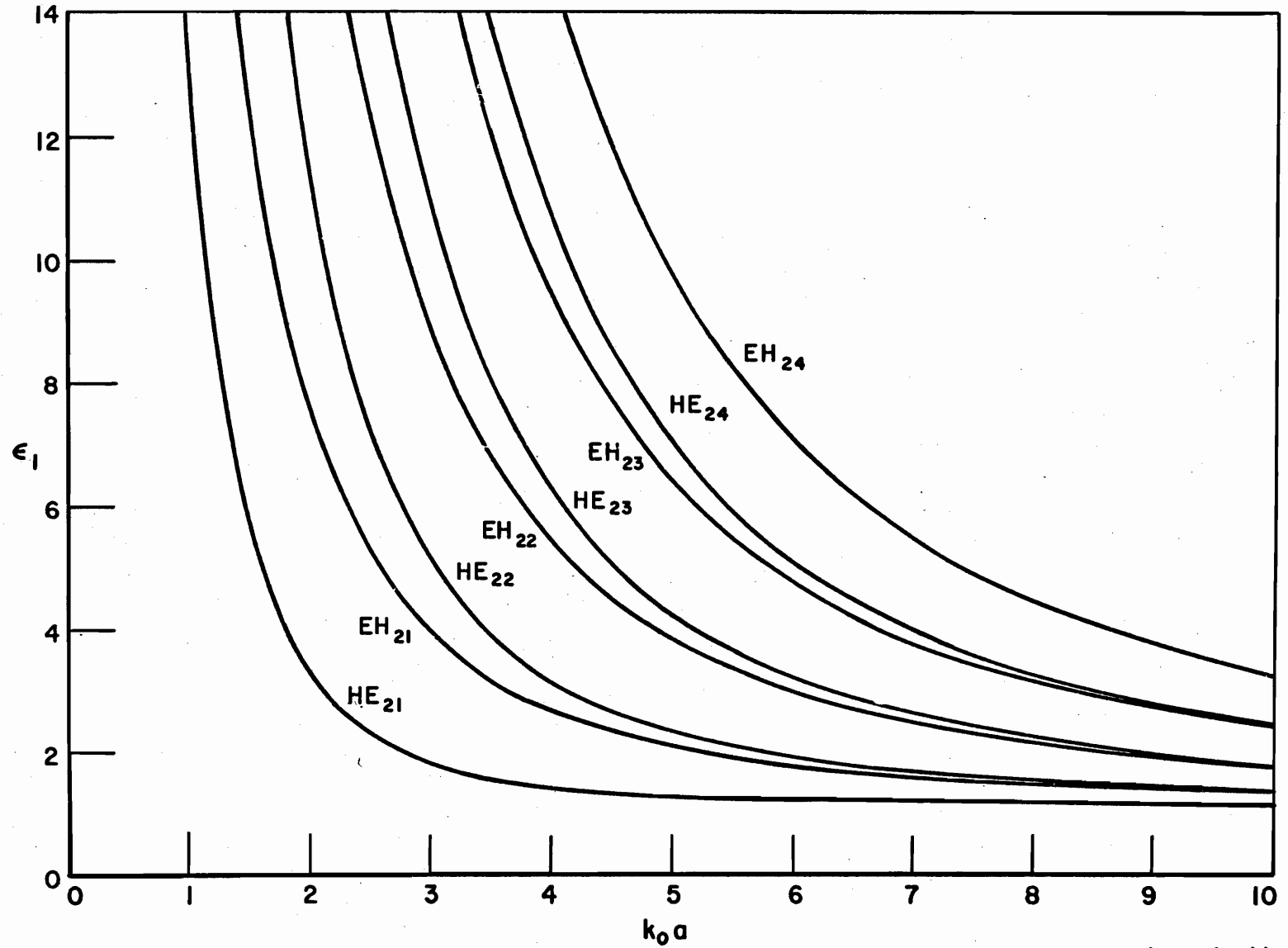

Fig. I-33.--Permittivity versus modal cutoff wavenumbers for dielectric rod waveguide (Eq. (42)).

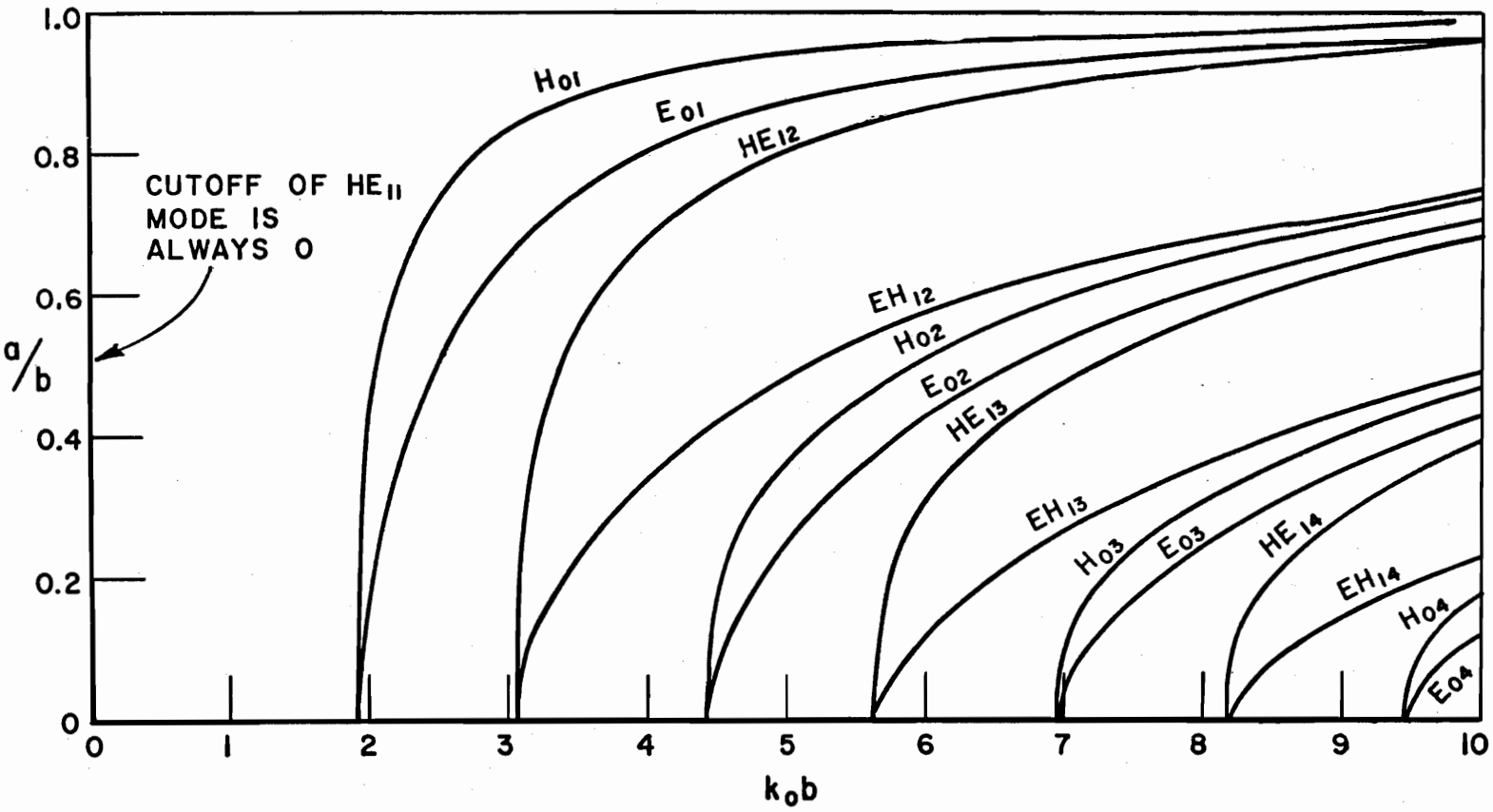

Fig. I-34.--Radii ratio (a/b) versus modal cutoff wavenumbers for airfilled dielectric tube waveguide: ϵ_2=2.55 (Eqs. (27), (31) and (32)).

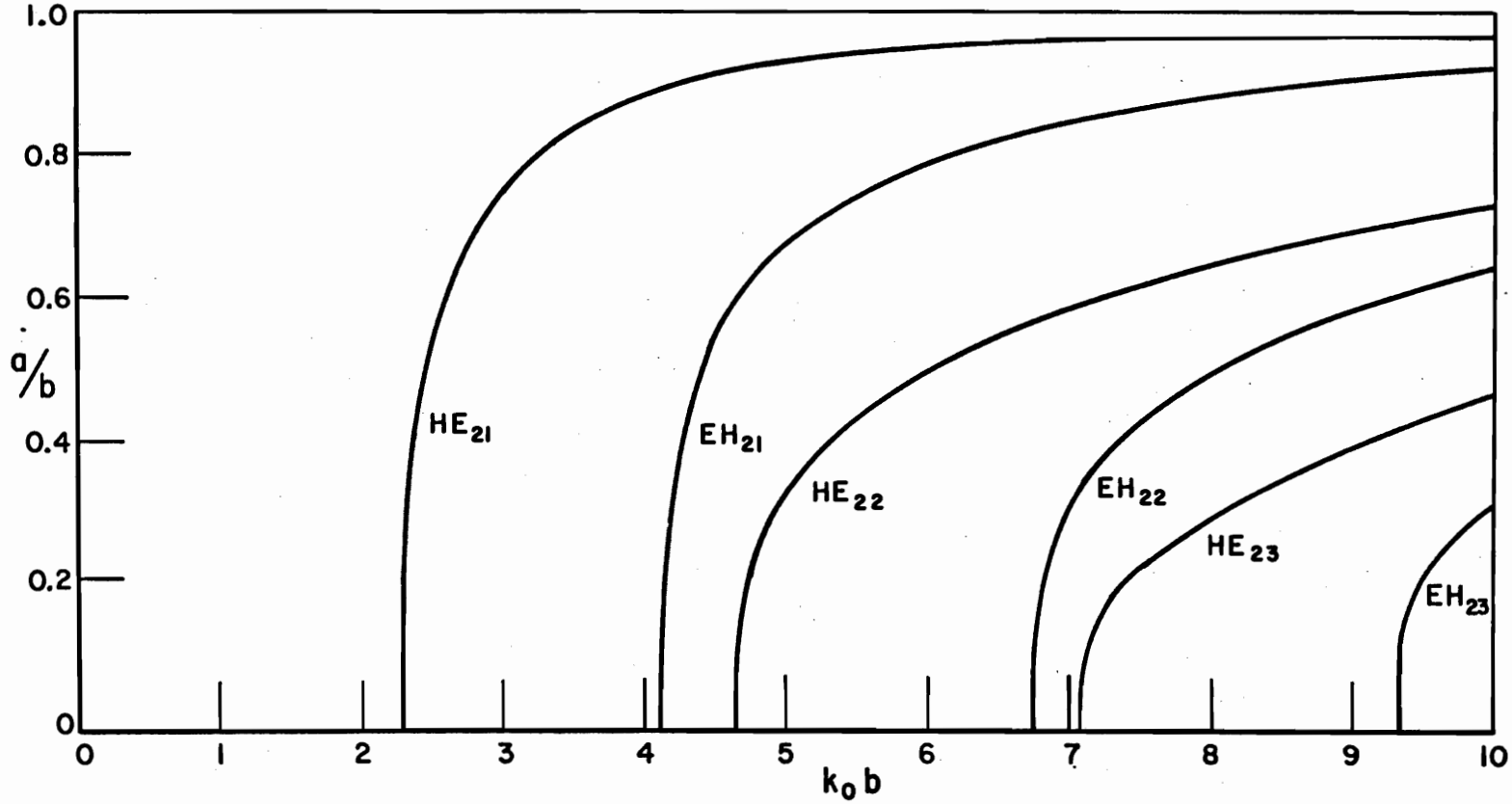

Fig. I-35.--Radii ratio (a/b) versus modal cutoff wavenumbers for airfilled dielectric tube waveguide: ϵ_2=2.55 (Eq. (28)).

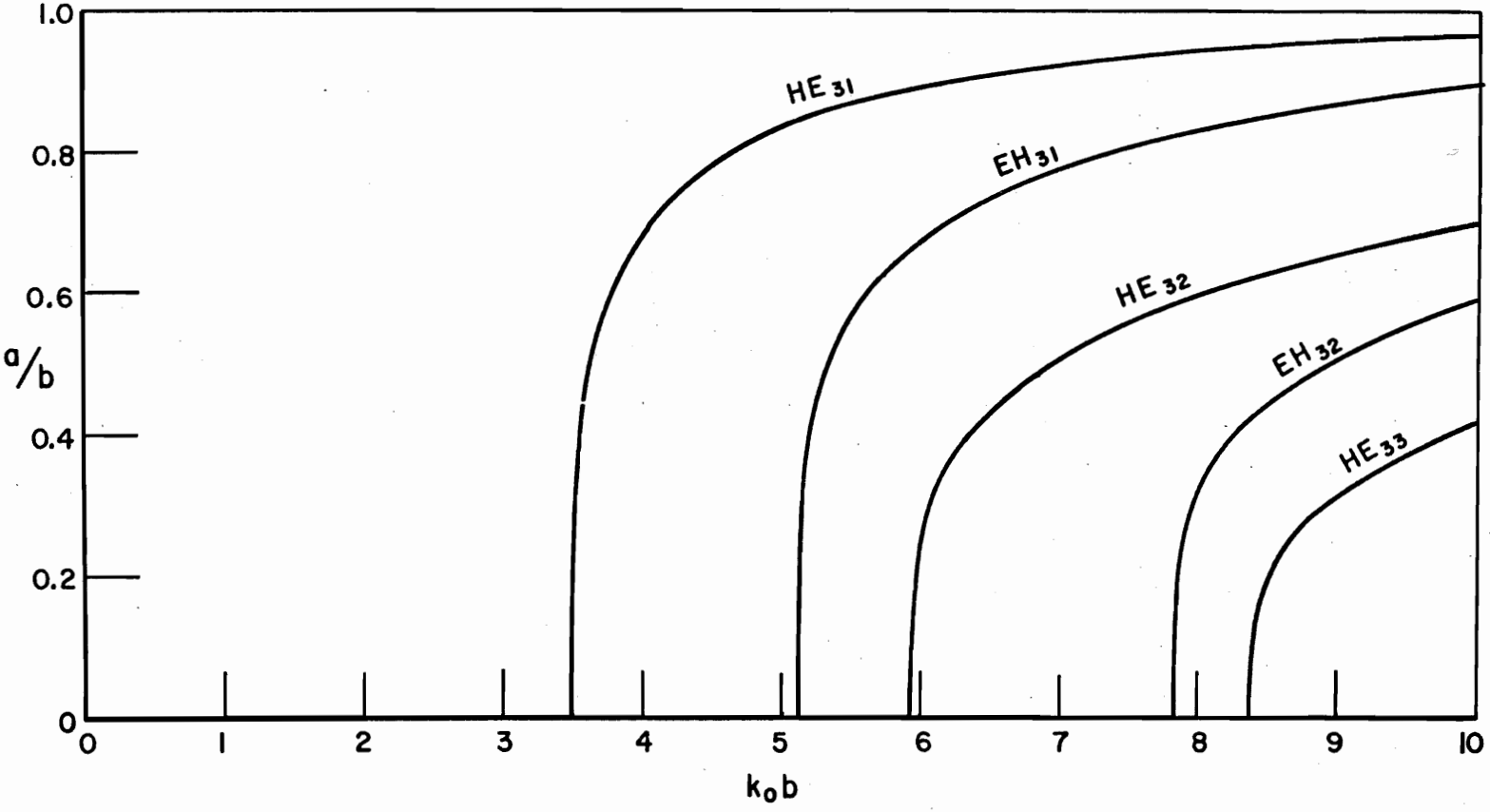

Fig. I-36.--Radii ratio (a/b) versus modal cutoff wavenumbers for airfilled dielectric tube waveguide: ϵ_2=2.55 (Eq. (28)).

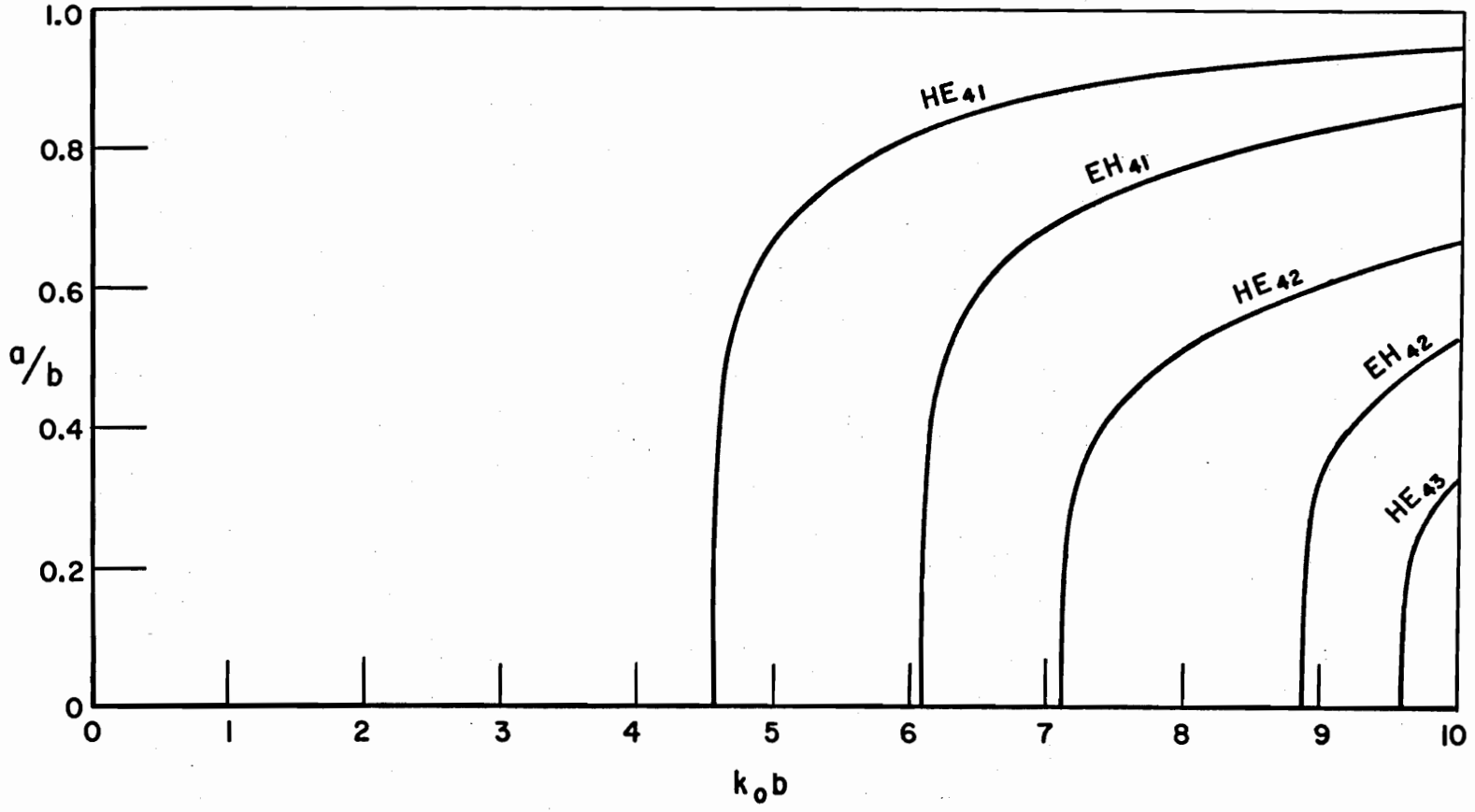

Fig. I-37.--Radii ratio (a/b) versus modal cutoff wavenumbers for airfilled dielectric tube waveguide: ϵ_2=2.55 (Eq. (28)).

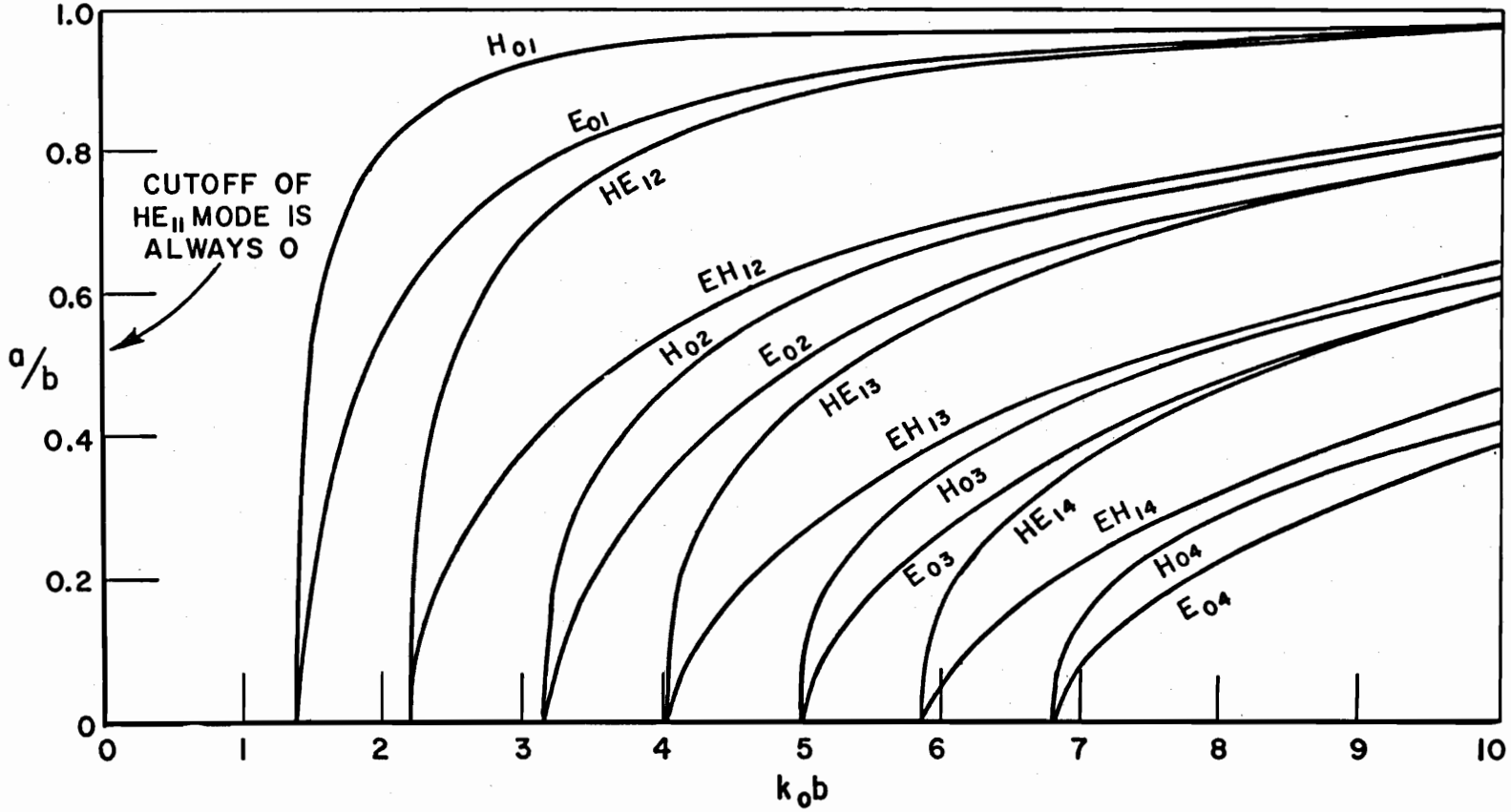

Fig. I-38.--Radii ratio (a/b) versus modal cutoff wavenumbers for airfilled dielectric tube waveguide: ϵ_2=4.0 (Eqs. (27), (31) and (32)).

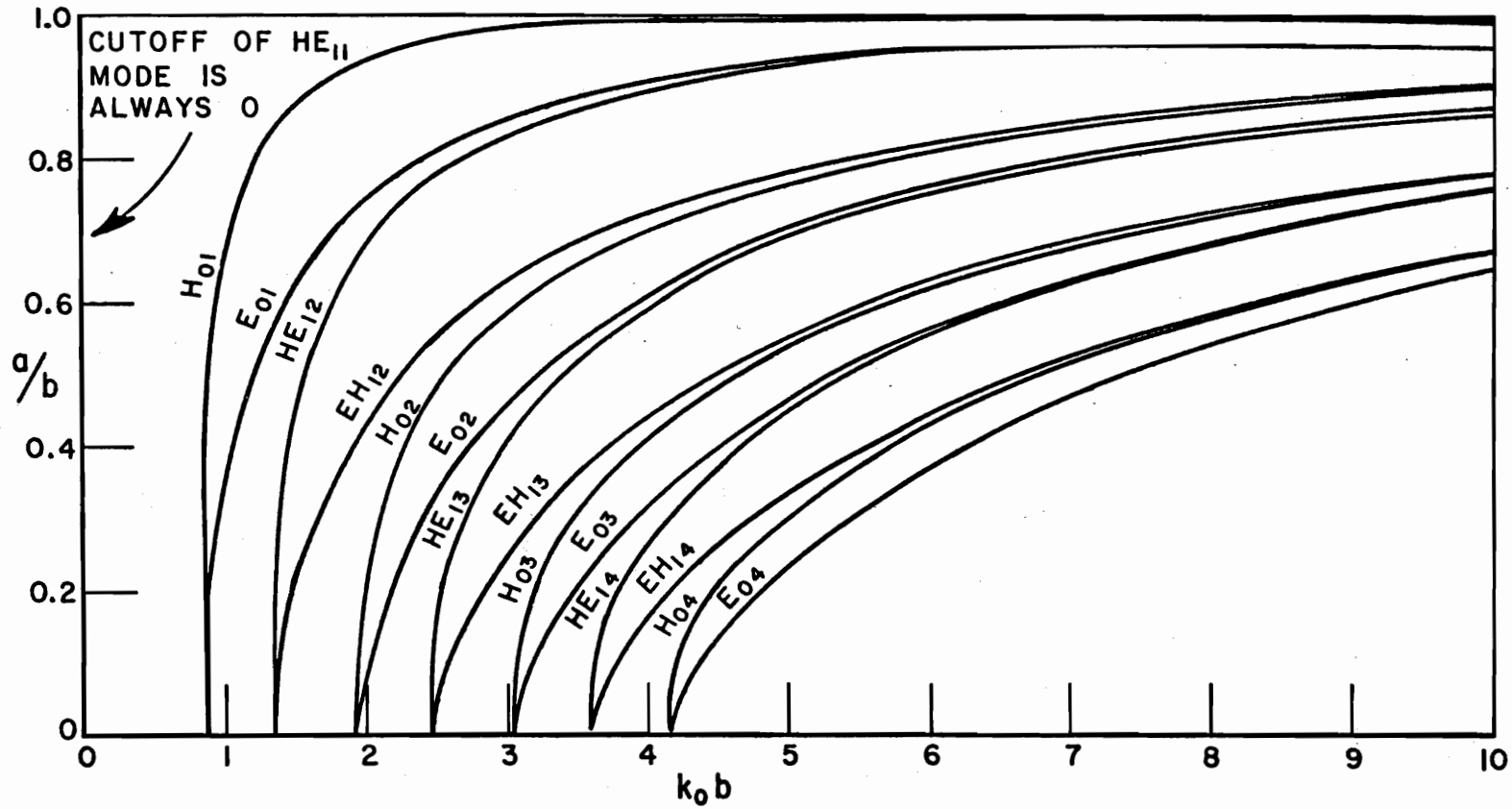

Fig. I-39.--Radii ratio (a/b) versus modal cutoff wavenumbers for airfilled dielectric tube waveguide: ϵ_3=9.0 (Eqs. (27), (31) and (32)).

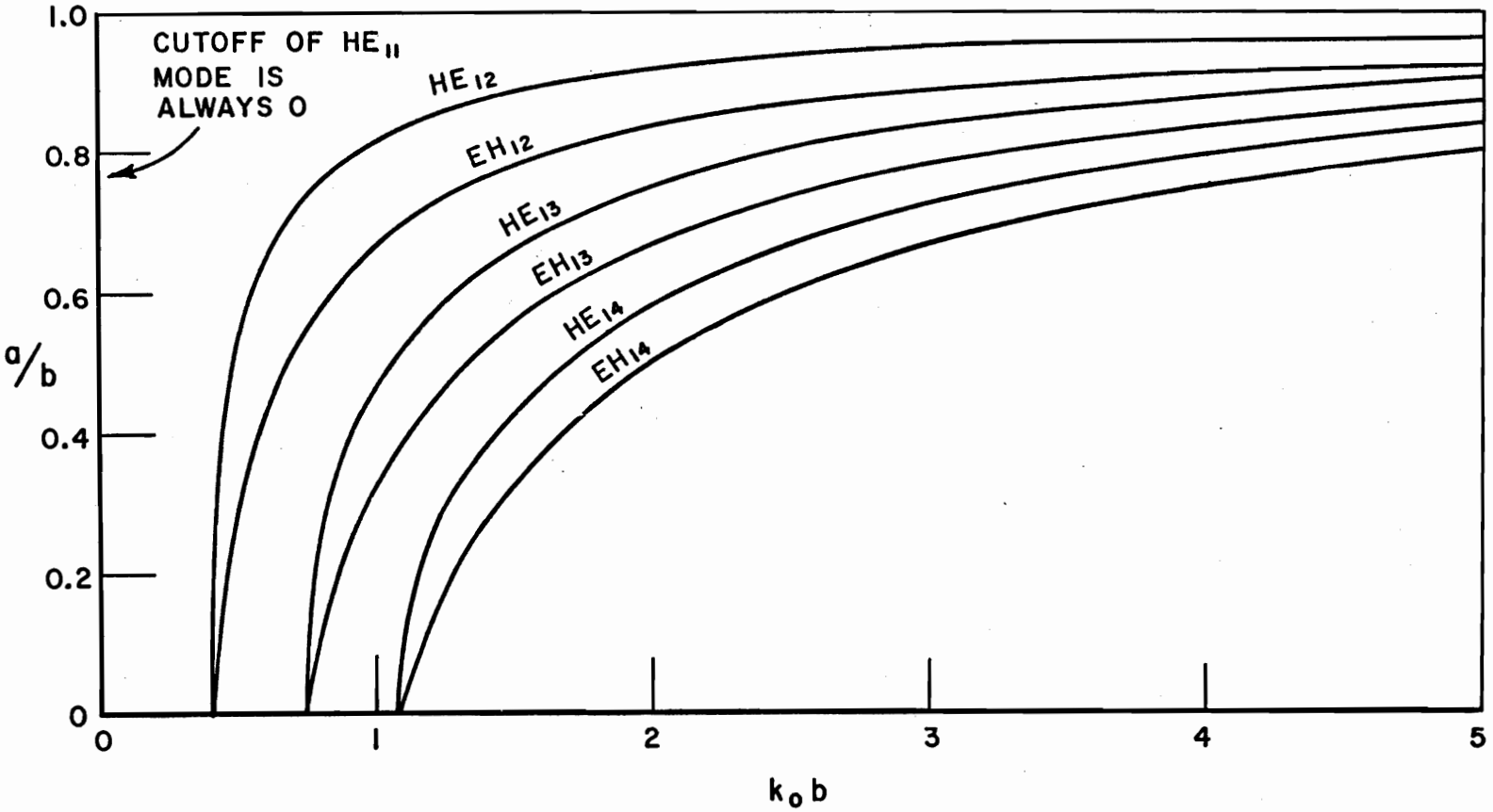

Fig. I-40.--Radii ratio (a/b) versus modal cutoff wavenumbers for airfilled dielectric tube waveguide: ϵ_2=90. (Eq. (27)).

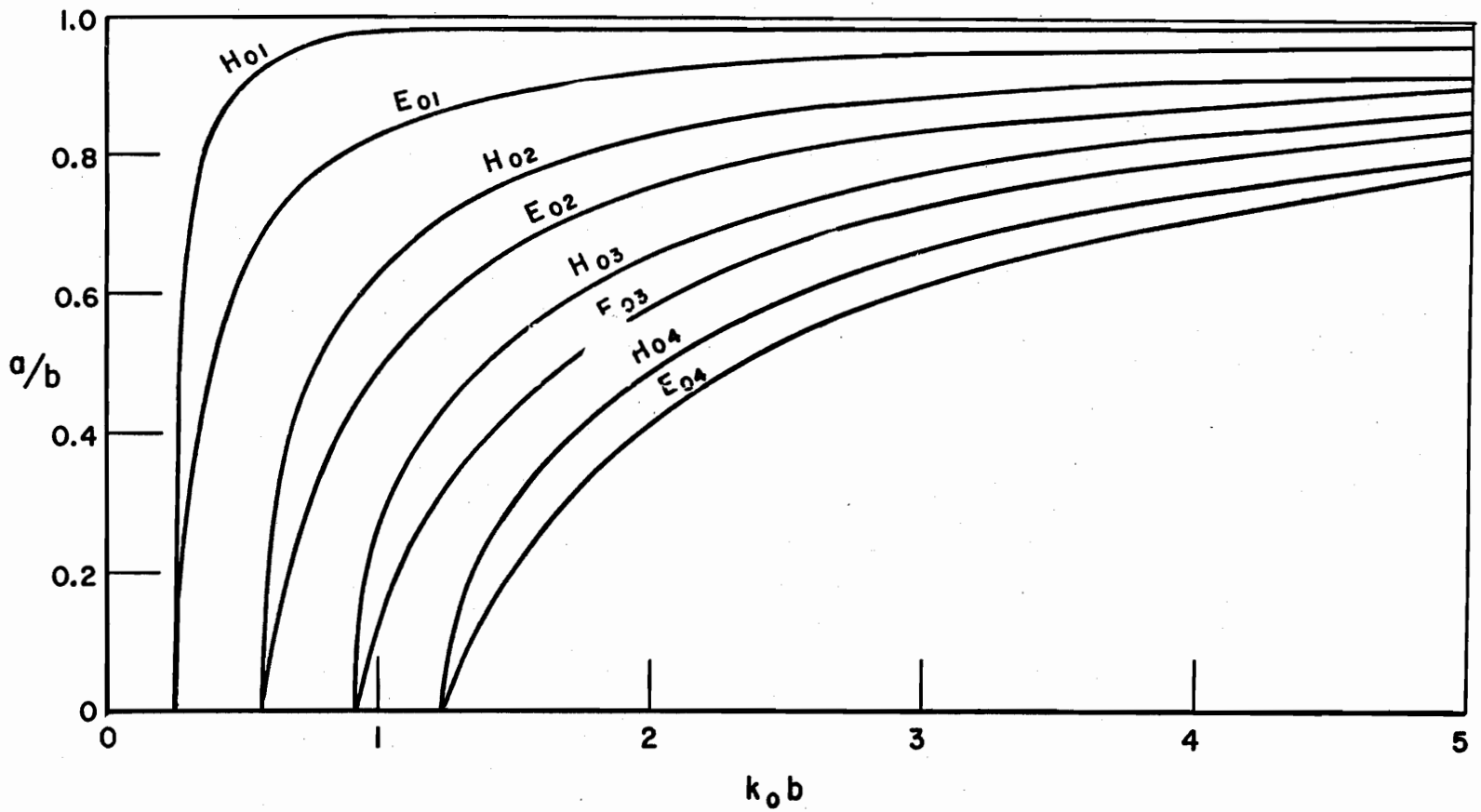

Fig. I-41.--Radii ratio (a/b) versus modal cutoff wavenumbers for airfilled dielectric tube waveguide: ϵ_2=90. (Eqs. (31) and (32)).

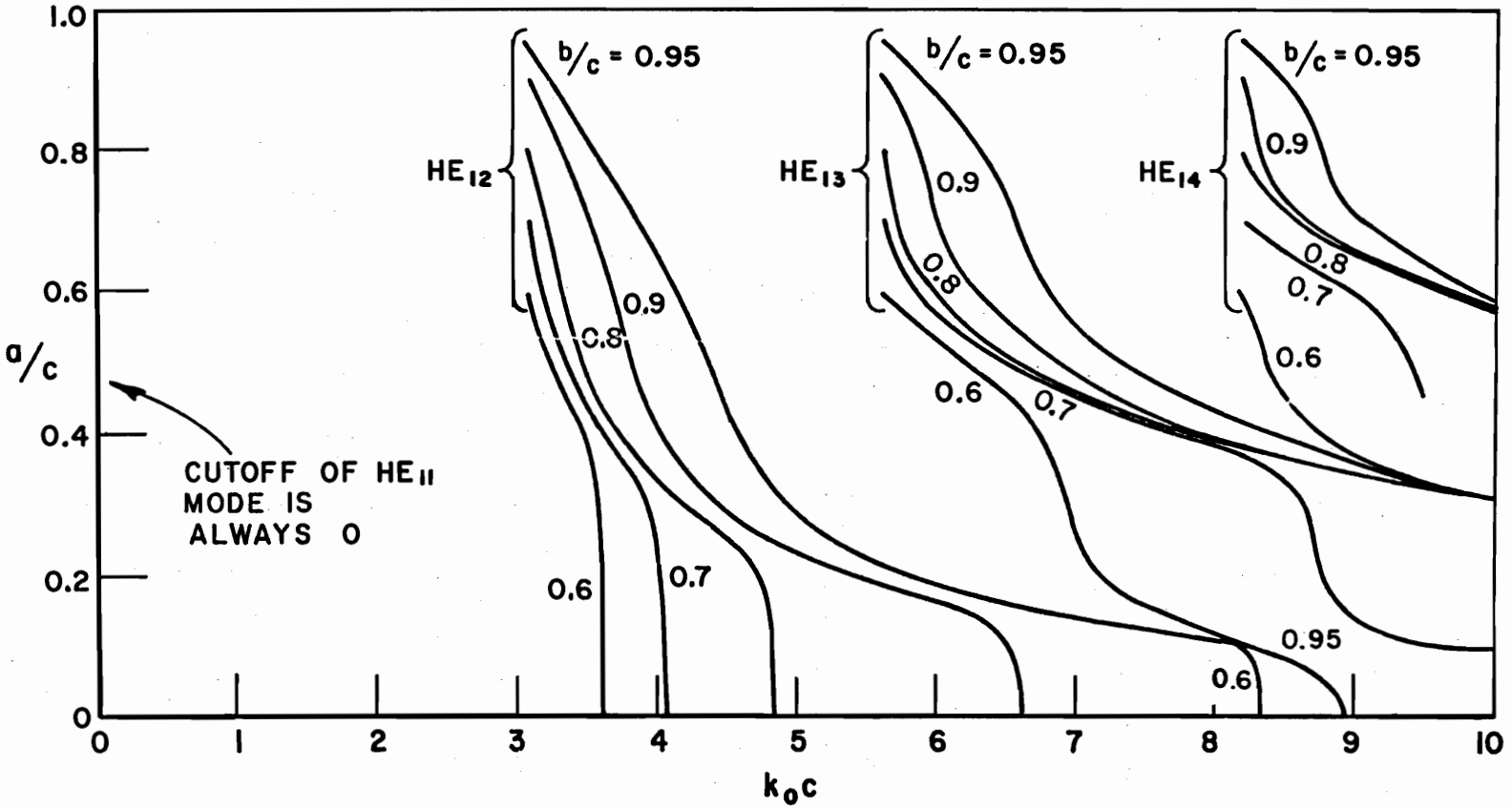

Fig. I-42.--Radii ratio (a/c) versus modal cutoff wavenumbers for dielectric coaxial waveguide: $\epsilon_1=\epsilon_3=2.55$, $\epsilon_2=1.03$ (Eq. (35)).

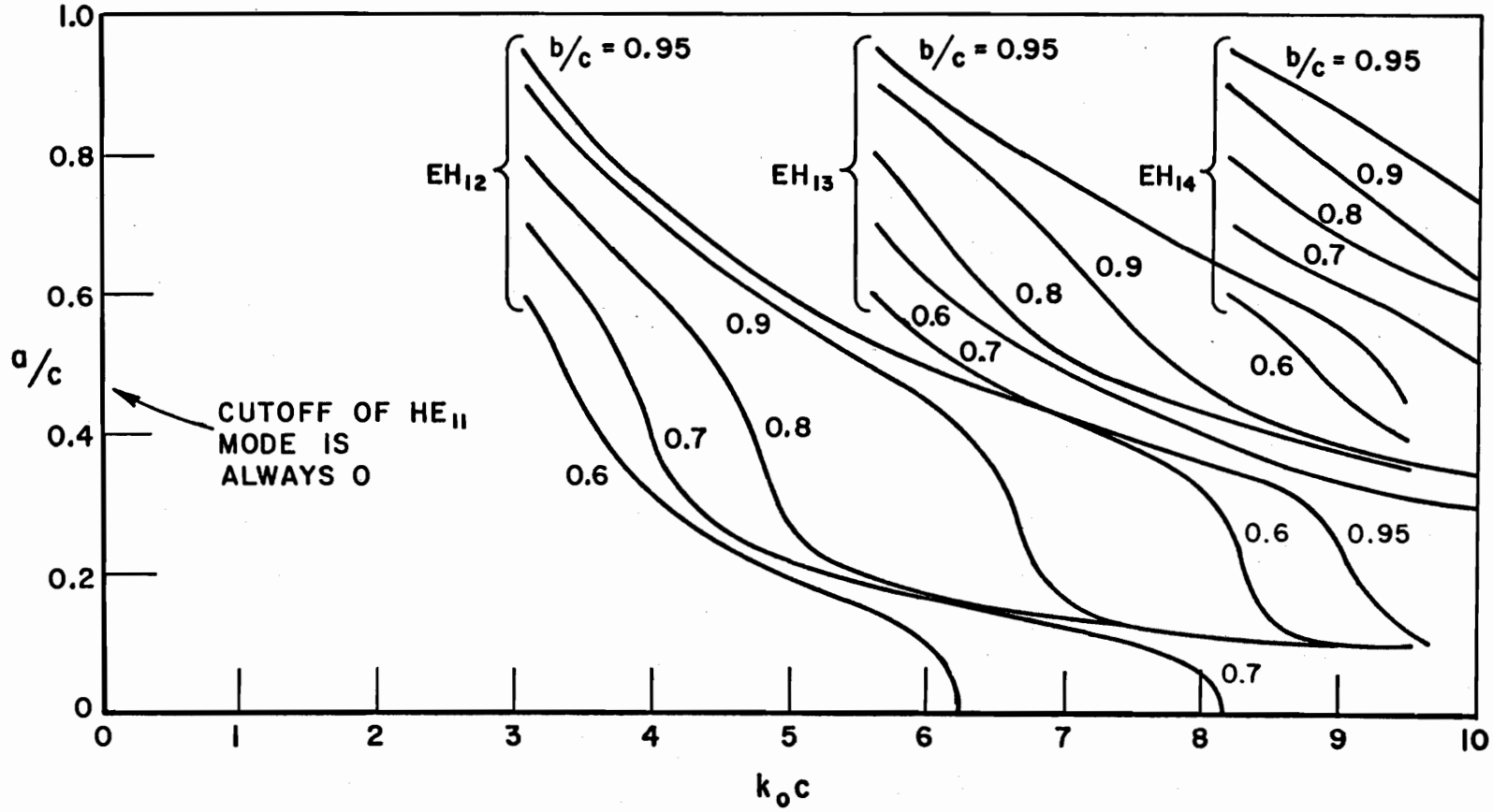

Fig. I-43.--Radii ratio (a/c) versus modal cutoff wavenumbers for dielectric coaxial waveguide: $\epsilon_1=\epsilon_3=2.55$, $\epsilon_2=1.03$ (Eq. (35)).

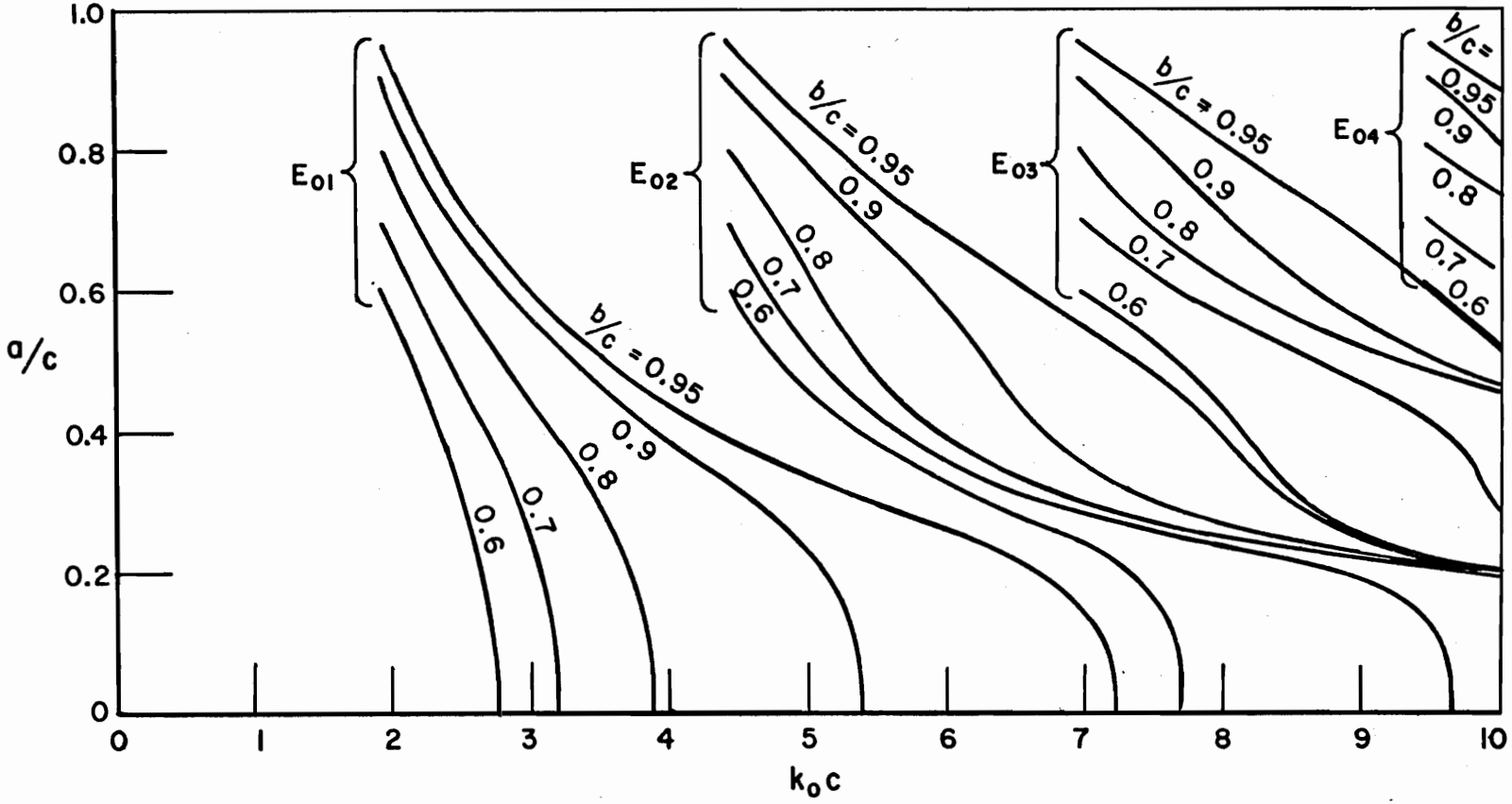

Fig. I-44.--Radii ratio (a/c) versus modal cutoff wavenumbers for dielectric coaxial waveguide: $\epsilon_1=\epsilon_3=2.55$, $\epsilon_2=1.03$ (Eq. (34)).

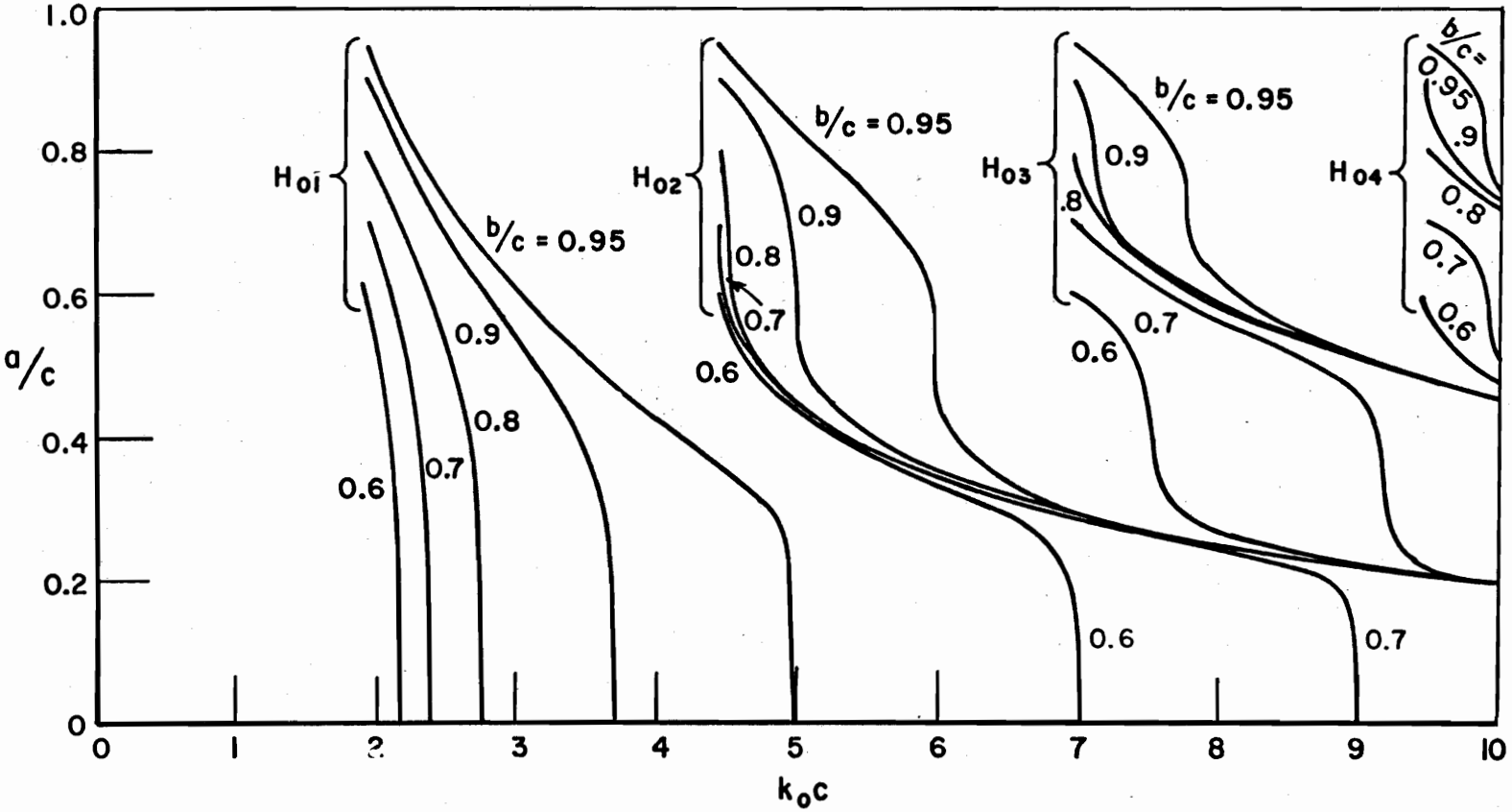

Fig. I-45.--Radii ratio (a/c) versus modal cutoff wavenumbers for dielectric coaxial waveguide: $\epsilon_1=\epsilon_3=2.55$, $\epsilon_2=1.03$ (Eq. (33)).

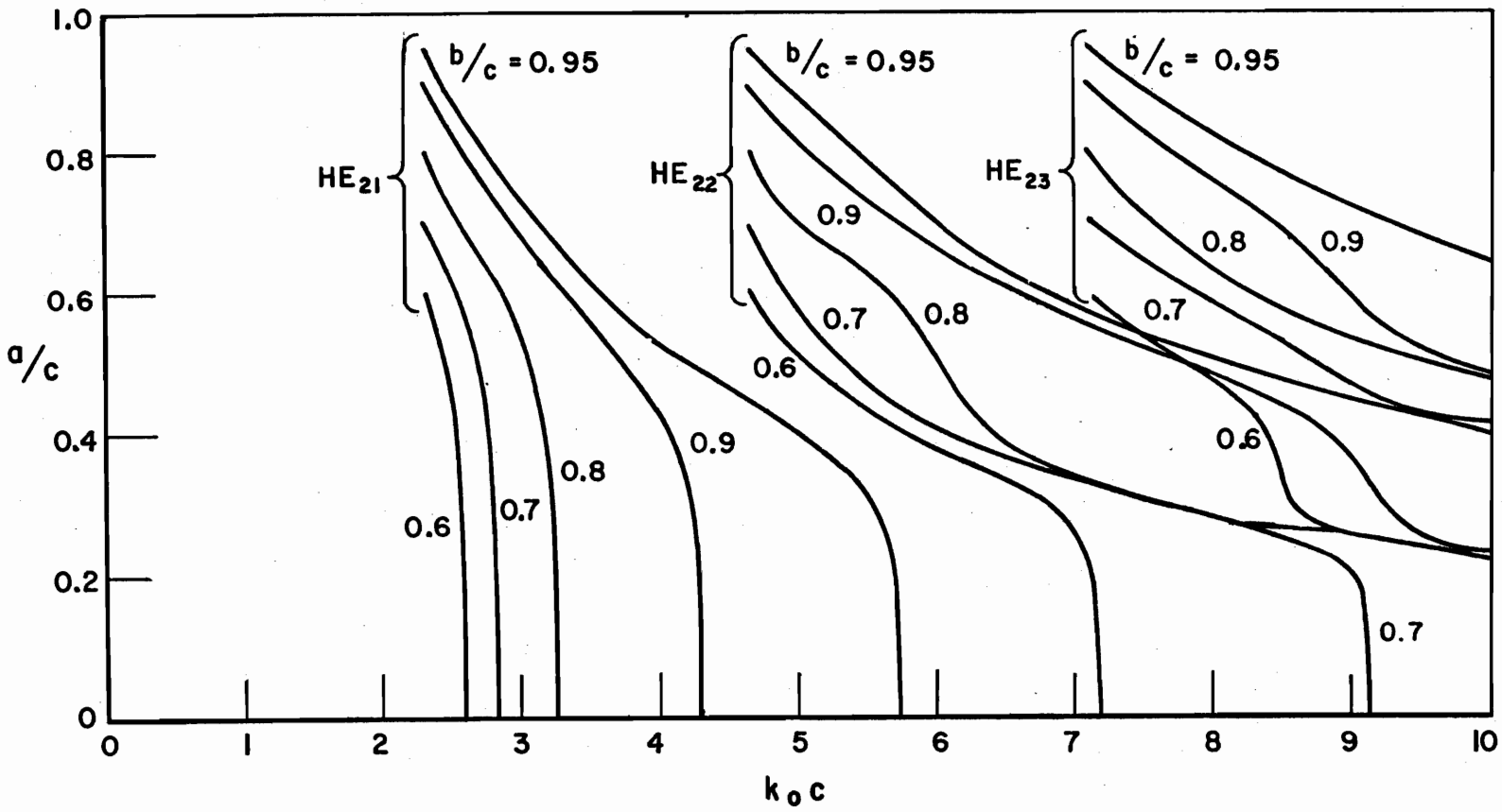

Fig. I-46.--Radii ratio (a/c) versus modal cutoff wavenumbers for dielectric coaxial waveguide: $\epsilon_1=\epsilon_3=2.55$, $\epsilon_2=1.03$ (Eq. (36)).

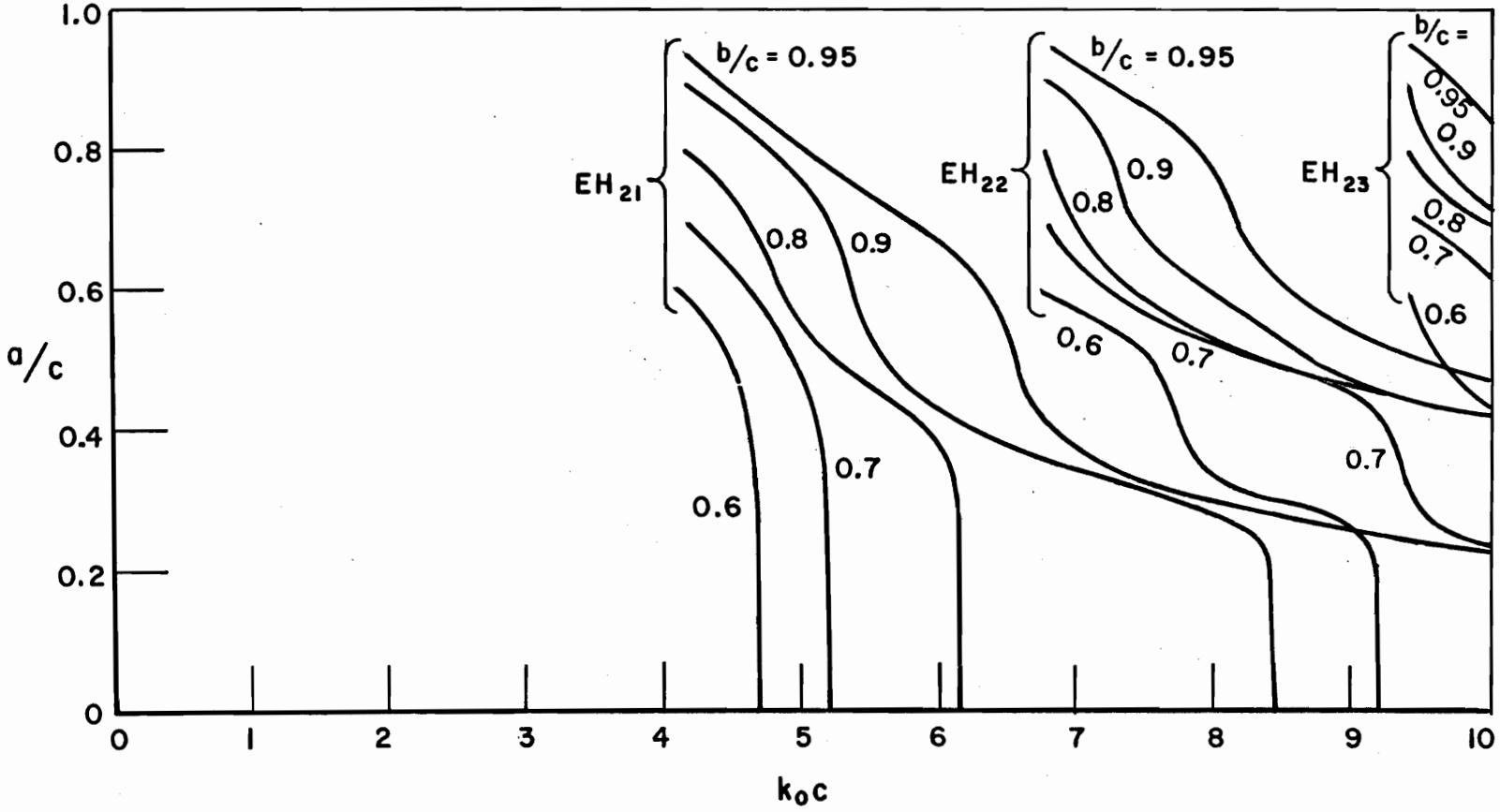

Fig. I-47.--Radii ratio (a/c) versus modal cutoff wavenumbers for dielectric coaxial waveguide: $\epsilon_1=\epsilon_3=2.55$, $\epsilon_2=1.03$ (Eq. (36)).

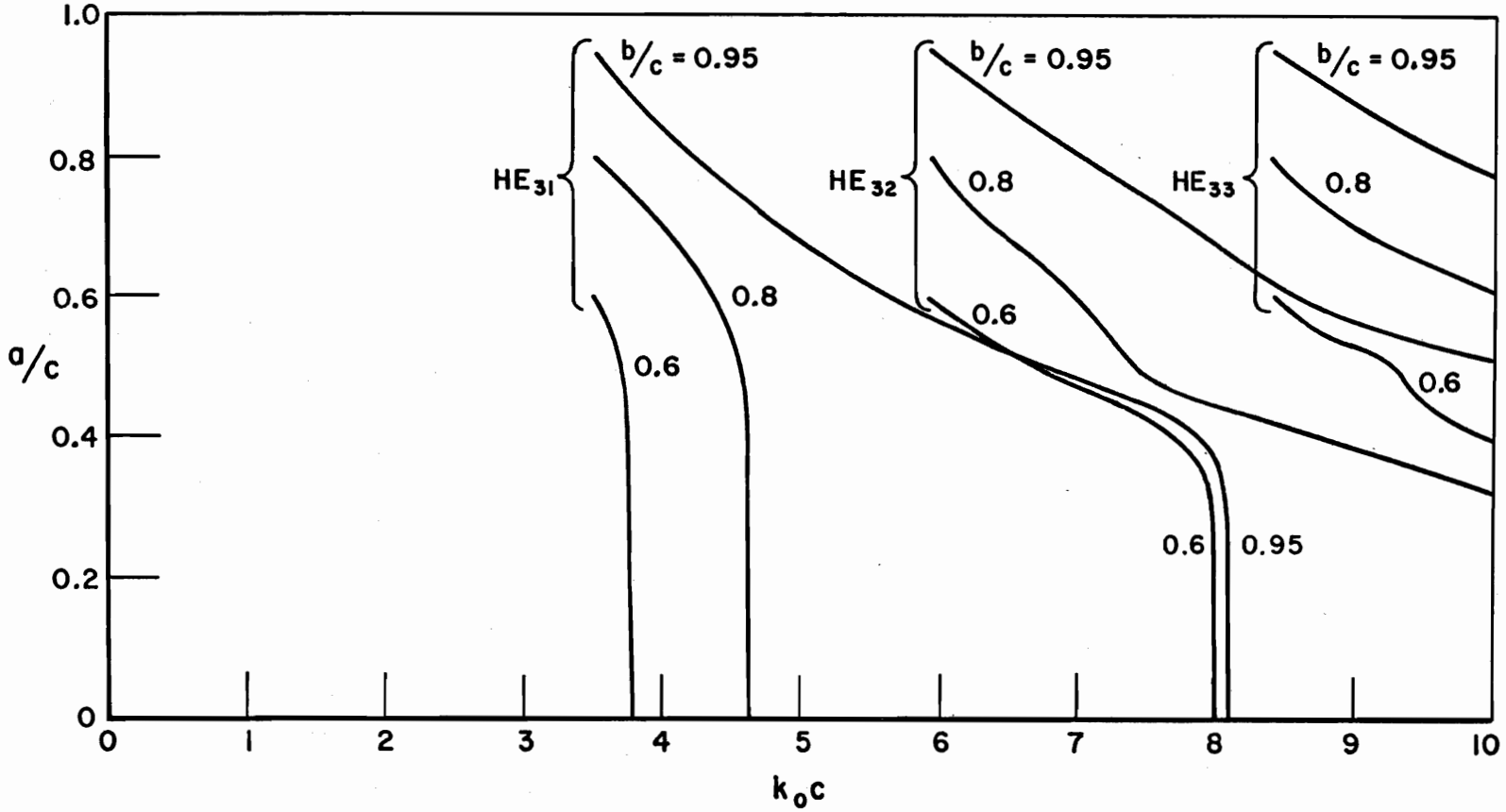

Fig. I-48.--Radii ratio (a/c) versus modal cutoff wavenumbers for dielectric coaxial waveguide: $\epsilon_1=\epsilon_3=2.55$, $\epsilon_2=1.03$ (Eq. (36)).

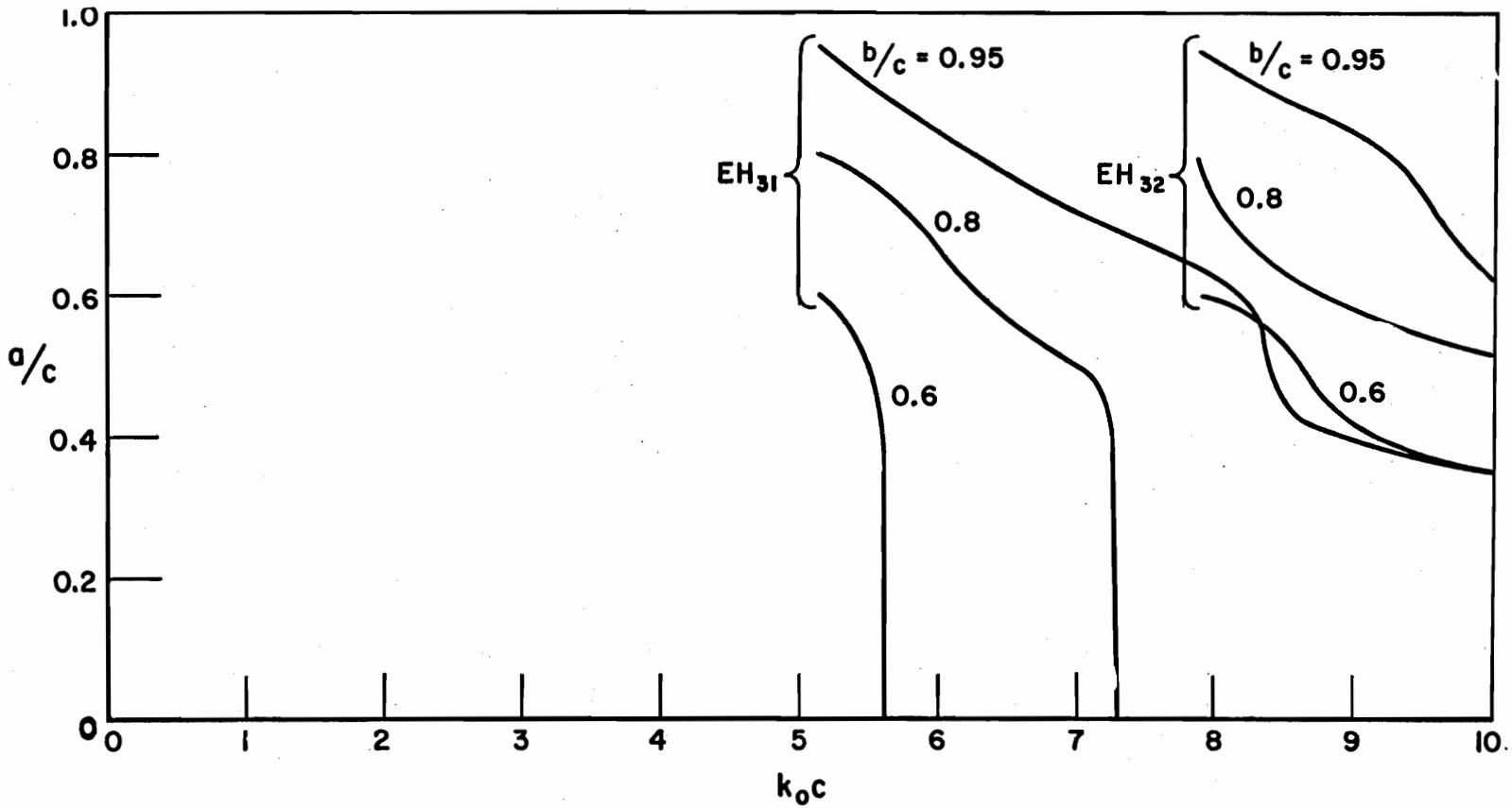

Fig. I-49.--Radii ratio (a/c) versus modal cutoff wavenumbers for dielectric coaxial waveguide: $\epsilon_1=\epsilon_3=2.55$, $\epsilon_2=1.03$ (Eq. (36)).

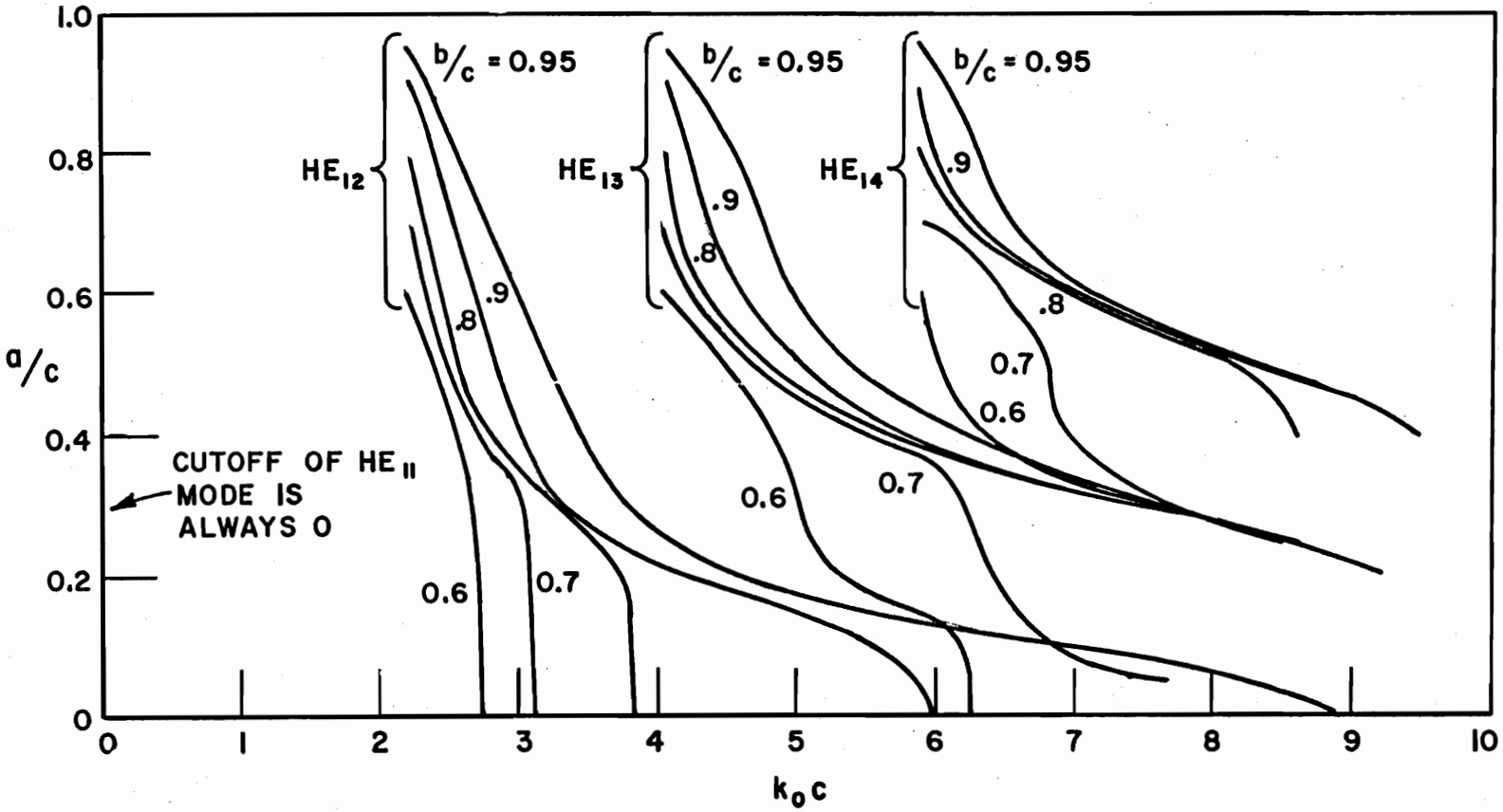

Fig. I-50.--Radii ratio (a/c) versus modal cutoff wavenumbers for dielectric coaxial waveguide: $\epsilon_1=\epsilon_3=4.0$, $\epsilon_2=1.03$ (Eq. (35)).

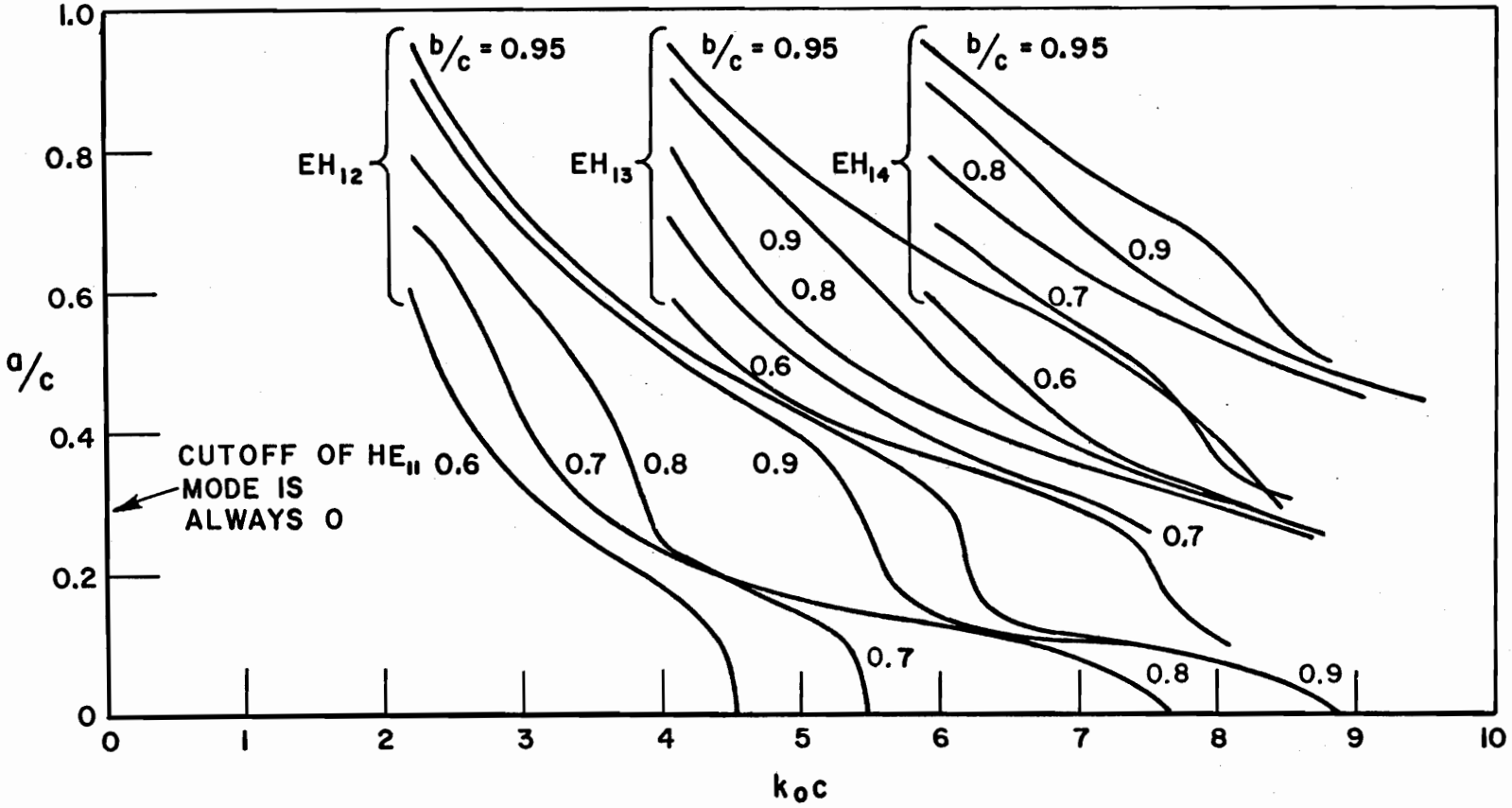

Fig. I-51.--Radii ratio (a/c) versus modal cutoff wavenumbers for dielectric coaxial waveguide: $\epsilon_1=\epsilon_3=4.0$, $\epsilon_2=1.03$ (Eq. (35)).

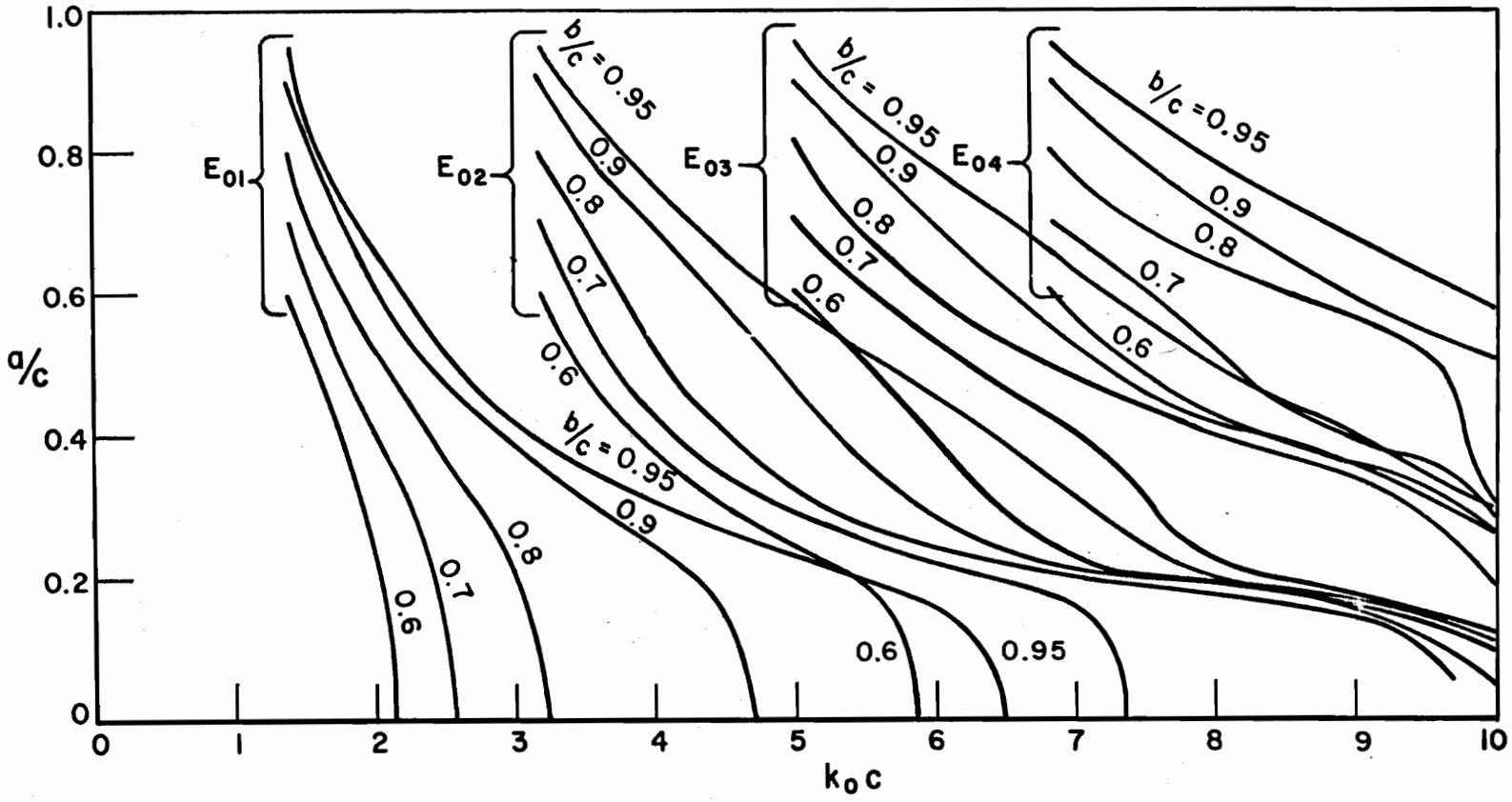

Fig. I-52.--Radii ratio (a/c) versus modal cutoff wavenumbers for dielectric coaxial waveguide: $\epsilon_1=\epsilon_3=4.0$, $\epsilon_2=1.03$ (Eq. (34)).

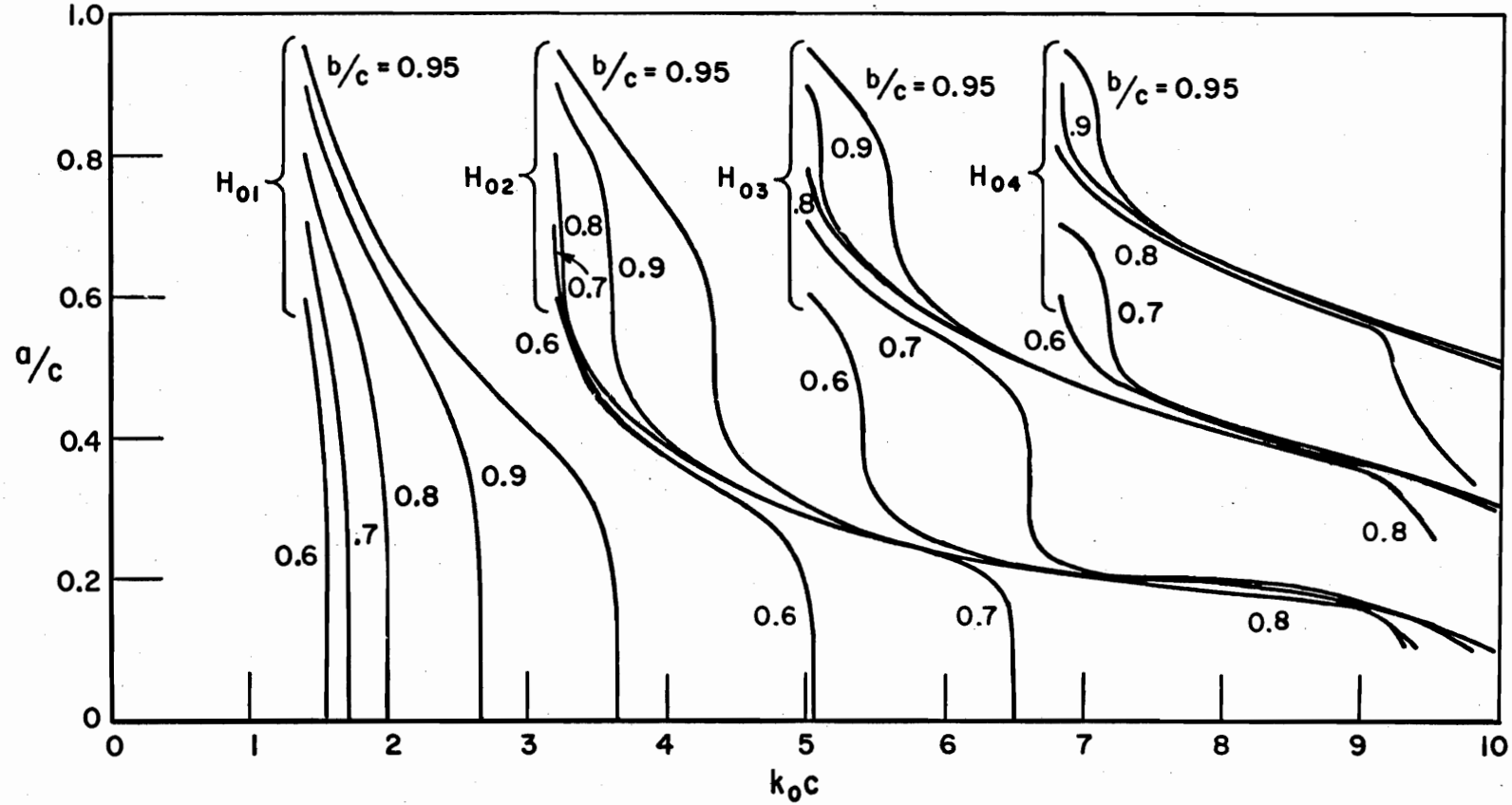

Fig. I-53.--Radii ratio (a/c) versus modal cutoff wavenumbers for dielectric coaxial waveguide: $\epsilon_1 = \epsilon_3 = 4.0$, $\epsilon_2 = 1.03$ (Eq. (33)).

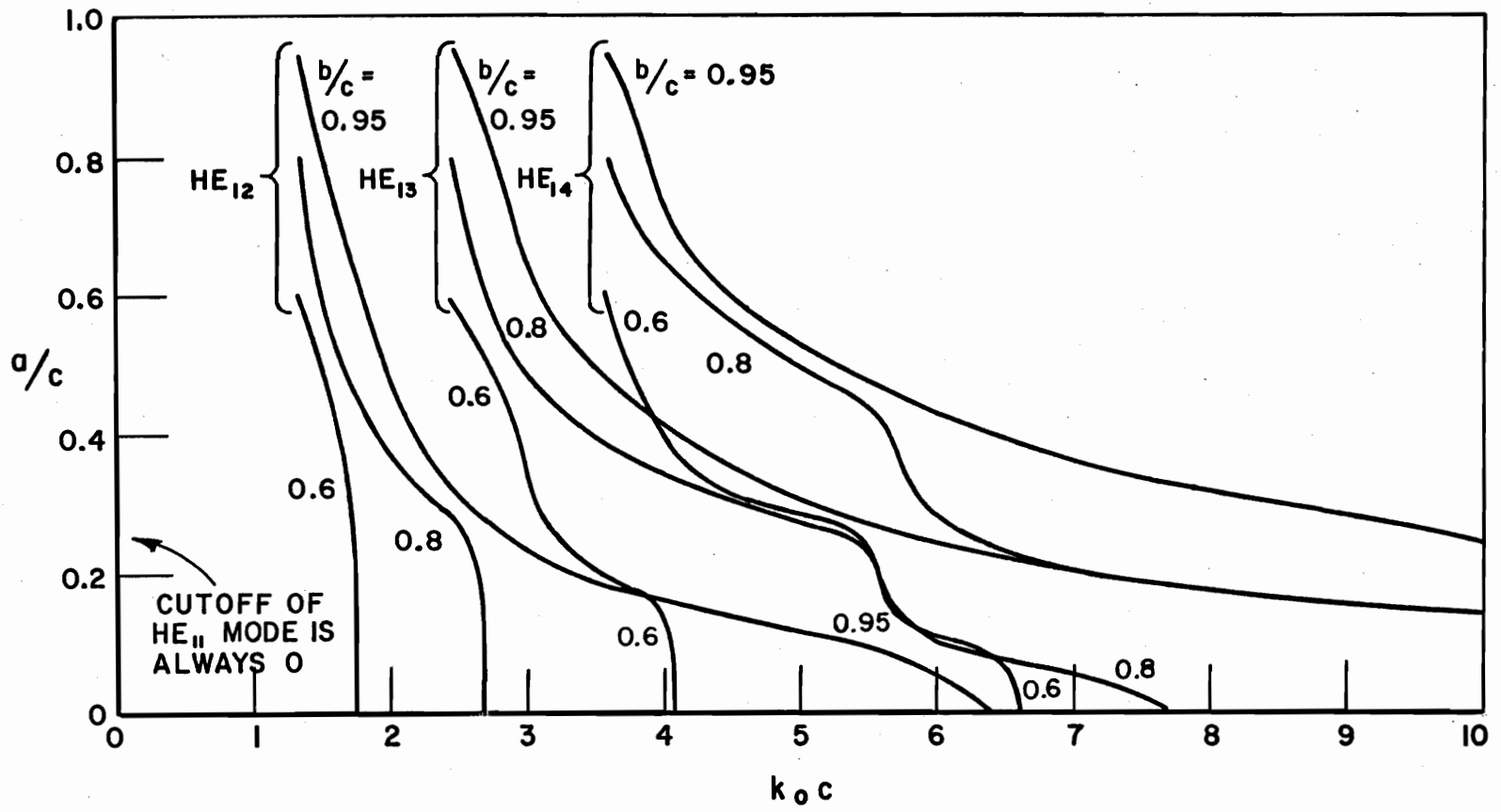

Fig. I-54.--Radii ratio (a/c) versus modal cutoff wavenumbers for dielectric coaxial waveguide: $\epsilon_1=\epsilon_3=9.0$, $\epsilon_2=1.03$ (Eq. (35)).

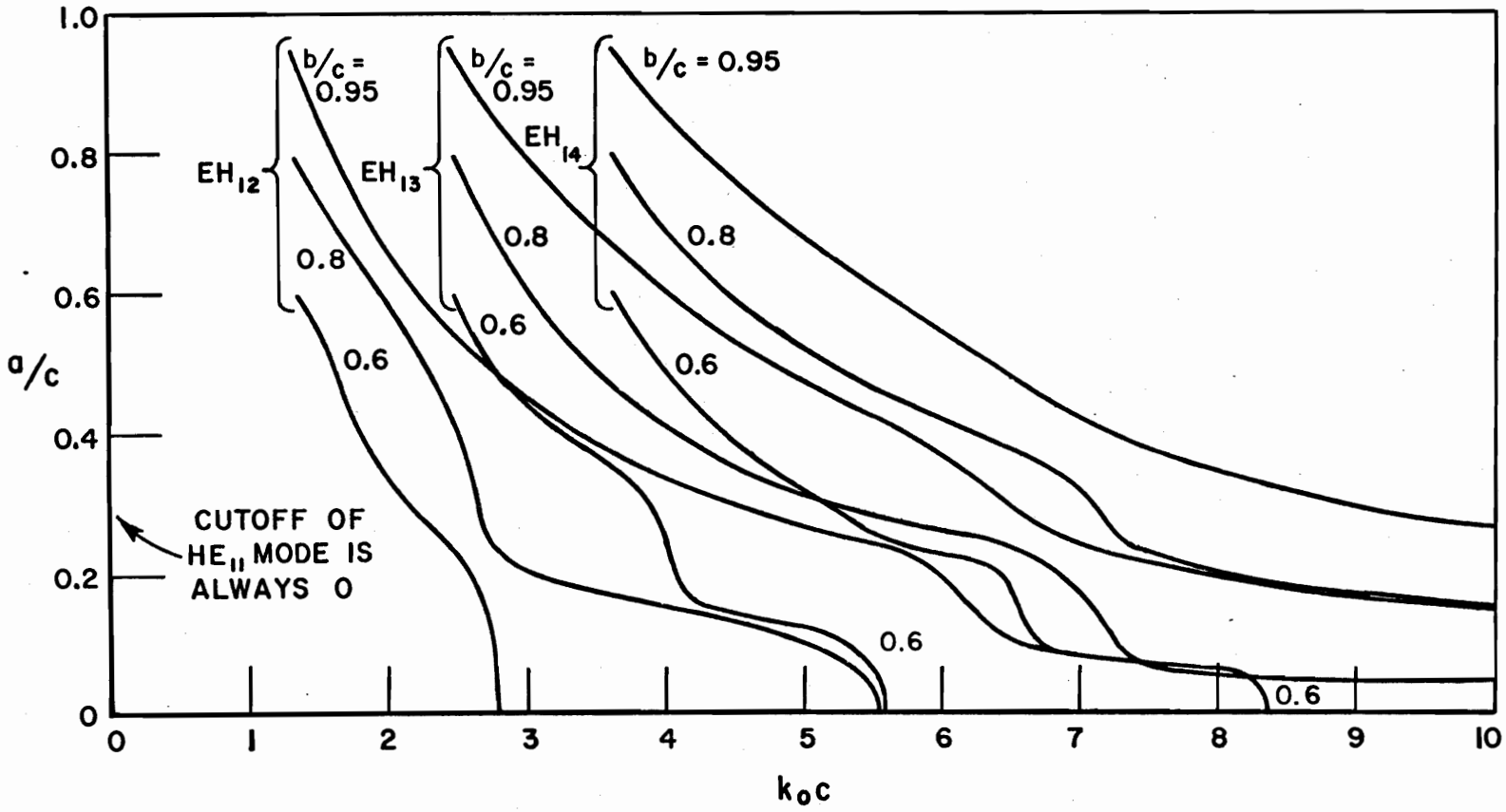

Fig. I-55.--Radii ratio (a/c) versus modal cutoff wavenumbers for dielectric coaxial waveguide: $\epsilon_1=\epsilon_3=9.0$, $\epsilon_2=1.03$ (Eq. (35)).

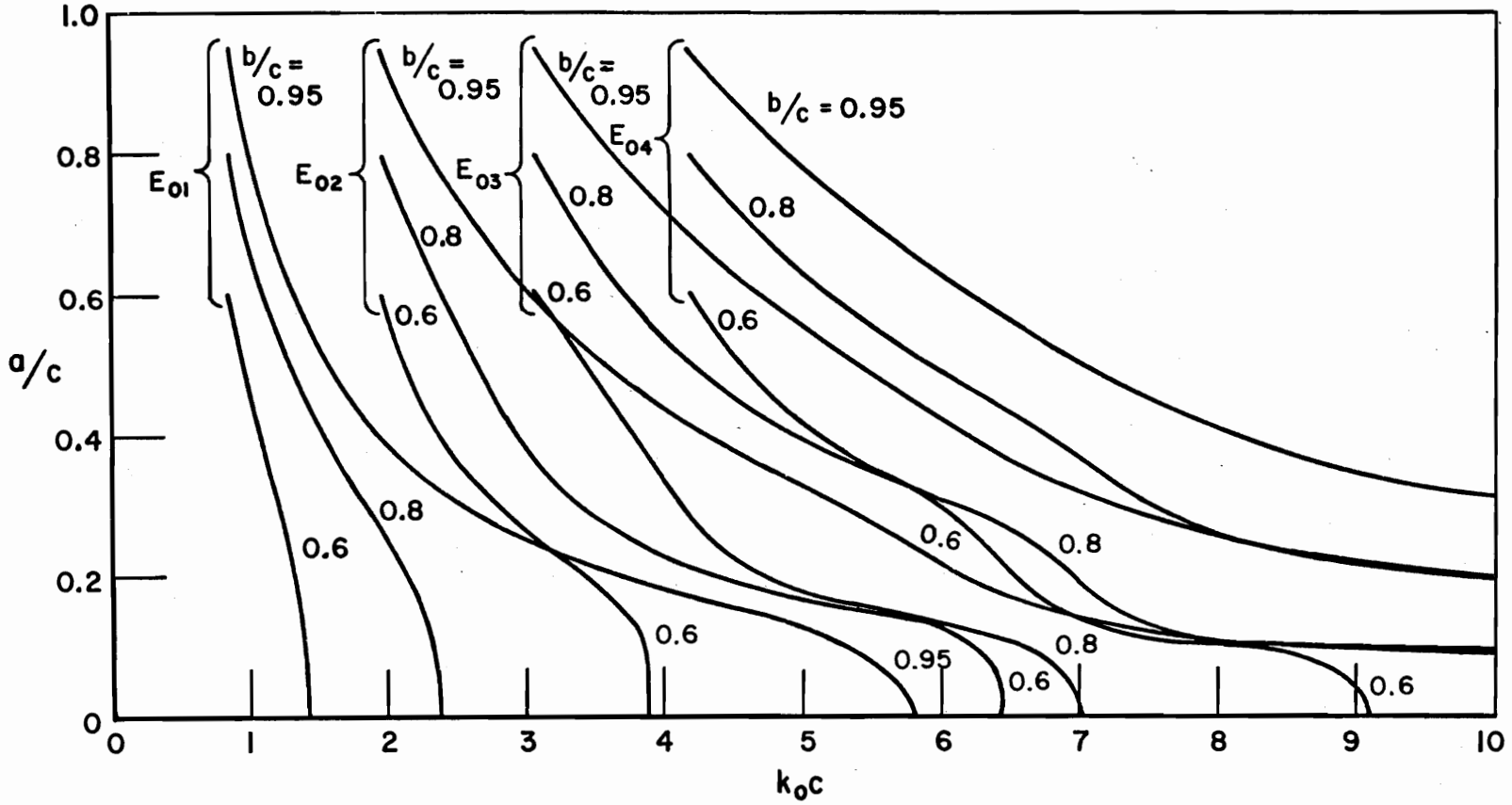

Fig. I-56.--Radii ratio (a/c) versus modal cutoff wavenumbers for dielectric coaxial waveguide: $\epsilon_1=\epsilon_3=9.0$, $\epsilon_2=1.03$ (Eq. (34)).

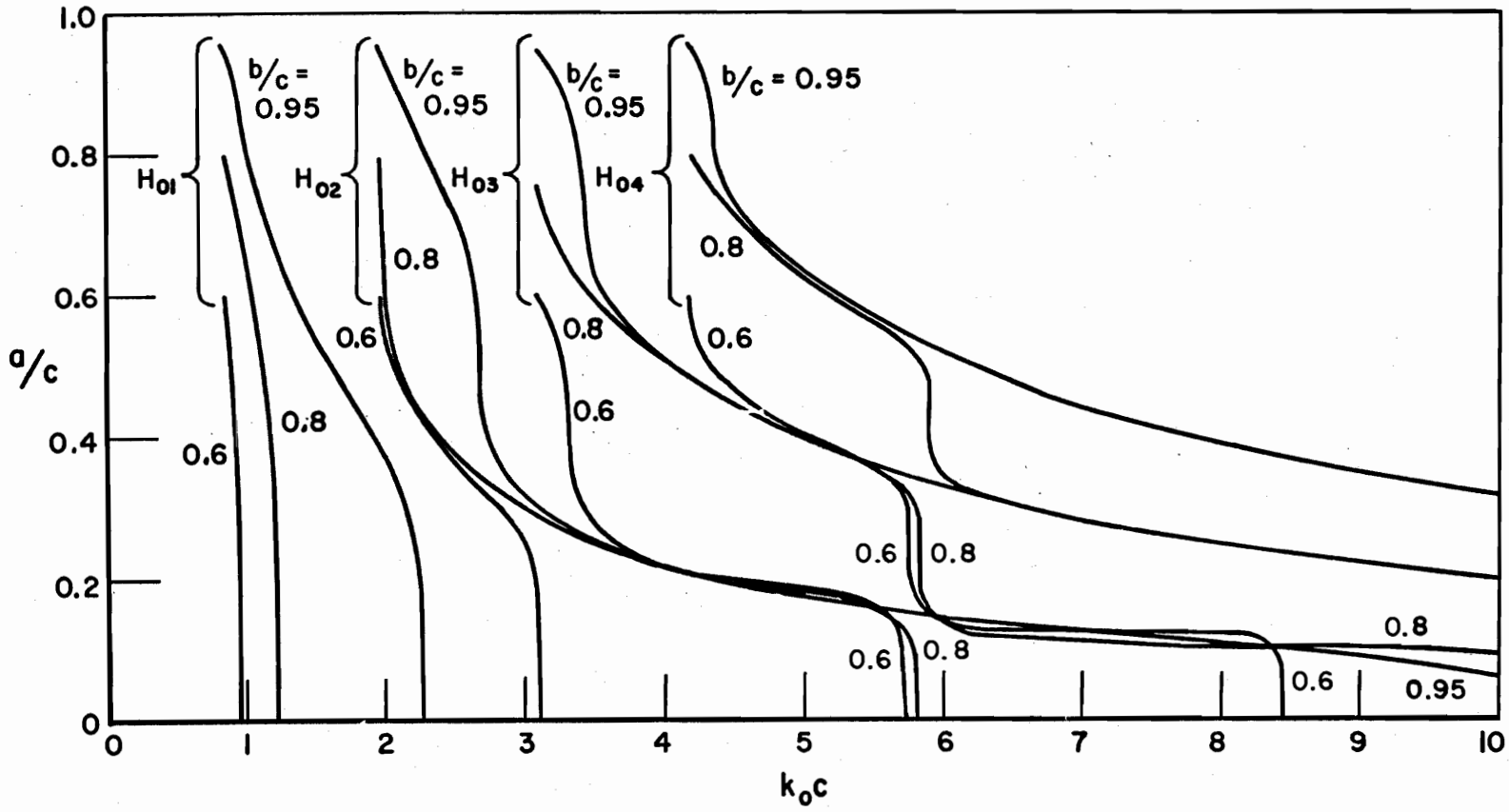

Fig. I-57.--Radii ratio (a/c) versus modal cutoff wavenumbers for dielectric coaxial waveguide: $\epsilon_1=\epsilon_3=9.0$, $\epsilon_2=1.03$ (Eq. (33)).

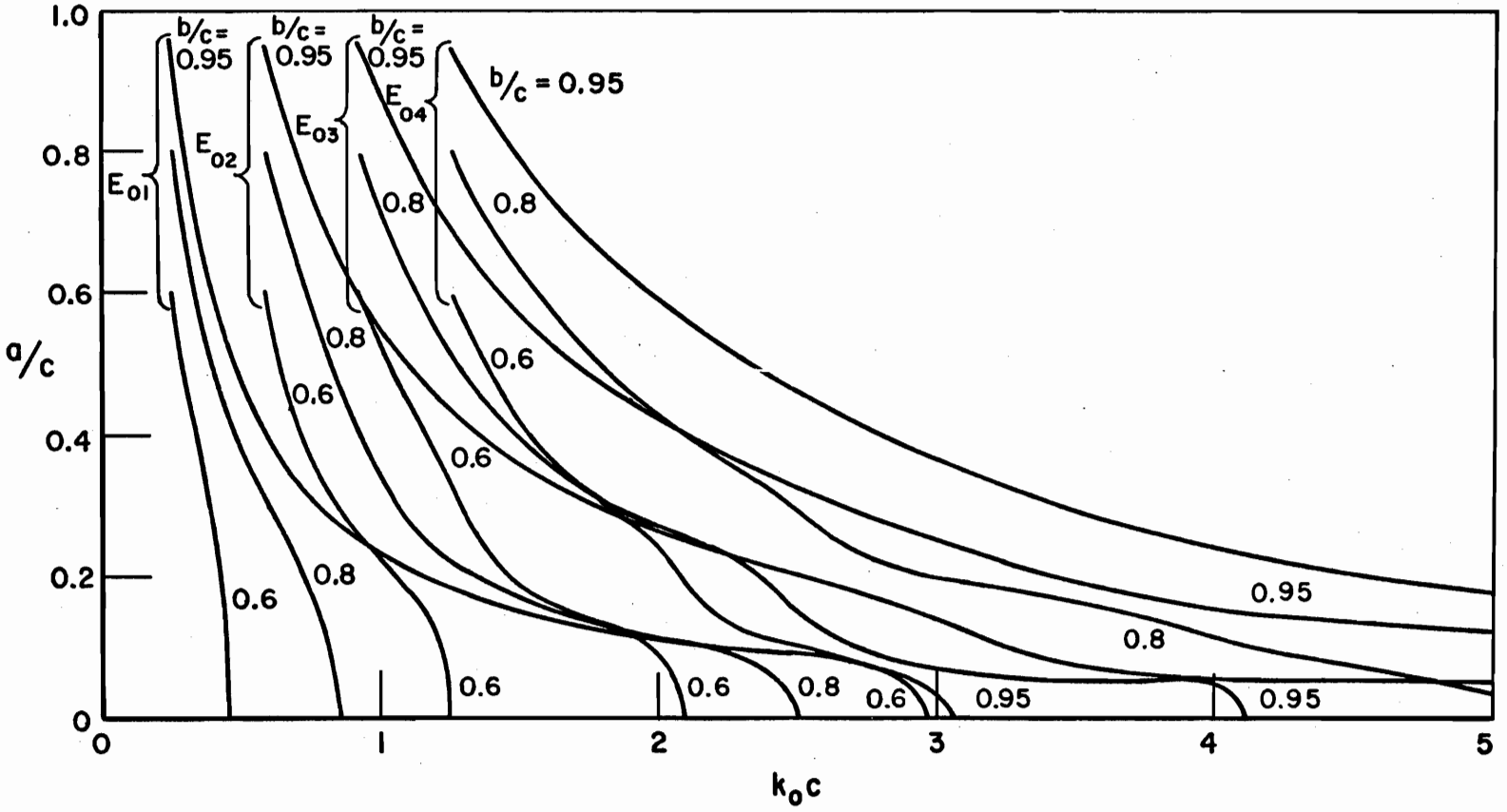

Fig. I-58.--Radii ratio (a/c) versus modal cutoff wavenumbers for dielectric coaxial waveguide: $\epsilon_1 = \epsilon_3 = 90.$, $\epsilon_2 = 1.03$ (Eq. (35)).

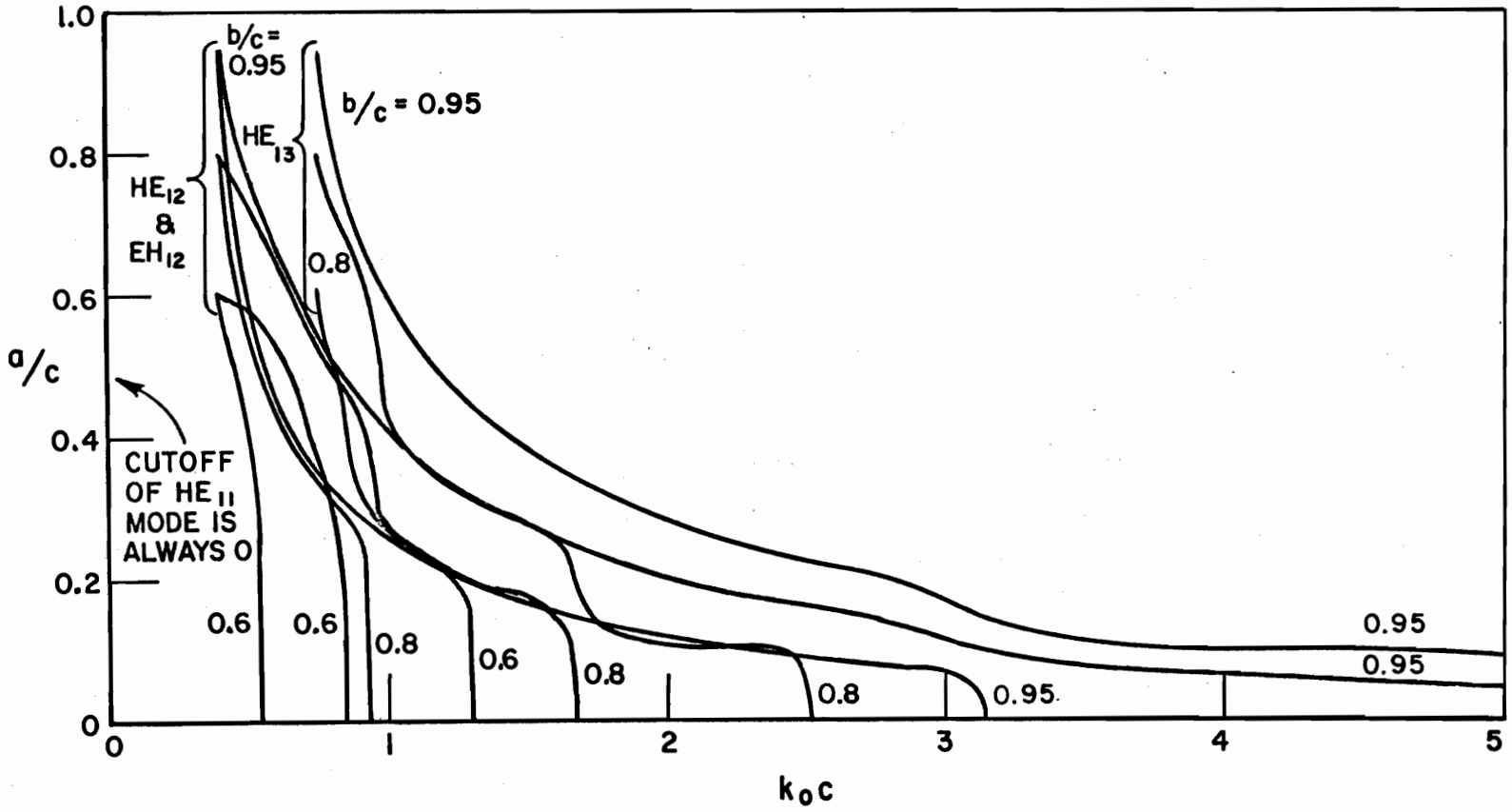

Fig. I-59.--Radii ratio (a/c) versus modal cutoff wavenumbers for dielectric coaxial waveguide: $\epsilon_1=\epsilon_3=90.$, $\epsilon_2=1.03$ (Eq. (34)).

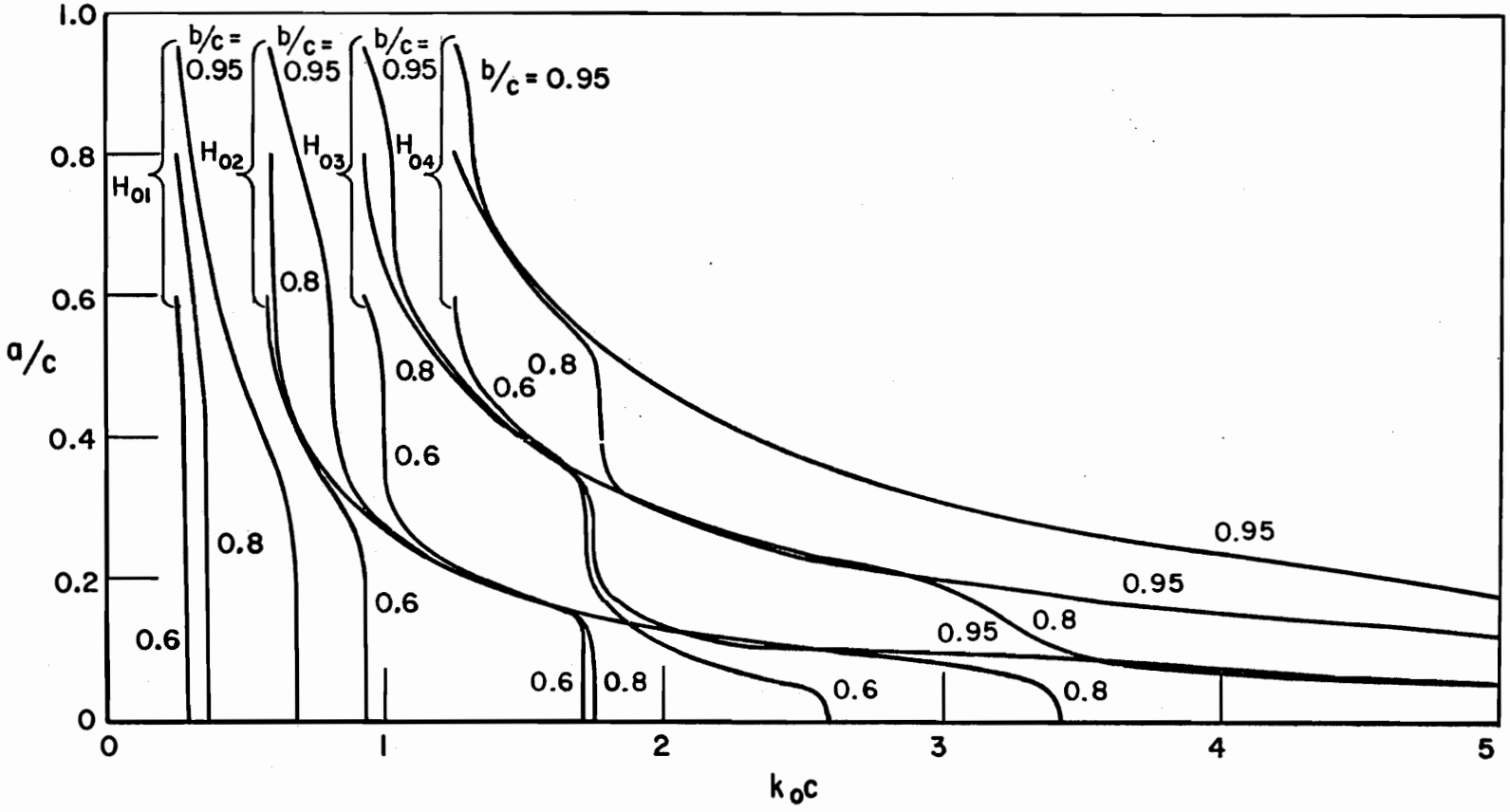
1.0
0.8
0.6
0.4
0.2
0
a/c
0
1
2
3
4
5
k_0c
b/c = 0.95
H_{01}
H_{02}
H_{03}
H_{04}
0.8
0.6
0.95

APPENDIX II
THE FIELDS AND DISPERSION RELATIONS FOR DIELECTRIC COAXIAL WAVEGUIDES

The three coaxial dielectric waveguides considered are shown in Fig. 1 with appropriate parameters and coordinates indicated. The dielectric rod waveguide (ℓ=1), a single dielectric with an infinite surrounding vacuum, has been treated extensively in the literature. Notably, the rod was first considered by Hondros and Debye[1] in 1910. Since that time numerous papers have been published concerning the characteristics of the dielectric rod.[1] The parameter ℓ denotes the number of dielectric interfaces, ℓ=1 for the rod, ℓ=2 for the tube etc. The dielectric tube, a hollow tube filled with another dielectric (usually air) and surrounded by vacuum, apparently was first considered by the Northwestern University Microwave Laboratory[4]. Much of what was known about dielectric rods and tubes by the year 1952 was compiled in a monograph on the subject of dielectric aerials by D. G. Kiely. The dielectric coaxial waveguide (ℓ=3), is constructed of a dielectric rod surrounded concentrically by two hollow dielectric tubes and an infinite surrounding vacuum. Investigation of this structure was forced to wait until very recent times when techniques for handling a computational problem of this size were available.

---

[1]Reference 7 provides an extensive bibliography on the dielectric rod and tube.

The cylindrical dielectric rod surrounded by a hollow cylindrical tube with air between was considered by Barnett[6].

Each configuration can support the H_{om}, E_{om} or hybrid (where both axial H and E components exist simultaneously) modes. Unlike metal waveguides which can support longitudinal conduction currents along their walls, dielectric waveguides unable to support conduction currents, give rise to displacement currents requiring both axial E and H components. The convention of denoting these hybrid modes as HE_{nm} or EH_{nm} (n>1) depending on whether the H_{nm} or E_{nm} metal waveguide type mode, respectively, predominates is used. The HE modes have a lower cutoff value than the corresponding EH modes of the same order. Further, the HE_{11} (hybrid) mode which has no cutoff value is referred to as the dominant mode. The first index n indicates that the phase around the circumference of the cylinder changes n times. The second index m gives the number of standing halfwaves between the guide axis and the outer guide boundary. Unlike ordinary metal guides, the number of halfwaves in a dielectric guide is a whole number only at the cutoff frequency of the mode. Therefore, m is the number of full halfwaves neglecting any portions of incomplete halfwaves.

Using the boundary condition that the tangential fields H_ϕ, E_ϕ, H_z and E_z are continuous across each dielectric interface, expressions relating the modal excitation constants in adjacent regions are found. For the hybrid modes, the number of boundary conditions which must be satisfied increases by four each time another dielectric shell is added.

Requiring the tangential fields to be continuous across all the boundaries gives rise to a set of 4ℓ (ℓ is the number of dielectric interfaces) homogeneous equations relating the modal excitation constants in adjoining regions. In order for a solution to exist for this system of homogeneous equations, the determinant of the coefficients of the modal excitation constants (referred hereafter as the dispersion determinant) must vanish. The order of this determinant which is originally 4ℓ for the hybrid modes is reduced by employing the relations resulting from imposition of the boundary conditions for H_z and E_z at the innermost and outermost interfaces. For each configuration and mode, these equations are shown following the field component expressions at the end of this appendix. For the hybrid modes when $\ell=1$, the outermost and innermost layers are the same and the order of the determinant can only be reduced by 2; but for $\ell>1$, the order of the determinant can be reduced by four. Summarizing, the order of the determinant relating the modal excitation constants of the hybrid modes is

$$\text{(II-1)} \qquad \text{Order of } D = \begin{cases} 2 & \text{if } \ell=1 \\ 4\ell-4 & \text{if } \ell>1 \end{cases}$$

The order of the dispersion determinant for either the H_{om} or E_{om} modes will be half that of the corresponding hybrid mode determinant since only half as many boundary conditions are involved

$$\text{(II-2)} \qquad \text{Order of } D = \begin{cases} 1 & \text{for } \ell=1 \\ 2\ell-2 & \text{for } \ell>1. \end{cases}$$

The dispersion determinant, D, is a function of the normalized propagation factor γ/k_o, the dielectric properties of the cylinder and the various radii of the coaxial layers. The radial wavenumber h_p of region p is related to γ/k_o by

$$\frac{h_p}{k_o} = \sqrt{\epsilon_p - (\gamma/k_o)^2} \qquad \text{(II-3)}$$

where ϵ_p is the relative permittivity of region p. The relative permittivity is

$$\epsilon_p = \frac{\epsilon_p}{\epsilon_o} (1-j \tan \delta_p) \qquad \text{(II-4)}$$

where ϵ_p is the dielectric constant and tan δ_p is the loss tangent of region p. The zeros of determinant D provide the dispersion and attenuation data for a particular configuration and mode. In each case, the determinant is ordered in such a way as to remove all singularities.

There are restrictions on the domain of the propagation factor γ and the external radial wavenumber h_{ext}. Since wave propagation is assumed of the form $e^{j(\omega t-\gamma z)}$, γ must lie in the fourth quadrant for waves traveling in the positive z direction. The function characterizing the external fields is $H_n^{(2)}(h_{ext}\ r)$. To provide the proper asymptotic field behavior, with this restriction on γ,

$$h_{ext} = k_o \sqrt{1 - (\gamma/k_o)^2}$$

must lie in the third quadrant.

Once the dispersion curve for the desired configuration and mode has been obtained, the field components in each region can be determined. This requires the determination of all the modal excitation constants for the given configuration and a particular frequency. Since the dispersion curve represents solutions to a homogeneous set of equations, one of the modal excitation constants must remain arbitrary. If one of the I modal excitation constants is set equal to unity, then the remaining I-1 constants can be determined uniquely from any I-1 of the I simultaneous equations. This procedure has the effect of normalizing the I-1 modal excitation constants to that constant which is set equal to unity.

A compilation of the field equations and dispersion determinants, D of all modes (H_{om}, E_{om} and hybrids) for the dielectric rod, tube, and coaxial waveguide configurations follow.

A. Dielectric Rod Waveguide

1. E_{om} modes

a. Field equations

$$\text{(II-5)} \quad \begin{cases} E_z^I = a_o^I J_o(h_1 r)\, \epsilon^{-j\gamma z} \\ E_z^{II} = b_o^{II} H_o^{(2)}(h_2 r)\, \epsilon^{-j\gamma z} \end{cases}$$

$$\text{(II-6)} \quad \begin{cases} E_r^I = -j a_o^I \frac{\gamma}{h_1} J_o'(h_1 r)\, \epsilon^{-j\gamma z} \\ E_r^{II} = -j b_o^{II} \frac{\gamma}{h_2} H_o^{(2)}(h_2 r)\, \epsilon^{-j\gamma z} \end{cases}$$

$$(II\text{-}7)\quad \begin{cases} H_\phi^I = -ja_o^I \dfrac{k_o\varepsilon_1}{h_1 z_o} J_o'(h_1 r)\ \epsilon^{-j\gamma z} \\ H_\phi^{II} = -jb_o^{II} \dfrac{k_o\varepsilon_2}{h_2 z_o} H_o^{(2)'}(h_2 r)\ \epsilon^{-j\gamma z} \end{cases}$$

where $b_o^{II}/a_o^I = \dfrac{J_o(h_1 a)}{H_o^{(2)}(h_2 a)}$ is obtained from the E_z boundary condition.

b. Dispersion determinant: $D(\gamma/k_o; k_o a)$

$$(II\text{-}8)\quad D = \begin{vmatrix} & \dfrac{b_o^{II}}{} & \dfrac{a_o^I}{} \\ -\varepsilon_1 (h_2 a)^2 J_1(h_1 a) + \varepsilon_2 (h_1 a) J_o(h_1 a) \left[(h_2 a) \dfrac{H_1^{(2)}(h_2 a)}{H_o^{(2)}(h_2 a)} \right] & 0 \\ 0 & 1 \end{vmatrix} = 0$$

2. H_{om} modes

a. Field equations

$$(II\text{-}9)\quad \begin{cases} H_z^I = c_o^I J_o(h_1 r)\ \epsilon^{-j\gamma z} \\ H_z^{II} = d_o^{II} H_o^{(2)}(h_2 r)\ \epsilon^{-j\gamma z} \end{cases}$$

$$(II\text{-}10)\quad \begin{cases} H_r^I = -jc_o^I \frac{\gamma}{h_1} J_o'(h_1 r)\, \epsilon^{-j\gamma z} \\ H_r^{II} = -jd_o^{II} \frac{\gamma}{h_2} H_o^{(2)'}(h_2 r)\, \epsilon^{-j\gamma z} \end{cases}$$

$$(II\text{-}11)\quad \begin{cases} E_\phi^I = jc_o^I \frac{k_o z_o}{h_1} J_o'(h_1 r)\, \epsilon^{-j\gamma z} \\ E_\phi^{II} = jd_o^{II} \frac{k_o z_o}{h_1} H_o^{(2)'}(h_2 r)\, \epsilon^{-j\gamma z} \end{cases}$$

where $d_o^{II}/c_o^I = \dfrac{J_o(h_1 a)}{H_o^{(2)}(h_2 a)}$ is obtained from the H_z boundary condition.

b. Dispersion determinant: $D(\gamma/k_o; k_o a)$

$$(II\text{-}12)\quad D = \begin{vmatrix} -(h_2a)^2 J_1(h_1a) + (h_1a) J_o(h_1a) \left[(h_2a) \dfrac{H_1^{(2)}(h_2a)}{H_o^{(2)}(h_2a)} \right] & \dfrac{d_o^{II}}{c_o^I} \\ 0 & 1 \end{vmatrix} = 0$$

3. Hybrid Modes [HE_{nm} and EH_{nm}]

a. Field equations

$$(II\text{-}13)\quad \begin{cases} E_z^I = a_n^I J_n(h_1 r) \cos n\phi \; \epsilon^{-j\gamma z} \\ E_z^{II} = b_n^{II} H_n^{(2)}(h_2 r) \cos n\phi \; \epsilon^{-j\gamma z} \end{cases}$$

$$(II\text{-}14)\quad \begin{cases} H_z^I = c_n^I J_n(h_1 r) \sin n\phi \; \epsilon^{-j\gamma z} \\ H_z^{II} = d_n^{II} H_n^{(2)}(h_2 r) \sin n\phi \; \epsilon^{-j\gamma z} \end{cases}$$

$$(II\text{-}15)\quad \begin{cases} E_r^I = -j\left[\dfrac{(\gamma/k_o)}{(h_1/k_o)} J_n'(h_1 r)\, a^I + n \dfrac{Z_o}{(h_1/k_o)^2} \dfrac{J_n(h_1 r)}{k_o r} c_n^I\right] \cos n\phi \; \epsilon^{-j\gamma z} \\ E_r^{II} = -j\left[\dfrac{(\gamma/k_o)}{(h_2/k_o)} H_n^{(2)'}(h_2 r)\, b_n^{II} + n \dfrac{Z_o}{(h_2/k_o)^2} \dfrac{H_n^{(2)}(h_2 r)}{k_o r} d_n^{II}\right] \cos n\phi \; \epsilon^{-j\gamma z} \end{cases}$$

(II-16)

$$\begin{cases} H_r^I = -j\left[n \dfrac{\varepsilon_1}{Z_o} \dfrac{1}{(h_1/k_o)^2} \dfrac{J_n(h_1 r)}{k_o r} a_n^I \right. \\ \qquad\qquad \left. + \dfrac{(\gamma/k_o)}{(h_1/k_o)} J_n'(h_1 r)\, c_n^I \right] \sin n\phi\, \epsilon^{-j\gamma z} \\ H_r^{II} = -j\left[n \dfrac{\varepsilon_2}{Z_o} \dfrac{1}{(h_2/k_o)^2} \dfrac{H_n^{(2)}(h_2 r)}{k_o r} b_n^{II} \right. \\ \qquad\qquad \left. + \dfrac{(\gamma/k_o)}{(h_2/k_o)} H_n^{(2)'}(h_2 r)\, d_n^{II} \right] \sin n\phi\, \epsilon^{-j\gamma z} \end{cases}$$

(II-17)

$$\begin{cases} E_\phi^I = j\left[n \dfrac{(\gamma/k_o)}{(h_1/k_o)^2} \dfrac{J_n(h_1 r)}{k_o r} a_n^I \right. \\ \qquad\qquad \left. + \dfrac{Z_o}{(h_1/k_o)} J_n'(h_1 r)\, c_n^I \right] \sin n\phi\, \epsilon^{-j\gamma z} \\ E_\phi^{II} = j\left[n \dfrac{(\gamma/k_o)}{(h_2/k_o)^2} \dfrac{H_n^{(2)}(h_2 r)}{k_o r} b_n^{II} \right. \\ \qquad\qquad \left. + \dfrac{Z_o}{(h_2/k_o)} H_n^{(2)'}(h_2 r)\, d_n^{II} \right] \sin n\phi\, \epsilon^{-j\gamma z} \end{cases}$$

$$
(II\text{-}18)\quad
\begin{cases}
H_\phi^I = -j\left[\dfrac{\varepsilon_1}{Z_o}\dfrac{1}{(h_1/k_o)}J_n'(h_1r)\,a_n^I \right. \\
\qquad\qquad \left. + n\dfrac{(\gamma/k_o)}{(h_1/k_o)^2}\dfrac{J_n(h_1r)}{k_or}\,c_n^I\right]\cos n\phi\;\epsilon^{-j\gamma z} \\
H_\phi^{II} = -j\left[\dfrac{\varepsilon_2}{Z_o}\dfrac{1}{(h_2/k_o)}H_n^{(2)'}(h_2r)\,b_n^{II} \right. \\
\qquad\qquad \left. + n\dfrac{(\gamma/k_o)}{(h_2/k_o)^2}\dfrac{H_n^{(2)}(h_2r)}{k_or}\,d_n^{II}\right]\cos n\phi\;\epsilon^{-j\gamma z}
\end{cases}
$$

where $a_n^I = \dfrac{H_n^{(2)}(h_2a)}{J_n(h_1a)}\,b_n^{II}$ and $c_n^I = \dfrac{H_n^{(2)}(h_2a)}{J_n(h_1a)}\,d_n^{II}$

are obtained from the H_z and E_z boundary conditions.

b. Dispersion determinant: $D(\gamma/k_o;k_oa)$

$$
(II\text{-}19)\quad D = \begin{vmatrix}
\dfrac{b_n^{II}}{(h_2a)^2(h_1a)\varepsilon_1J_n'(h_1a) \\ -(h_2a)(h_1a)^2\varepsilon_2J_n(h_1a)\dfrac{H_n^{(2)'}(h_2a)}{H_n^{(2)}(h_2a)}} & \dfrac{d_n^{II}}{n(\gamma/k_o)[(h_2a)^2-(h_1a)^2]J_n(h_1a)} \\
n(\gamma/k_o)[(h_2a)^2-(h_1a)^2]J_n(h_1a) & \dfrac{(h_2a)^2(h_1a)J_n'(h_1a) \\ -(h_2a)(h_1a)^2J_n(h_1a)\dfrac{H_n^{(2)'}(h_2a)}{H_n^{(2)}(h_2a)}}
\end{vmatrix} = 0
$$

B. Dielectric Tube Waveguide

1. E_{om} modes

a. Field equations

$$(II\text{-}20)\quad \begin{cases} E_z^I = a_o^I\, J_o(h_1 r)\, \epsilon^{-j\gamma z} \\ E_z^{II} = [a_o^{II}\, J_o(h_2 r) + b_o^{II}\, N_o(h_2 r)]\epsilon^{-j\gamma z} \\ E_z^{III} = b_o^{III}\, H_o^{(2)}(h_3 r)\, \epsilon^{-j\gamma z} \end{cases}$$

$$(II\text{-}21)\quad \begin{cases} E_r^I = -j\, \dfrac{(\gamma/k_o)}{(h_1/k_o)}\, J_o'(h_1 r)\, a_o^I\, \epsilon^{-j\gamma z} \\ E_r^{II} = -j\, \dfrac{(\gamma/k_o)}{(h_2/k_o)}\, [J_o'(h_2 r)\, a_o^{II} + N_o'(h_2 r)\, b_o^{II}]\epsilon^{-j\gamma z} \\ E_r^{III} = -j\, \dfrac{(\gamma/k_o)}{(h_3/k_o)}\, H_o^{(2)'}(h_3 r)\, b_o^{III}\, \epsilon^{-j\gamma z} \end{cases}$$

$$(II\text{-}22)\quad \begin{cases} H_\phi^I = -j\, \dfrac{\varepsilon_1}{Z_o}\, \dfrac{1}{(h_1/k_o)}\, J_o'(h_1 r)\, a_o^I\, \epsilon^{-j\gamma z} \\ H_\phi^{II} = -j\, \dfrac{\varepsilon_2}{Z_o}\, \dfrac{1}{(h_2/k_o)}\, [J_o'(h_2 r)\, a_o^{II} + N_o'(h_2 r)\, b_o^{II}]\epsilon^{-j\gamma z} \\ H_\phi^{III} = -j\, \dfrac{\varepsilon_3}{Z_o}\, \dfrac{1}{(h_3/k_o)}\, H_o^{(2)'}(h_3 r)\, b_o^{III}\, \epsilon^{-j\gamma z} \end{cases}$$

where

$$\begin{cases} a_o^I = \dfrac{J_o(h_2 a)}{J_o(h_1 a)}\, a_o^{II} + \dfrac{N_o(h_2 a)}{J_o(h_1 a)}\, b_o^{II} \\ b_o^{III} = \dfrac{J_o(h_2 b)}{H_o^{(2)}(h_3 b)}\, a_o^{II} + \dfrac{N_o(h_2 b)}{H_o^{(2)}(h_3 b)}\, b_o^{II} \end{cases}$$

are obtained from the boundary conditions on E_z at the innermost and outermost boundaries.

b. Dispersion determinant: $D(\gamma/k_o; k_o a; k_o b)$

$$(II\text{-}23)\quad D = \begin{vmatrix} \overbrace{\epsilon_1\left(\frac{h_2}{k_o}\right) J_o'(h_1 a) J_o(h_2 a) - \epsilon_2\left(\frac{h_1}{k_o}\right) J_o(h_1 a) J_o'(h_2 a)}^{a_o^{II}} & \overbrace{\epsilon_1\left(\frac{h_2}{k_o}\right) J_o'(h_1 a) N_o(h_2 a) - \epsilon_2\left(\frac{h_1}{k_o}\right) J_o(h_1 a) N_o'(h_2 a)}^{b_o^{II}} \\ \frac{h_2}{k_o} J_o(h_2 b) + \frac{\epsilon_2}{\epsilon_3} J_o'(h_2 b) \frac{(h_3/k_o) H_o^{(2)}(h_3 b)}{H_1^{(2)}(h_3 b)} & \left(\frac{h_2}{k_o}\right) N_o(h_2 b) + \frac{\epsilon_2}{\epsilon_3} N_o'(h_2 b) \frac{(h_3/k_o) H_o^{(2)}(h_3 b)}{H_1^{(2)}(h_3 b)} \end{vmatrix} = 0$$

2. H_{om} modes

a. Field equations

$$(II\text{-}24)\quad \begin{cases} H_z^I = c_o^I J_o(h_1 r)\, \epsilon^{-j\gamma z} \\ H_z^{II} = [c_o^{II} J_o(h_2 r) + d_o^{II} N_o(h_2 r)]\, \epsilon^{-j\gamma z} \\ H_z^{III} = d_o^{III} H_o^{(2)}(h_3 r)\, \epsilon^{-j\gamma z} \end{cases}$$

$$(II\text{-}25)\quad \begin{cases} H_r^I = -j \dfrac{(\gamma/k_o)}{(h_1/k_o)} J_o'(h_1 r)\, c_o^I\, \epsilon^{-j\gamma z} \\ H_r^{II} = -j \dfrac{(\gamma/k_o)}{(h_2/k_o)} [J_o'(h_2 r)\, c_o^{II} + N_o'(h_2 r)\, d_o^{II}]\, \epsilon^{-j\gamma z} \\ H_r^{III} = -j \dfrac{(\gamma/k_o)}{(h_3/k_o)} H_o^{(2)'}(h_3 r)\, d_o^{III}\, \epsilon^{-j\gamma z} \end{cases}$$

$$(II\text{-}26)\quad \begin{cases} E_\phi^I = j\,\dfrac{Z_o}{(h_1/k_o)}\,J_o'(h_1 r)\,c_o^I\,\epsilon^{-j\gamma z} \\ E_\phi^{II} = j\,\dfrac{Z_o}{(h_2/k_o)}\,[J_o'(h_2 r)\,c_o^{II} + N_o'(h_2 r)\,d_o^{II}]\,\epsilon^{-j\gamma z} \\ E_\phi^{III} = j\,\dfrac{Z_o}{(h_3/k_o)}\,H_o^{(2)'}(h_3 r)\,d_o^{III}\,\epsilon^{-j\gamma z} \end{cases}$$

where

$$\begin{cases} c_o^I = \dfrac{J_o(h_2 a)}{J_o(h_1 a)}\,c_o^{II} + \dfrac{N_o(h_2 a)}{J_o(h_1 a)}\,d_o^{II} \\ d_o^{III} = \dfrac{J_o(h_2 b)}{H_o^{(2)}(h_3 b)}\,c_o^{II} + \dfrac{N_o(h_2 b)}{H_o^{(2)}(h_3 b)}\,d_o^{II} \end{cases}$$

are obtained from the boundary conditions on H_z at the innermost and outermost boundaries.

b. Dispersion determinant: $D(\gamma/k_o; k_o a; k_o b)$

$$(II\text{-}27)\quad D = \begin{vmatrix} \left(\frac{h_2}{k_o}\right) J_o'(h_1 a) J_o(h_2 a) - \left(\frac{h_1}{k_o}\right) J_o(h_1 a) J_o'(h_2 a) & \left(\frac{h_2}{k_o}\right) J_o'(h_1 a) N_o(h_2 a) - \left(\frac{h_1}{k_o}\right) J_o(h_1 a) N_o'(h_2 a) \\ \left(\frac{h_2}{k_o}\right) J_o(h_2 b) + J_o'(h_2 b)\,\dfrac{(h_3/k_o) H_o^{(2)}(h_3 b)}{H_1^{(2)}(h_3 b)} & \left(\frac{h_2}{k_o}\right) N_o(h_2 b) + N_o'(h_2 b)\,\dfrac{(h_3/k_o) H_o^{(2)}(h_3 b)}{H_1^{(2)}(h_3 b)} \end{vmatrix} = 0$$

3. Hybrid Modes [HE_{nm} and EH_{nm}]

a. Field equations

$$(II\text{-}28)\quad \begin{cases} E_z^I = a_n^I\, J_n(h_1 r)\cos n\phi\, \epsilon^{-j\gamma z} \\ E_z^{II} = [a_n^{II}\, J_n(h_2 r) + b_n^{II}\, N_n(h_2 r)]\cos n\phi\, \epsilon^{-j\gamma z} \\ E_z^{III} = b_n^{III}\, H_n^{(2)}(h_3 r)\cos n\phi\, \epsilon^{-j\gamma z} \end{cases}$$

$$(II\text{-}29)\quad \begin{cases} H_z^I = c_n^I\, J_n(h_1 r)\sin n\phi\, \epsilon^{-j\gamma z} \\ H_z^{II} = [c_n^{II}\, J_n(h_2 r) + d_n^{II}\, N_n(h_2 r)]\sin n\phi\, \epsilon^{-j\gamma z} \\ H_z^{III} = d_n^{III}\, H_n^{(2)}(h_3 r)\sin n\phi\, \epsilon^{-j\gamma z} \end{cases}$$

$$(II\text{-}30)\quad \begin{cases} H_\phi^I = -j\left[\dfrac{\varepsilon_1}{(h_1/k_o)Z_o}\, J_n'(h_1 r)a_n^I + \dfrac{n(\gamma/k_o)}{(h_1/k_o)^2}\,\dfrac{J_n(h_1 r)}{(k_o r)}\, c_n^I\right]\cos n\phi\, \epsilon^{-j\gamma z} \\ H_\phi^{II} = -j\left[\dfrac{\varepsilon_2}{(h_2/k_o)Z_o}\,(J_n'(h_2 r)a_n^{II} + N_n'(h_2 r)b_n^{II}) + \dfrac{n(\gamma/k_o)}{(h_2/k_o)^2}\left(\dfrac{J_n(h_2 r)}{(k_o r)}\, c_n^{II} + \dfrac{N_n(h_2 r)}{(k_o r)}\, d_n^{II}\right)\right]\cos n\phi\, \epsilon^{-j\gamma z} \\ H_\phi^{III} = -j\left[\dfrac{\varepsilon_3}{(h_3/k_o)Z_o}\, H_n^{(2)'}(h_3 r)\, b_n^{III} + \dfrac{n(\gamma/k_o)}{(h_3/k_o)^2}\,\dfrac{H_n^{(2)}(h_3 r)}{(k_o r)}\, d_n^{III}\right]\cos n\phi\, \epsilon^{-j\gamma z} \end{cases}$$

(II-31)

$$
\begin{cases}
E_\phi^I = j\left[\dfrac{n(\gamma/k_o)}{(h_1/k_o)^2}\dfrac{J_n(h_1r)}{(k_or)}\,a_n^I + \dfrac{Z_o}{(h_1/k_o)}\,J_n'(h_1r)\,c_n^I\right]\sin n\phi\;\epsilon^{-j\gamma z} \\
E_\phi^{II} = j\left[\dfrac{n(\gamma/k_o)}{(h_2/k_o)^2}\left(\dfrac{J_n(h_2r)}{(k_or)}\,a_n^{II} + \dfrac{N_n(h_2r)}{(k_or)}\,b_n^{II}\right) + \dfrac{Z_o}{(h_2/k_o)}\left(J_n'(h_2r)\,c_n^{II} + N_n'(h_2r)\,d_n^{II}\right)\right]\sin n\phi\;\epsilon^{-j\gamma z} \\
E_\phi^{III} = j\left[\dfrac{n(\gamma/k_o)}{(h_3/k_o)^2}\dfrac{H_n^{(2)}(h_3r)}{(k_or)}\,b_n^{III} + \dfrac{Z_o}{(h_3/k_o)}\,H_n^{(2)'}(h_3r)\,d_n^{III}\right]\sin n\phi\;\epsilon^{-j\gamma z}
\end{cases}
$$

(II-32)

$$
\begin{cases}
H_r^I = -j\left[\dfrac{n\varepsilon_1}{(h_1/k_o)^2 Z_o}\dfrac{J_n(h_1r)}{(k_or)}\,a_n^I + \dfrac{(\gamma/k_o)}{(h_1/k_o)}\,J_n'(h_1r)\,c_n^I\right]\sin n\phi\;\epsilon^{-j\gamma z} \\
H_r^{II} = -j\left[\dfrac{n\varepsilon_2}{(h_2/k_o)^2 Z_o}\left(\dfrac{J_n(h_2r)}{(k_or)}\,a_n^{II} + \dfrac{N_n(h_2r)}{(k_or)}\,b_n^{II}\right) + \dfrac{(\gamma/k_o)}{(h_2/k_o)}\left(J_n'(h_2r)\,c_n^{II} + N_n'(h_2r)\,d_n^{II}\right)\right]\sin n\phi\;\epsilon^{-j\gamma z} \\
H_r^{III} = -j\left[\dfrac{n\varepsilon_3}{(h_3/k_o)^2 Z_o}\dfrac{H_n^{(2)}(h_3r)}{(k_or)}\,b_n^{III} + \dfrac{(\gamma/k_o)}{(h_3/k_o)}\,H_n^{(2)'}(h_3r)\,d_n^{III}\right]\sin n\phi\;\epsilon^{-j\gamma z}
\end{cases}
$$

$$
(II\text{-}33)\quad
\begin{cases}
E_r^I = -j\left[\dfrac{(\gamma/k_o)}{(h_1/k_o)}\, J_n'(h_1 r)\, a_n^I \right. \\
\qquad \left. + \dfrac{nZ_o}{(h_1/k_o)^2}\, \dfrac{J_n(h_1 r)}{(k_o r)}\, c_n^I \right] \cos n\phi\ \epsilon^{-j\gamma z} \\
E_r^{II} = -j\left[\dfrac{(\gamma/k_o)}{(h_2/k_o)} \left(J_n'(h_2 r)\, a_n^{II} + N_n'(h_2 r)\, b_n^{II}\right) \right. \\
\qquad \left. + \dfrac{nZ_o}{(h_2/k_o)^2} \left(\dfrac{J_n(h_2 r)}{(k_o r)}\, c_n^{II} + \dfrac{N_n(h_2 r)}{(k_o r)}\, d_n^{II}\right)\right] \cos n\phi\ \epsilon^{-j\gamma z} \\
E_r^{III} = -j\left[\dfrac{(\gamma/k_o)}{(h_3/k_o)}\, H_n^{(2)'}(h_3 r)\, b_n^{III} \right. \\
\qquad \left. + \dfrac{nZ_o}{(h_3/k_o)^2}\, \dfrac{H_n^{(2)}(h_3 r)}{(k_o r)}\, d_n^{III}\right] \cos n\phi\ \epsilon^{-j\gamma z}
\end{cases}
$$

$$
\text{where}\quad
\begin{cases}
a_n^I = \dfrac{J_n(h_2 a)}{J_n(h_1 a)}\, a_n^{II} + \dfrac{N_n(h_2 a)}{J_n(h_1 a)}\, b_n^{II} \\
c_n^I = \dfrac{J_n(h_2 a)}{J_n(h_1 a)}\, c_n^{II} + \dfrac{N_n(h_2 a)}{J_n(h_1 a)}\, d_n^{II} \\
b_n^{III} = \dfrac{J_n(h_2 b)}{H_n^{(2)}(h_3 b)}\, a_n^{II} + \dfrac{N_n(h_2 b)}{H_n^{(2)}(h_3 b)}\, b_n^{II} \\
d_n^{III} = \dfrac{J_n(h_2 b)}{H_n^{(2)}(h_3 b)}\, c_n^{II} + \dfrac{N_n(h_2 b)}{H_n^{(2)}(h_3 b)}\, d_n^{II}
\end{cases}
$$

are obtained from the boundary conditions on E_z and H_z at the innermost and outermost boundaries.

b. Dispersion determinant: $D(\gamma/k_o; k_o a; k_o b)$

(II-34)

$$D = \begin{vmatrix} a_n^{II} & b_n^{II} & c_n^{II} & d_n^{II} \\ \left[\left(\frac{h_1}{k_o}\right)\left(\frac{h_2}{k_o}\right)^2 \epsilon_1 J_n'(h_1 a) J_n(h_2 a) - \left(\frac{h_1}{k_o}\right)^2\left(\frac{h_2}{k_o}\right)\epsilon_2 J_n(h_1 a) J_n'(h_2 a)\right] & \left[\left(\frac{h_1}{k_o}\right)\left(\frac{h_2}{k_o}\right)^2 \epsilon_1 J_n'(h_1 a) N_n(h_2 a) - \left(\frac{h_1}{k_o}\right)^2\left(\frac{h_2}{k_o}\right)\epsilon_2 J_n(h_1 a) N_n'(h_2 a)\right] & \frac{n(\gamma/k_o)}{(k_o a)}\left[\left(\frac{h_2}{k_o}\right)^2 - \left(\frac{h_1}{k_o}\right)^2\right] J_n(h_1 a) J_n(h_2 a) & \frac{n(\gamma/k_o)}{(k_o a)}\left[\left(\frac{h_2}{k_o}\right)^2 - \left(\frac{h_1}{k_o}\right)^2\right] J_n(h_1 a) N_n(h_2 a) \\ \left[\left(\frac{h_2}{k_o}\right)^2 \epsilon_3 J_n(h_2 b)\left\{\left(\frac{h_3}{k_o}\right)\frac{H_n^{(2)'}(h_3 b)}{H_n^{(2)}(h_3 b)}\right\} - \left(\frac{h_2}{k_o}\right)\left(\frac{h_3}{k_o}\right)^2 \epsilon_2 J_n'(h_2 b)\right] & \left[\left(\frac{h_2}{k_o}\right)^2 \epsilon_3 N_n(h_2 b)\left\{\left(\frac{h_3}{k_o}\right)\frac{H_n^{(2)'}(h_3 b)}{H_n^{(2)}(h_3 b)}\right\} - \left(\frac{h_2}{k_o}\right)\left(\frac{h_3}{k_o}\right)^2 \epsilon_2 N_n'(h_2 b)\right] & \frac{n(\gamma/k_o)}{(k_o b)}\left[\left(\frac{h_2}{k_o}\right)^2 - \left(\frac{h_3}{k_o}\right)^2\right] J_n(h_2 b) & \frac{n(\gamma/k_o)}{(k_o b)}\left[\left(\frac{h_2}{k_o}\right)^2 - \left(\frac{h_3}{k_o}\right)^2\right] N_n(h_2 b) \\ \frac{n(\gamma/k_o)}{(k_o a)}\left[\left(\frac{h_2}{k_o}\right)^2 - \left(\frac{h_1}{k_o}\right)^2\right] J_n(h_1 a) J_n(h_2 a) & \frac{n(\gamma/k_o)}{(k_o a)}\left[\left(\frac{h_2}{k_o}\right)^2 - \left(\frac{h_1}{k_o}\right)^2\right] J_n(h_1 a) N_n(h_2 a) & \left[\left(\frac{h_1}{k_o}\right)\left(\frac{h_2}{k_o}\right)^2 J_n'(h_1 a) J_n(h_2 a) - \left(\frac{h_1}{k_o}\right)^2\left(\frac{h_2}{k_o}\right) J_n(h_1 a) J_n'(h_2 a)\right] & \left[\left(\frac{h_1}{k_o}\right)\left(\frac{h_2}{k_o}\right)^2 J_n'(h_1 a) N_n(h_2 a) - \left(\frac{h_1}{k_o}\right)^2\left(\frac{h_2}{k_o}\right) J_n(h_1 a) N_n'(h_2 a)\right] \\ \frac{n(\gamma/k_o)}{(k_o b)}\left[\left(\frac{h_2}{k_o}\right)^2 - \left(\frac{h_3}{k_o}\right)^2\right] J_n(h_2 b) & \frac{n(\gamma/k_o)}{(k_o b)}\left[\left(\frac{h_2}{k_o}\right)^2 - \left(\frac{h_3}{k_o}\right)^2\right] N_n(h_2 b) & \left[\left(\frac{h_2}{k_o}\right)^2 J_n(h_2 b)\left\{\left(\frac{h_3}{k_o}\right)\frac{H_n^{(2)'}(h_3 b)}{H_n^{(2)}(h_3 b)}\right\} - \left(\frac{h_2}{k_o}\right)\left(\frac{h_3}{k_o}\right)^2 J_n'(h_2 b)\right] & \left[\left(\frac{h_2}{k_o}\right)^2 N_n(h_2 b)\left\{\left(\frac{h_3}{k_o}\right)\frac{H_n^{(2)'}(h_3 b)}{H_n^{(2)}(h_3 b)}\right\} - \left(\frac{h_2}{k_o}\right)\left(\frac{h_3}{k_o}\right)^2 N_n'(h_2 b)\right] \end{vmatrix} = 0$$

C. Coaxial Dielectric Waveguide

1. E_{om} modes

a. Field equations

$$(II\text{-}35)\quad \begin{cases} E_z^I = a_o^I\, J_o(h_1 r)\,\epsilon^{-j\gamma z} \\ E_z^{II} = [a_o^{II}\, J_o(h_2 r) + b_o^{II}\, N_o(h_2 r)]\,\epsilon^{-j\gamma z} \\ E_z^{III} = [a_o^{III}\, J_o(h_3 r) + b_o^{III}\, N_o(h_3 r)]\,\epsilon^{-j\gamma z} \\ E_z^{IV} = b_o^{IV}\, H_o^{(2)}(h_4 r)\,\epsilon^{-j\gamma z} \end{cases}$$

$$(II\text{-}36)\quad \begin{cases} E_r^I = -j\dfrac{(\gamma/k_o)}{(h_1/k_o)}\, J_o'(h_1 a)\, a_o^I\, \epsilon^{-j\gamma z} \\ E_r^{II} = -j\dfrac{(\gamma/k_o)}{(h_2/k_o)}\, [J_o'(h_2 r)\, a_o^{II} + N_o'(h_2 r)\, b_o^{II}]\,\epsilon^{-j\gamma z} \\ E_r^{III} = -j\dfrac{(\gamma/k_o)}{(h_3/k_o)}\, [J_o'(h_3 r)\, a_o^{III} + N_o'(h_3 r)\, b_o^{III}]\,\epsilon^{-j\gamma z} \\ E_r^{IV} = -j\dfrac{(\gamma/k_o)}{(h_4/k_o)}\, H_o^{(2)'}(h_4 r)\, b_o^{IV}\, \epsilon^{-j\gamma z} \end{cases}$$

$$(II\text{-}37)\quad \begin{cases} H_\phi^I = -j\,\dfrac{\varepsilon_1}{Z_o}\dfrac{1}{(h_1/k_o)}\, a_o^I\, J_o'(h_1 r)\,\epsilon^{-j\gamma z} \\ H_\phi^{II} = -j\,\dfrac{\varepsilon_2}{Z_o}\dfrac{1}{(h_2/k_o)}\, [J_o'(h_2 r)\, a_o^{II} + N_o'(h_2 r)\, b_o^{II}]\,\epsilon^{-j\gamma z} \\ H_\phi^{III} = -j\,\dfrac{\varepsilon_3}{Z_o}\dfrac{1}{(h_3/k_o)}\, [J_o'(h_3 r)\, a_o^{III} + N_o'(h_3 r)\, b_o^{III}]\,\epsilon^{-j\gamma z} \\ H_\phi^{IV} = -j\,\dfrac{\varepsilon_4}{Z_o}\dfrac{1}{(h_4/k_o)}\, H_o^{(2)'}(h_4 r)\, b_o^{IV}\, \epsilon^{-j\gamma z} \end{cases}$$

$$\text{where} \begin{cases} a_o^I = \dfrac{J_o(h_2a)}{J_o(h_1a)}\, a_o^{II} + \dfrac{N_o(h_2a)}{J_o(h_1a)}\, b_o^{II} \\ b_o^{IV} = \dfrac{J_o(h_3c)}{H_o^{(2)}(h_4c)}\, a_o^{III} + \dfrac{N_o(h_3c)}{H_o^{(2)}(h_4c)}\, b_o^{III} \end{cases}$$

are obtained from the boundary conditions on E_z at the innermost and outermost boundaries.

b. Dispersion determinant: $D(\gamma/k_o; k_oa; k_ob; k_oc)$

(II-38) AS AMENDED →

$$D = \begin{vmatrix} a_o^{II} & b_o^{II} & a_o^{III} & b_o^{III} \\ \epsilon_1\left(\frac{h_2}{k_o}\right)J_o'(h_1a)J_o(h_2a) & \epsilon_1\left(\frac{h_2}{k_o}\right)J_o'(h_1a)N_o(h_2a) & 0 & 0 \\ -\epsilon_2\left(\frac{h_1}{k_o}\right)J_o(h_1a)J_o'(h_2a) & -\epsilon_2\left(\frac{h_1}{k_o}\right)J_o(h_1a)N_o'(h_2a) & & \\ 0 & 0 & \epsilon_4\left(\frac{h_3}{k_o}\right)J_o(h_3c)\left\{\frac{(h_4/k_o)H_o^{(2)'}(h_4c)}{H_o^{(2)}(h_4c)}\right\} & \epsilon_4\left(\frac{h_3}{k_o}\right)N_o(h_3c)\left\{\frac{(h_4/k_o)H_o^{(2)'}(h_4c)}{H_o^{(2)}(h_4c)}\right\} \\ & & -\epsilon_3\left(\frac{h_4}{k_o}\right)^2 J_o'(h_3c) & -\epsilon_3\left(\frac{h_4}{k_o}\right)^2 N_o'(h_3c) \\ J_o(h_2b) & N_o(h_2b) & -J_o(h_3b) & -N_o(h_3b) \\ \epsilon_2\left(\frac{h_3}{k_o}\right)J_o'(h_2b) & \epsilon_2\left(\frac{h_3}{k_o}\right)N_o'(h_2b) & -\epsilon_3\left(\frac{h_2}{k_o}\right)J_o'(h_3b) & -\epsilon_3\left(\frac{h_2}{k_o}\right)N_o'(h_3b) \end{vmatrix} = 0$$

2. H_{om} modes

a. Field equations

$$(\text{II-39}) \begin{cases} H_z^I = c_o^I\, J_o(h_1r)\epsilon^{-j\gamma z} \\ H_z^{II} = [c_o^{II}\, J_o(h_2r) + d_o^{II}\, N_o(h_2r)]\epsilon^{-j\gamma z} \\ H_z^{III} = [c_o^{III}\, J_o(h_3r) + d_o^{III}\, N_o(h_3r)]\epsilon^{-j\gamma z} \\ H_z^{IV} = d_o^{IV}\, H_o^{(2)}(h_4r)\epsilon^{-j\gamma z} \end{cases}$$

$$
(II\text{-}40)\quad
\begin{cases}
H_r^{I} = -j\,\dfrac{(\gamma/k_o)}{(h_1/k_o)}\,c_o^{I}\,J_o'(h_1 r)\epsilon^{-j\gamma z} \\
H_r^{II} = -j\,\dfrac{(\gamma/k_o)}{(h_2/k_o)}\,[J_o'(h_2 r)\,c_o^{II} + N_o'(h_2 r)\,d_o^{II}]\epsilon^{-j\gamma z} \\
H_r^{III} = -j\,\dfrac{(\gamma/k_o)}{(h_3/k_o)}\,[J_o'(h_3 r)\,c_o^{III} + N_o'(h_3 r)\,d_o^{III}]\epsilon^{-j\gamma z} \\
H_r^{IV} = -j\,\dfrac{(\gamma/k_o)}{(h_4/k_o)}\,d_o^{IV}\,H_o^{(2)'}(h_4 r)\epsilon^{-j\gamma z}
\end{cases}
$$

$$
(II\text{-}41)\quad
\begin{cases}
E_\phi^{I} = j\,\dfrac{Z_o}{(h_1/k_o)}\,c_o^{I}\,J_o'(h_1 r)\epsilon^{-j\gamma z} \\
E_\phi^{II} = j\,\dfrac{Z_o}{(h_4/k_o)}\,[c_o^{II}\,J_o'(h_2 r) + d_o^{II}N_o'(h_2 r)\epsilon^{-j\gamma z} \\
E_\phi^{III} = j\,\dfrac{Z_o}{(h_3/k_o)}\,[J_o'(h_3 r)\,c_o^{III} + N_o'(h_3 r)\,d_o^{III}]\epsilon^{-j\gamma z} \\
E_\phi^{IV} = j\,\dfrac{Z_o}{(h_4/k_o)}\,d_o^{IV}\,H_o^{(2)'}(h_4 r)\epsilon^{-j\gamma z}
\end{cases}
$$

where

$$
\begin{cases}
c_o^{I} = \dfrac{J_o(h_2 a)}{J_o(h_1 a)}\,c_o^{II} + \dfrac{N_o(h_2 a)}{J_o(h_1 a)}\,d_o^{II} \\
d_o^{IV} = \dfrac{J_o(h_3 c)}{H_o^{(2)}(h_4 c)}\,c_o^{III} + \dfrac{N_o(h_3 c)}{H_o^{(2)}(h_4 c)}\,d_o^{III}
\end{cases}
$$

are obtained from the boundary conditions on H_z at the innermost and outermost boundaries.

b. Dispersion determinant: $D(\gamma/k_o; k_o a; k_o b; k_o c)$

$$
(\text{II-42})\quad D = \begin{vmatrix}
\overset{c_o^{II}}{\overbrace{}} & \overset{d_o^{II}}{\overbrace{}} & \overset{c_o^{III}}{\overbrace{}} & \overset{d_o^{III}}{\overbrace{}} \\
\left(\frac{h_3}{k_o}\right) J_o'(h_2 b) & \left(\frac{h_3}{k_o}\right) N_o'(h_2 b) & -\left(\frac{h_2}{k_o}\right) J_o'(h_3 b) & -\left(\frac{h_2}{k_o}\right) N_o'(h_3 b) \\
\left(\frac{h_2}{k_o}\right) J_o'(h_1 a) J_o(h_2 a) - \left(\frac{h_1}{k_o}\right) J_o(h_1 a) J_o'(h_2 a) & \left(\frac{h_2}{k_o}\right) J_o'(h_1 a) N_o(h_2 a) - \left(\frac{h_1}{k_o}\right) J_o(h_1 a) N_o'(h_2 a) & 0 & 0 \\
J_o(h_2 b) & N_o(h_2 b) & -J_o(h_3 b) & -N_o(h_3 b) \\
0 & 0 & \left(\frac{h_3}{k_o}\right) J_o(h_3 c)\left\{\frac{(h_4/k_o)H_o^{(2)'}(h_4 c)}{H_o^{(2)}(h_4 c)}\right\} - \left(\frac{h_4}{k_o}\right)^2 J_o'(h_3 c) & \left(\frac{h_3}{k_o}\right) N_o(h_3 c)\left\{\frac{(h_4/k_o)H_o^{(2)'}(h_4 c)}{H_o^{(2)}(h_4 c)}\right\} - \left(\frac{h_4}{k_o}\right)^2 N_o'(h_3 c)
\end{vmatrix} = 0
$$

3. Hybrid modes [HE_{nm} and EH_{nm}]

a. Field equations

$$
(\text{II-43})\quad \begin{cases}
E_z^I = a_n^I J_n(h_1 r) \cos n\phi \, \epsilon^{-j\gamma z} \\
E_z^{II} = [a_n^{II} J_n(h_2 r) + b_n^{II} N_n(h_2 r)] \cos n\phi \, \epsilon^{-j\gamma z} \\
E_z^{III} = [a_n^{III} J_n(h_3 r) + b_n^{III} N_n(h_3 r)] \cos n\phi \, \epsilon^{-j\gamma z} \\
E_z^{IV} = b_n^{IV} H_n^{(2)}(h_4 r) \cos n\phi \, \epsilon^{-j\gamma z}
\end{cases}
$$

$$
(\text{II-44})\quad \begin{cases}
H_z^I = c_n^I J_n(h_1 r) \sin n\phi \, \epsilon^{-j\gamma z} \\
H_z^{II} = [c_n^{II} J_n(h_2 r) + d_n^{II} N_n(h_2 r)] \sin n\phi \, \epsilon^{-j\gamma z} \\
H_z^{III} = [c_n^{III} J_n(h_3 r) + d_n^{III} N_n(h_3 r)] \sin n\phi \, \epsilon^{-j\gamma z} \\
H_z^{IV} = d_n^{IV} H_n^{(2)}(h_4 r) \sin n\phi \, \epsilon^{-j\gamma z}
\end{cases}
$$

$$
(\text{II-45}) \quad
\begin{cases}
H_r^{I} = -j\left[n \dfrac{\varepsilon_1}{Z_o} \dfrac{1}{(h_1/k_o)^2} \dfrac{J_n(h_1 r)}{k_o r} a_n^{I} \right. \\
\qquad \left. + \dfrac{(\gamma/k_o)}{(h_1/k_o)} J_n'(h_1 r)\, c_n^{I} \right] \sin n\phi\, \epsilon^{-j\gamma z} \\
\\
H_r^{II} = -j\left[n \dfrac{\varepsilon_2}{Z_o} \dfrac{1}{(h_2/k_o)^2} \left(\dfrac{J_n(h_2 r)}{k_o r} a_n^{II} + \dfrac{N_n(h_2 r)}{k_o r} b_n^{II} \right) \right. \\
\qquad \left. + \dfrac{(\gamma/k_o)}{(h_2/k_o)} \left(J_n'(h_2 r)\, c_n^{II} + N_n'(h_2 r)\, d_n^{II} \right) \right] \sin n\phi\, \epsilon^{-j\gamma z} \\
\\
H_r^{III} = -j\left[n \dfrac{\varepsilon_3}{Z_o} \dfrac{1}{(h_3/k_o)^2} \left(\dfrac{J_n(h_3 r)}{k_o r} a_n^{III} + \dfrac{N_n(h_3 r)}{k_o r} b_n^{III} \right) \right. \\
\qquad \left. + \dfrac{(\gamma/k_o)}{(h_3/k_o)} \left(J_n'(h_3 r)\, c_n^{II} + N_n'(h_3 r)\, d_n^{III} \right) \right] \sin n\phi\, \epsilon^{-j\gamma z} \\
\\
H_r^{IV} = -j\left[n \dfrac{\varepsilon_4}{Z_o} \dfrac{1}{(h_4/k_o)^2} \dfrac{H_n^{(2)}(h_4 r)}{k_o r} b_n^{IV} \right. \\
\qquad \left. + \dfrac{(\gamma/k_o)}{(h_4/k_o)} H_n^{(2)'}(h_4 r)\, d_n^{IV} \right] \sin n\phi\, \epsilon^{-j\gamma z}
\end{cases}
$$

$$
(\text{II-46})\quad
\begin{cases}
E_r^{I} = -j\left[\dfrac{(\gamma/k_o)}{(h_1/k_o)}\, J_n'(h_1 r)\, a_n^{I} \right. \\
\qquad \left. + nZ_o\, \dfrac{1}{(h_1/k_o)^2}\, \dfrac{J_n(h_1 r)}{k_o r}\, c_n^{I}\right] \cos n\phi\, \epsilon^{-j\gamma z} \\
\\
E_r^{II} = -j\left[\dfrac{(\gamma/k_o)}{(h_2/k_o)}\left(J_n'(h_2 r)\, a_n^{II} + N_n'(h_2 r)\, b_n^{II}\right)\right. \\
\qquad \left. + n\, \dfrac{Z_o}{(h_2/k_o)^2}\left(\dfrac{J_n(h_2 r)}{k_o r}\, c_n^{II} + \dfrac{N_n(h_2 r)}{k_o r}\, d_n^{II}\right)\right] \cos n\phi\, \epsilon^{-j\gamma z} \\
\\
E_r^{III} = -j\left[\dfrac{(\gamma/k_o)}{(h_3/k_o)}\left(J_n'(h_3 r)\, a_n^{III} + N_n'(h_3 r)\, b_n^{III}\right)\right. \\
\qquad \left. + n\, \dfrac{Z_o}{(h_3/k_o)^2}\left(\dfrac{J_n(h_3 r)}{k_o r}\, c_n^{III} + \dfrac{N_n(h_3 r)}{k_o r}\, d_n^{III}\right)\right] \cos n\phi\, \epsilon^{-j\gamma z} \\
\\
E_r^{IV} = -j\left[\dfrac{(\gamma/k_o)}{(h_4/k_o)}\, H_n^{(2)'}(h_4 r)\, b_n^{IV} \right. \\
\qquad \left. + n\, \dfrac{Z_o}{(h_4/k_o)^2}\, \dfrac{H_n^{(2)}(h_4 r)}{k_o r}\, d_n^{IV}\right] \cos n\phi\, \epsilon^{-j\gamma z}
\end{cases}
$$

$$
\begin{cases}
H_\phi^{I} = -j\left[\dfrac{\varepsilon_1}{Z_o}\dfrac{1}{(h_1/k_o)}\,J_n'(h_1 r)\,a_n^{I} \right. \\
\qquad \left. + n\,\dfrac{(\gamma/k_o)}{(h_1/k_o)^2}\dfrac{J_n(h_1 r)}{k_o r}\,c_n^{I}\right]\cos n\phi\;\epsilon^{-j\gamma z} \\
\\
H_\phi^{II} = -j\left[\dfrac{\varepsilon_2}{Z_o}\dfrac{1}{(h_2/k_o)}\left(J_n'(h_2 r)\,a_n^{II} + N_n'(h_2 r)\,b_n^{II}\right)\right. \\
\qquad \left. + n\,\dfrac{(\gamma/k_o)}{(h_2/k_o)^2}\left(\dfrac{J_n(h_2 r)}{k_o r}\,c_n^{II} + \dfrac{N_n(h_2 r)}{k_o r}\,d_n^{II}\right)\right]\cos n\phi\;\epsilon^{-j\gamma z} \\
\\
H_\phi^{III} = -j\left[\dfrac{\varepsilon_3}{Z_o}\dfrac{1}{(h_3/k_o)}\left(J_n'(h_3 r)\,a_n^{III} + N_n'(h_3 r)\,b_n^{III}\right)\right. \\
\qquad \left. + n\,\dfrac{(\gamma/k_o)}{(h_3/k_o)^2}\left(\dfrac{J_n(h_3 r)}{k_o r}\,c_n^{III} + \dfrac{N_n(h_3 r)}{k_o r}\,d_n^{III}\right)\right]\cos n\phi\;\epsilon^{-j\gamma z} \\
\\
H_\phi^{IV} = -j\left[\dfrac{\varepsilon_4}{Z_o}\dfrac{1}{(h_4/k_o)}\,H_n^{(2)'}(h_4 r)\,b_n^{IV} \right. \\
\qquad \left. + n\,\dfrac{(\gamma/k_o)}{(h_4/k_o)^2}\dfrac{H_n^{(2)}(h_4 r)}{k_o r}\,d_n^{IV}\right]\cos n\phi\;\epsilon^{-j\gamma z}
\end{cases}
\tag{II-47}
$$

$$
\begin{cases}
E_\phi^I = j\left[n \dfrac{(\gamma/k_o)}{(h_1/k_o)^2} \dfrac{J_n(h_1 r)}{k_o r} a_n^I \right. \\
\qquad \left. + \dfrac{Z_o}{(h_1/k_o)} J_n'(h_1 r)\, c_n^I \right] \sin n\phi\, \epsilon^{-j\gamma z} \\
E_\phi^{II} = j\left[n \dfrac{(\gamma/k_o)}{(h_2/k_o)^2} \left(\dfrac{J_n(h_2 r)}{k_o r} a_n^{II} + \dfrac{N_n(h_2 r)}{k_o r} b_n^{II} \right) \right. \\
\qquad \left. + \dfrac{Z_o}{(h_2/k_o)} \left(J_n'(h_2 r)\, c_n^{II} + N_n'(h_2 r)\, d_n^{II} \right) \right] \sin n\phi\, \epsilon^{-j\gamma z} \\
E_\phi^{III} = j\left[n \dfrac{(\gamma/k_o)}{(h_3/k_o)^2} \left(\dfrac{J_n(h_3 r)}{k_o r} a_n^{III} + \dfrac{N_n(h_3 r)}{k_o r} b_n^{III} \right) \right. \\
\qquad \left. + \dfrac{Z_o}{(h_3/k_o)} \left(J_n'(h_3 r)\, c_n^{III} + N_n'(h_3 r)\, d_n^{III} \right) \right] \sin n\phi\, \epsilon^{-j\gamma z} \\
E_\phi^{IV} = j\left[n \dfrac{(\gamma/k_o)}{(h_4/k_o)^2} \dfrac{H_n^{(2)}(h_4 r)}{k_o r} b_n^{IV} \right. \\
\qquad \left. + \dfrac{Z_o}{(h_4/k_o)} H_n^{(2)'}(h_4 r)\, d_n^{IV} \right] \sin n\phi\, \epsilon^{-j\gamma z}
\end{cases}
\tag{II-48}
$$

where

$$
\begin{cases}
a_n^I = \dfrac{J_n(h_2 a)}{J_n(h_1 a)} a_n^{II} + \dfrac{N_n(h_2 a)}{J_n(h_1 a)} b_n^{II} \\
c_n^I = \dfrac{J_n(h_2 a)}{J_n(h_1 a)} c_n^{II} + \dfrac{N_n(h_2 a)}{J_n(h_1 a)} d_n^{II} \\
b_n^{IV} = \dfrac{J_n(h_3 c)}{H_n^{(2)}(h_4 c)} a_n^{III} + \dfrac{N_n(h_3 c)}{H_n^{(2)}(h_4 c)} b_n^{III} \\
d_n^{IV} = \dfrac{J_n(h_3 c)}{H_n^{(2)}(h_4 c)} c_n^{III} + \dfrac{N_n(h_3 c)}{H_n^{(2)}(h_4 c)} d_n^{III}
\end{cases}
$$

are obtained from the boundary conditions on H_z and E_z at the innermost and outermost boundaries.

b. Dispersion determinant: $D(\gamma/k_o; k_o a; k_o b; k_o c)$

(II-49) $D =$

a_n^{II}	b_n^{II}	c_n^{II}	d_n^{II}
$\epsilon_1\left(\frac{h_1}{k_o}\right)\left(\frac{h_2}{k_o}\right)^2 J_n'(h_1 a) J_n(h_2 a)$	$\epsilon_1\left(\frac{h_1}{k_o}\right)\left(\frac{h_2}{k_o}\right)^2 J_n'(h_1 a) N_n(h_2 a)$	$\frac{n(\gamma/k_o)}{(k_o a)}\left[\left(\frac{h_2}{k_o}\right)^2 - \left(\frac{h_1}{k_o}\right)^2\right] J_n(h_1 a) J_n(h_2 a)$	$\frac{n(\gamma/k_o)}{(k_o a)}\left[\left(\frac{h_2}{k_o}\right)^2 - \left(\frac{h_1}{k_o}\right)^2\right] J_n(h_1 a) N_n(h_2 a)$
$-\epsilon_2\left(\frac{h_1}{k_o}\right)^2\left(\frac{h_2}{k_o}\right) J_n(h_1 a) J_n'(h_2 a)$	$-\epsilon_2\left(\frac{h_1}{k_o}\right)^2\left(\frac{h_2}{k_o}\right) J_n(h_1 a) N_n'(h_2 a)$		
0	0	0	0
$\epsilon_2\left(\frac{h_2}{k_o}\right)\left(\frac{h_3}{k_o}\right)^2 J_n'(h_2 b)$	$\epsilon_2\left(\frac{h_2}{k_o}\right)\left(\frac{h_3}{k_o}\right)^2 N_n'(h_2 b)$	$\frac{n(\gamma/k_o)}{(k_o b)}\left(\frac{h_3}{k_o}\right)^2 J_n(h_2 b)$	$\frac{n(\gamma/k_o)}{(k_o b)}\left(\frac{h_3}{k_o}\right)^2 N_n(h_2 b)$
$J_n(h_2 b)$	$N_n(h_2 b)$	0	0
0	0	$J_n(h_2 b)$	$N_n(h_2 b)$
$\frac{n(\gamma/k_o)}{(k_o b)}\left(\frac{h_3}{k_o}\right)^2 J_n(h_2 b)$	$\frac{n(\gamma/k_o)}{(k_o b)}\left(\frac{h_3}{k_o}\right)^2 N_n(h_2 b)$	$\left(\frac{h_2}{k_o}\right)\left(\frac{h_3}{k_o}\right)^2 J_n'(h_2 b)$	$\left(\frac{h_2}{k_o}\right)\left(\frac{h_3}{k_o}\right)^2 N_n'(h_2 b)$
$\frac{n(\gamma/k_o)}{(k_o a)}\left[\left(\frac{h_2}{k_o}\right)^2 - \left(\frac{h_1}{k_o}\right)^2\right] J_n(h_1 a) J_n(h_2 a)$	$\frac{n(\gamma/k_o)}{(k_o a)}\left[\left(\frac{h_2}{k_o}\right)^2 - \left(\frac{h_1}{k_o}\right)^2\right] J_n(h_1 a) N_n(h_2 a)$	$\left(\frac{h_1}{k_o}\right)\left(\frac{h_2}{k_o}\right)^2 J_n'(h_1 a) J_n(h_2 a)$	$\left(\frac{h_1}{k_o}\right)\left(\frac{h_2}{k_o}\right)^2 J_n'(h_1 a) N_n(h_2 a)$
		$-\left(\frac{h_1}{k_o}\right)^2\left(\frac{h_2}{k_o}\right) J_n(h_1 a) J_n'(h_2 a)$	$-\left(\frac{h_1}{k_o}\right)^2\left(\frac{h_2}{k_o}\right) J_n(h_1 a) N_n'(h_2 a)$
0	0	0	0

$a_n^{I\ldots}$	b_n^{III}	c_n^{III}	d_n^{III}
0	0	0	0
$\epsilon_4\left(\frac{h_3}{k_o}\right)^2 J_n(h_3 c)\left\{\frac{(h_4/k_o)H_n^{(2)'}(h_4 c)}{H_n^{(2)}(h_4 c)}\right\}$	$\epsilon_4\left(\frac{h_3}{k_o}\right)^2 N_n(h_3 c)\left\{\frac{(h_4/k_o)H_n^{(2)'}(h_4 c)}{H_n^{(2)}(h_4 c)}\right\}$	$\frac{n(\gamma/k_o)}{(k_o c)}\left[\left(\frac{h_3}{k_o}\right)^2 - \left(\frac{h_4}{k_o}\right)^2\right] J_n(h_3 c)$	$\frac{n(\gamma/k_o)}{(k_o c)}\left[\left(\frac{h_3}{k_o}\right)^2 - \left(\frac{h_4}{k_o}\right)^2\right] N_n(h_3 c)$
$-\epsilon_3\left(\frac{h_3}{k_o}\right)\left(\frac{h_4}{k_o}\right)^2 J_n'(h_3 c)$	$-\epsilon_3\left(\frac{h_3}{k_o}\right)\left(\frac{h_4}{k_o}\right)^2 N_n'(h_3 c)$		
$-\epsilon_3\left(\frac{h_2}{k_o}\right)^2\left(\frac{h_3}{k_o}\right) J_n'(h_3 b)$	$-\epsilon_3\left(\frac{h_2}{k_o}\right)^2\left(\frac{h_3}{k_o}\right) N_n'(h_3 b)$	$\frac{-n(\gamma/k_o)}{(k_o b)}\left(\frac{h_2}{k_o}\right)^2 J_n(h_3 b)$	$\frac{-n(\gamma/k_o)}{(k_o b)}\left(\frac{h_2}{k_o}\right)^2 N_n(h_3 b)$
$-J_n(h_3 b)$	$-N_n(h_3 b)$	0	0
0	0	$-J_n(h_3 b)$	$-N_n(h_3 b)$
$\frac{-n(\gamma/k_o)}{(k_o b)}\left(\frac{h_2}{k_o}\right)^2 J_n(h_3 b)$	$\frac{-n(\gamma/k_o)}{(k_o b)}\left(\frac{h_2}{k_o}\right)^2 N_n(h_3 b)$	$-\left(\frac{h_2}{k_o}\right)^2\left(\frac{h_3}{k_o}\right) J_n'(h_3 b)$	$-\left(\frac{h_2}{k_o}\right)^2\left(\frac{h_3}{k_o}\right) N_n'(h_3 b)$
0	0	0	0
$\frac{n(\gamma/k_o)}{(k_o c)}\left[\left(\frac{h_3}{k_o}\right)^2 - \left(\frac{h_4}{k_o}\right)^2\right] J_n(h_3 c)$	$\frac{n(\gamma/k_o)}{(k_o c)}\left[\left(\frac{h_3}{k_o}\right)^2 - \left(\frac{h_4}{k_o}\right)^2\right] N_n(h_3 c)$	$\left(\frac{h_3}{k_o}\right)^2 J_n(h_3 c)\left\{\frac{(h_4/k_o)H_n^{(2)'}(h_4 c)}{H_n^{(2)}(h_4 c)}\right\}$	$\left(\frac{h_3}{k_o}\right)^2 N_n(h_3 c)\left\{\frac{(h_4/k_o)H_n^{(2)'}(h_4 c)}{H_n^{(2)}(h_4 c)}\right\}$
		$-\left(\frac{h_3}{k_o}\right)\left(\frac{h_4}{k_o}\right)^2 J_n'(h_3 c)$	$-\left(\frac{h_3}{k_o}\right)\left(\frac{h_4}{k_o}\right)^2 N_n'(h_3 c)$

$= 0$

REFERENCES

1. Hondros, D. and Debye, P., "Elektromagnetesche Wellen an dielektrischen Drähten," ~~Annalen der Physik, V 32, 1910.~~ AS AMENDED Ann. d. Phys. 32, 465, (1910) AS AMENDED

2. Schelkunoff, S.A., Electromagnetic Waves, D. VanNostrand ~~Co.~~ Space AS AMENDED AS AMENDED Inc., New York, N.Y., (1943)

3. Scheslinger, S.P., "On Higher-Order Hybrid Modes of Dielectric Cylinders," IRE Transactions on Microwave Theory and Techniques, MTT-8, ~~March~~ 252, (1960) AS AMENDED

4. Beam, R., Astrahan, M., Jakes, W., Wachowski, H., and Firestone, W., "Dielectric Tube Waveguides," Final Report, Investigation of Multimode Propagation in Waveguides and Microwave Optics, Chap. V, Northwestern University, Report AS AMENDED ATI 194929 (1950) ~~ASTIA, AD98814, 1956.~~ AS AMENDED

5. Unger, H.G., "Dielektrische Rohre als Wellenleiter," Archiv der Elektrischen Ubertragung (A.E.Ü.), ~~June, 1954.~~ 8, 241 (1954) AS AMENDED

6. Barnett, R.I., "An All Dielectric Coaxial Waveguide and Antenna," Phd. Dissertation; Department of Electrical Engineering, The Ohio State University, (1963) AS AMENDED

7. Vzyatyshev, V.F., Dielectric Wave Guides, (Dielektricheskiye volnovody), Moscow Sovitshoye Radio, (1970) AS AMENDED

8. Kiely, D.G., Dielectric Aerials, Methuen's Monographs on Physical Subjects, London: Methuen and Co., Ltd., New York: John Wiley and Sons, Inc., 1953.

9. Moreno, T., Microwave Transmission Design Data, Dover Publications, Inc., New York, N.Y., 1958.

10. Goldman, S., Frequency Analysis, Modulation and Noise, McGraw-Hill Book Co., Inc., New York, 1948.